Polymer film heat transfer elements for multi - effect and vapour compression desalination

by

ANTÓNIO JOSÉ LEÃO

A thesis submitted in partial fulfilment of the requirements
for the degree of

PHILOSOPHIAE DOCTOR

in the

FACULTY OF NATURAL AND AGRICULTURAL SCIENCES

UNIVERSITY OF PRETORIA

April 2004

Polymer film heat transfer elements for multi-effect and vapour compression desalination

by

António José Leão

Supervisor: Dr TB Scheffler

Faculty: Natural and Agricultural Sciences

Department: Physics

Degree: Philosophiae Doctor

ABSTRACT

The continuing improvement of existing desalination processes – both distillation and membrane – is contributing significantly to reducing the cost of desalted water, and to the rapid growth of the desalination industry. Thus the world capacity has more than *doubled* during the two years 2000 - 2001, and desalination of seawater is at present the major source of potable water in arid coastal regions such as the Arabian Gulf region.

Conventional multi-effect distillation (MED) and multi-stage flash (MSF) desalinators use cupro-nickel and/or titanium heat transfer surfaces. Polyolefins such as high density polyethylene (HDPE) and polypropylene (PP) have better corrosion resistance than these, which permits much thinner walls. Depending on the internal & external convection coefficients, 20-50μ thick HDPE and PP film heat transfer elements have from 60-105% of the U value of 1mm cupro-nickel tubes. Experience has shown them to last as well as – and in some high-scaling water re-use applications better than – titanium elements. But per unit area they cost only about 1% as much.

In chapter 2 we show how the low cost permits the installation of much more thermal conductance (UA) than is economically feasible with metal heat transfer surfaces. This leads to a lower temperature difference ΔT_1 between the condensing and evaporating sides, and *a lower specific energy consumption.*

This thesis further describes the design, building and testing of a simple falling saline film

mechanical vapour compression (MVC) desalinator. With air mattress-shaped polyolefin film heat transfer elements. Designed for operation (under vacuum) at various temperatures in the range 50-65°C, with a *small* temperature difference ΔT_i between the condensing and evaporating sides.

In chapter 3 we determine the pressure drop of the condensing vapour for laminar flow inside a film tube, to obtain the relation between film tube diameter, length, U value, temperature and the ratio $R_T = \Delta T_i/\Delta T_f$ of temperature difference ΔT_i to frictional temperature drop ΔT_f.

We also determine, for $\Delta T_i = 1K$ and $R_T = 8$, the relation between tensile stress and temperature for the HDPE and PP films that we have used to fabricate HTE's. For 39μ HDPE film elements up to 60 - 65°C, and for 50μ PP ones up to 90 - 95°C, the stress is below 0.4 MPa – and in most cases well below the creep strength of the materials for a 10 year design life.

In chapter 4 we discuss the welding of thin HDPE and PP films on specially developed apparatuses to produce air mattress-like heat transfer elements (HTE's). Some of these were pressure tested (up to several bars at room temperature) to determine the strength of the weld lines.

Chapter 5 discusses the successful vapour inlet manifolding of the heat transfer elements into heat transfer units. Also the design, construction and testing of a vacuum vessel and a turbo vapour compressor. And of the other auxiliaries (feed water heater, vacuum pump with protecting pre-condenser, water pumps, instrumentation . .).

It also discusses problems encountered, and the merits of various possible remedies.

Chapter 6 discusses suitable surface treatments to increase their surface tension and wettabilityof the air mattress-like heat transfer elements (HTE's). As these are of a non-polar hydrophobic material, such treatment – aimed at creating charged, polar or polarizable sites – is essential for film evaporation. As our original process – oxyfluorination – was only partially successful after several year's work, we have started another surface treatment – sulfonation – which is in the early stages of evaluation.

Polimeerfilm hitte-oordrag elemente vir multi-effek en dampsaampersingsontsouting

deur

António José Leão

Studieleier: Dr TB Scheffler

Fakulteit: Natuur- en Landbouwetenskappe

Departement: Fisika

Graad: Philosophiae Doctor

SAMEVATTING

Die voortgesette verbetering van bestaande ontsoutingsprosesse – beide distillasie- en membraan- – dra beduidend by tot die vermindering van die koste van ontsoute water, en tot die snelle groei van die ontsoutingbedryf. So het die wêreld-ontsoutingsvermoë meer as verdubbel gedurende die jare 2000-2001, en is ontsouting reeds die vernaamste bron van drinkbare water in droë kusstreke soos die Arabiese golfgebied.

Konvensionele multi-effek distillasie (MED) en multi-stadium flits (MSF) distilleerders gebruik kupro-nikkel en titaan hitte-oordrag-oppervlakke. Poli-olefiene soos hoë-digtheid polietileen (HDPE) en polipropileen (PP) is meer bestand teen korrosie as hierdie materiale, en maak dit moontlik om veel dunner wande te gebruik. Vir redelike aannames oor die interne en eksterne konveksie-koëffisiënte, sal 20-50μ HDPE en PP film hitte-oordrag-elemente 60-105% van die U-waarde hê van 1mm wand kupro-nikkel buise. Die ervaring wys dat hulle netso goed soos – en in sommige skaalvormende hergebruik toepassings beter as – titaan elemente hou. Maar per m^2 kos hulle slegs 1% soveel.

In hoofstuk 2 toon ons hoe die lae koste die installering van veel meer hitte-oordrag oppervlak toelaat as wat ekonomies is met metaal oppervlakke. Dit lei tot 'n kleiner temperatuurverskil ΔT_1 tussen die kondenseer- en verdampingskante, en tot 'n laer energie-verbruik per m^3 distillaat.

Die proefskrif beskryf ook die ontwerp, bou en evaluering van 'n eenvoudige vallende

soutwater film meganiese dampsaampersings-distilleerder – met parallele buis poli-olefien film hitte-oordrag elemente (HOE) in 'n lugmatras-tipe konfigurasie. Ontwerp vir bedryf (onder vakuum) by temperature tussen 50 en 65°C, met 'n klein temperatuurverskil ΔT_l tussen die kondensasie- en verdampingskante van die HOE.

In hoofstuk 3 bepaal ons die drukval van die damp vir laminêre vloei binne 'n filmbuis – om die verband te bepaal tussen filmbuis deursnee, lengte, U-waarde, temperatuur en die verhouding $R_T = \Delta T_l/\Delta T_f$ van ΔT_l tot die vloeiweerstand-geïnduseerde temperatuurval ΔT_f.

Ons bepaal ook, vir $\Delta T_l = 1K$ en $R_T = 8$, die verband tussen trekspanning en temperatuur vir die HDPE en PP films wat ons gebruik het om HOE te fabriseer. Vir 39μ HDPE film-elemente tot 60-65°C, en vir 50μ PP film tot 90-95°C, is die spanning minder as 0.4 MPa – en in die meeste gevalle minder as die kruip-sterkte van die materiale vir 'n 10 jaar ontwerpleeftyd.

In hoofstuk 4 bespreek ons die sweis van dun HDPE en PP films met spesiaal ontwikkelde apparate om lugmatras-vormige hitte-oordrag elemente (HOE) te vervaardig. Sommige hiervan is met druklug getoets (tot verskeie bar by kamertemperatuur) om die sterkte van die lyn-sweislasse te bepaal.

Hoofstuk 5 bespreek die suksesvolle ontwerp en konstruksie van die damp-inlate tot die HOE, en die saamvoeg van HOE tot hitte-oordrag eenhede. Ook die ontwerp, konstruksie en toets van 'n vakuum-houer, en van 'n turbo dampsaamperser. Ook van die ander toebehore (toevoerwater verwarmer, vakuumpomp met beskermende kondenseerder, waterpompe, instrumentasie . .).

Dit bespreek ook probleme met die bestaande apparaat en bedryfsmetode, en die meriete van verskillende potensiële oplossings.

Hoofstuk 6 bespreek geskikte oppervlak-behandelings om die oppervlak-spanning en benatbaarheid van die HOE te verhoog. Aangesien hulle van 'n nie-polêre hidrofobiese materiaal is, is sodanige behandeling – daarop gemik om polêre of polariseerbare plekke op die polimeer-oppervlakte te skep – essensieel vir film-verdamping. Aangesien ons

eerste proses – oksifluorinering – slegs gedeeltelik geslaagd was na jare se werk, het ons begin met 'n tweede proses – sulfonering – wat tans in 'n vroeë stadium van evaluering is.

To my family:

"My mother would have been proud of me!!"

ACKNOWLEDGEMENTS

I am greatly indebted to

- my supervisor Dr. T. B. Scheffler for his able and valued assistance and guidance,
- C. Thompson for valued support and cooperation,
- the technicians G. Pretorius, J. Taljaard and R. Van Weele for their assistance and fruitful support,
- my family, for support and encouragement,
- my friend Q. Odendaal for valuable help
- the Nuclear Energy Corporation of South Africa for the opportunity to use their facilities, and
- finally to SAREC for funding my studies.

TABLE OF CONTENTS

3. FLOW IN A THIN-WALLED POLYMER TUBE

4. FABRICATION OF POLYMER FILM HEAT TRANSFER ELEMENTS

5. ASSEMBLY

6. WETTABILITY AND WETTING

LIST OF FIGURES

LIST OF TABLES

1 Introduction

In nature, high quality potable water results from rain (or snow). Most rain results from the solar evaporation of sea water, followed by condensation in the atmosphere. That is, from a natural process of distillation.

In the laboratory, water of high purity can likewise be produced by distillation. As the energy required to evaporate water is very high, this process – called simple distillation - is not energy efficient, and not economical for producing large quantities of water. The enthalpy of evaporation of water - about 2.45×10^6 J/kg at 20°C – exceeds the theoretical minimum work required for separating a kilogram of pure water from sea water by a factor of about 800 [16].

But distillation entails both evaporation and condensation. On condensing vapour, about 99.88% of the heat of evaporation of the sea water is recovered – but normally at a lower temperature than the heat supplied for evaporation. Indeed, the higher the temperature difference, the higher the rate of heat transfer, and the higher the production rate from the distiller. In a vapour compression distiller (VCD) the vapour resulting from the evaporation of saline water is compressed, whereby its temperature is raised. What is important is that at the higher pressure, the vapour will condense at a temperature above the evaporation of saline water.

Thus if the evaporation of saline water takes place on the outside of a set of heat transfer tubes, then condensation of the vapour into pure water takes place inside this same set of tubes, after the vapour has been compressed. The very large latent heat of evaporation/condensation is efficiently recycled, by which the total energy requirement is drastically reduced. Indeed, in a well designed well-insulated VC distiller with a suitable counterflow heat exchanger for heat recovery, the primary energy input during steady operation is to the vapour compressor (and much smaller amounts to the water circulation pumps and vacuum pump). Except during start-up, no heat input is needed during operation.

The main energy needed is to compress the vapour and raise its pressure - and thereby

raise its saturation (condensing) temperature sufficiently above the evaporation temperature for effective heat transfer from the condensation inside the tubes through the heat exchange tube walls to the evaporation of saline water outside them.

This chapter provides some background by describing the need for widespread use of inexpensive and reliable desalination technologies, and defines the thesis objectives. Some attention is also given to the most used distillation technologies, especially vapour compression distillation.

1.1 Background

All terrestrial species, including humans, depend heavily on fresh water. Humans use water for different basic purposes, such as drinking, cooking, washing and sanitation. Human development and civilization requires a reliable supply of fresh water. However, the amount of *non-saline* water available on earth is less than 3% of the water on earth [1] - much of it locked up in glaciers and ice sheets.

As living standards develop, water consumption increases. The demand for potable water is increasing however, not only because of rising domestic and urban consumption but also to meet the needs of industry & agriculture. The improvement of living conditions is slow or is not happening in many "developing" countries. In these countries a considerable number of people still lack clean drinking water and have to use contaminated water. According to the World Health Organization, contaminated drinking water is involved in 80% of all human illnesses and diseases (gastroenteritis, dysentery, cholera, and other waterborne diseases) which claim many lives each year.

Fresh water is an essential commodity both for developed and developing countries. The biggest challenge many countries are facing is to ensure that enough water resources are available for future generations. This will require from some countries, especially in water-scarce regions, a reduction of water wastage and a better water conservation strategy.

The demand for potable water due to the rapid increase of world population, the rising domestic consumption, and increasing needs of the industry and irrigation, cannot be fully

satisfied by the natural sources of water supply (e.g. rain, rivers). Therefore other means of water production have to be found to supplement these natural sources. Several attempts have been made to solve this problem through better water conservation and demand management or by building more, costly dams. The increasing population and increasing *per capita* consumption cannot in the long run be satisfied by these measures alone.

An alternative way to supplement water for human consumption is the artificial desalination of seawater. Due to technological improvements, desalinated seawater is becoming more and more viable as an alternative water source for many applications, and in many regions.

Thus by the end of 2001, a total of 15, 233 large desalinating plants (each over 100 m^3 per plant) had been installed or contracted over the previous decades, with a total capacity of 32.4 million cubic metres per day [4]. This represents a *doubling in world desalination capacity* - **in less than 24 months!** In the same 2 years, the *seawater desalination capacity grew by 140%!*

Saudi Arabia (18.7%), the USA (15.8%) and the United Arab Emirates (14.6%), had the biggest share of the total desalination capacity [4].

Desalination of seawater is at present the major source of potable water in arid coastal regions such as the Arabian Gulf region. Most of the countries there rely to a large extent on desalination in order to supply their increasing fresh water requirement.

1.2 Thesis Objectives

This thesis describes research in the field of desalination for the production of potable water: Vapour compression distillation (VCD) using thin high density polyethylene (HDPE) and polypropylene (PP) film heat transfer elements in a laboratory model. The aim is to design, build and test this model desalinator.

The model is to enable us to:

- ✦ understand and improve the energy efficiency of a desalinator by using air mattress-

like polymer heat transfer elements instead of metal heat transfer tubes.

- develop methods to further increase the energy efficiency of the model.

The activities carried out for the accomplishment of the specific objectives are listed in chapter 2.

1.3 Desalination Technologies

Over the past century several processes have been developed for desalination, including evaporative processes (distillation), reverse osmosis, electrodialysis, freezing, and other crystallization processes. Some of these processes are of no economical importance. At present, developments concentrate on three general processes, namely, membrane processes, crystallization and distillation.

In the membrane processes, (reverse osmosis and electrodialysis), desalination occurs without phase change.

In reverse osmosis, saline water is forced under high pressure through a semi-permeable membrane which allows mainly fresh water to penetrate. It was originally applied to desalination of brackish water but successive developments have shown its viability for desalination of seawater.

Electrodialysis uses an electric field placed across the membranes to move salt ions out of the solution via the membranes. It is mainly applied for desalination of water sources with low salinity (due to energy required with increasing salt content) sometimes in the presence of hydrocarbons or clathrates.

Crystallization is characterized by phase change from liquid to solid. The obtained ice crystals contain pure water. However, brine clings to the surface of the ice crystals, and the needed washing with pure water makes the process inefficient.

Distillation is the oldest method of desalination. It was employed for the first time over 400 years ago [7] for production of fresh water from seawater. Modern distillation includes three processes: multi-effect distillation (MED), multistage flash distillation

(MSF), and vapour compression distillation (VCD).

All traditional desalination systems do have some constraints: high energy consumption, high initial cost, corrosion and scaling of the heat transfer surfaces. In the following sections the three distillation processes are described.

1.3.1 Multi-Effect Distillation

Multi-effect distillation (MED) was developed around 1900 in replacement of the existing simple stills (single effect) used over centuries. The single effect stills were *bulky* and *inefficient* due to factors such as high energy consumption due to the high heat of evaporation of water, severe scaling, and the carry-over of saline droplets into the distillate. The introduction of the multi-effect (MSF) process reduced scaling - which can be very efficiently managed in this process today [14,15]. Later the change from pool boiling to film boiling (in MED and VCD) enabled a much lower ΔT and a more or less proportional decrease in primary energy consumption.

Distillation involves evaporation of saline water, followed by condensation of the vapour, in which nearly all of the heat of evaporation can be recovered – at a lower temperature. In a simple (single effect) still, the heat of condensation is rejected to the environment by a cooling system.

In a multi-effect system, however, the heat of condensation is used to evaporate more saline water at a lower temperature. Figure 1.1 illustrates, in a schematic way, the principle of MED. Steam at 60°C in the leftmost chamber flows (arrows), condenses (dotted line) on a thin heat transfer surface (single solid line) and gives up heat of condensation, which passes through the surface to its cooler side. Saline water (dashed) trickling down as a film on this cooler side of the surface receives the heat, and is partly evaporated to form more vapour at say 58°C. This vapour flows (arrows) and condenses (dotted) on the next heat transfer surface, causing more (dashed) saline water to evaporate on its opposite side. Condensed vapour (dotted) collects as pure water (distillate – honeycomb) on the left of the heat transfer surfaces, and concentrate brine (dashed) on theright. In this simplified diagram, each chamber represents an "effect". The multi-effect distillation technology has been applied in industry for some decades - for example,

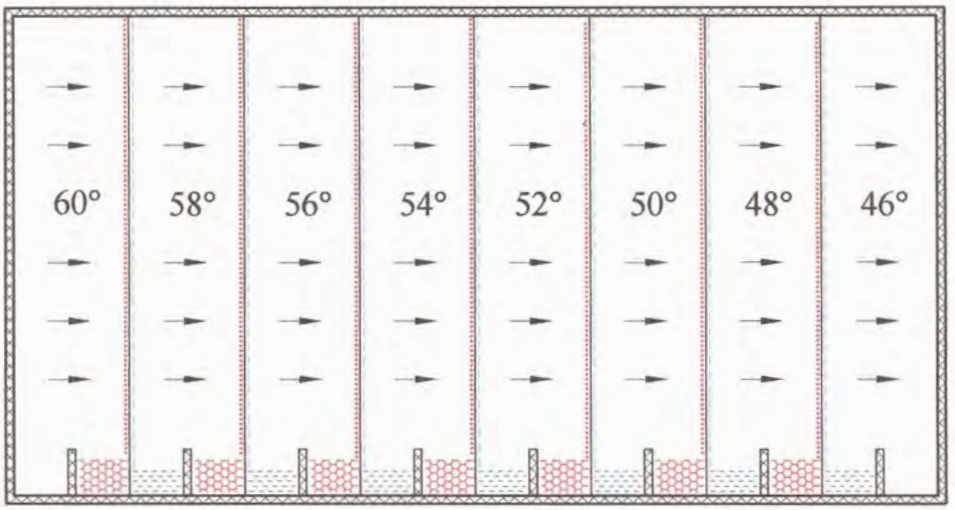

Fig. 1.1 Principle of multi-effect distillation.

in sugar production. Although thermodynamically more efficient than the Multistage Flash (MSF) process, the MED share of total desalination decreased from 1960 to 1998. The reason for its displacement by the simpler MSF process is its relative complexity, and problems with scaling and fouling at high temperatures.

Modern MED systems operate at lower temperature (LTMED) which has contributed to the renewed interest in this process. The operation at low temperature greatly reduces the scaling potential as saline water is kept below the saturation condition for low solubility salts. This also allows the employment of less expensive materials which reduces the capital cost and consequently the water cost.

1.3.2 Multistage Flash Distillation

Multistage flash distillation (MSF) for seawater desalination was proposed in the early 1950's by Prof. R.S. Silver as an alternative to overcome scaling problems affecting the heat transfer surfaces of MED units. As result of its "*morphological simplicity*" [6] MSF soon became the dominant desalination process for production of fresh water from seawater. 43.5% of world's seawater desalination is by multi-stage flash distillation [4].

Figure 1.2 shows the conceptual design of a MSF process. MSF technology uses steam as its primary energy source. The saline water is pumped through all stages in succession, where it is preheated by vapour condensing on outer tube surface. The condensation of external steam in the brine heater further heats this preheated water to just below its

boiling point. It then enters the first evaporation chamber (stage) at reduced pressure. This, results in flash boiling of part of the raw water.

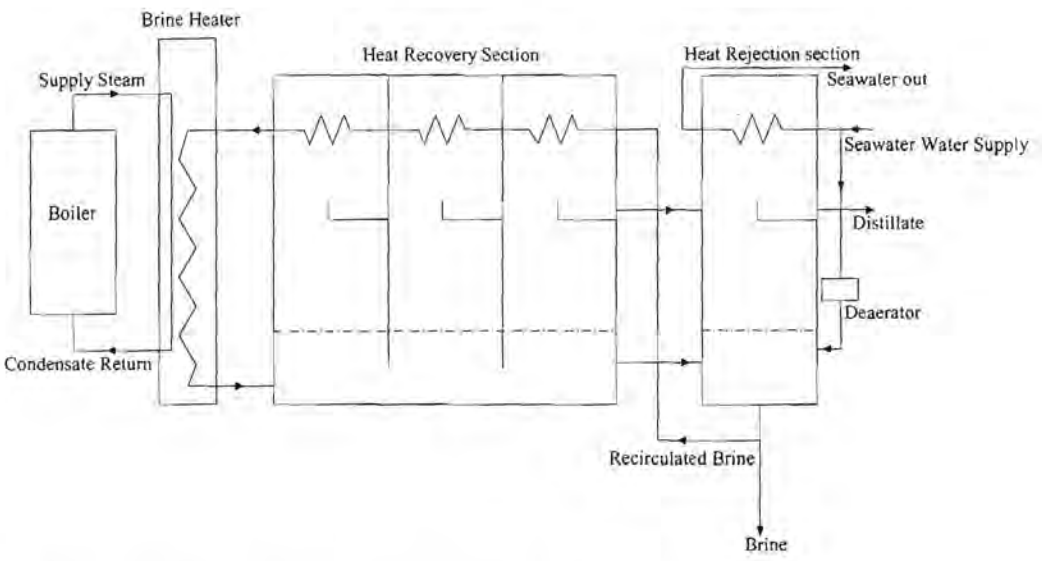

Fig. 1.2 Simplified flow diagram of multistage flash distillation.

Consequently, vapour is released in quantity in striving for equilibrium with conditions of the stage. It then condenses on the outer surface of the stage tubes. Both the condensate and the unevaporated brine flow into the next stage. More vapour is produced from the brine due to the drop in pressure in the stage. The process repeats itself in the remaining stages resulting in the production of more distillate. The condensate produced in all stages is collected and the concentrated brine is discharged before being used in the pre-heating of further incoming raw water.

The energy efficiency (G O R or performance ratio R) of a MSF plant depends on the *ratio* of the overall temperature range ΔT_{ov} to the typical (log mean) temperature difference ΔT_{l} between the flashing brine and the saline water being heated in the tubes [10]. If the number of stages is too small, this will negatively affect either R or the productivity of the still.

1.3.3 Vapor Compression Distillation

1.3.3.1 Historical Perspective

Vapour compression distillation (VCD) technology was developed by the military during

World War II to improve fuel efficiency. It is the most thermodynamically energy efficient single-purpose distillation process. It takes two forms: thermal (TVC) and mechanical (MVC). The former process uses a supersonic jet from high-pressure steam to drive an ejector (thermocompressor) to compress vapour to a required pressure. The latter compresses vapour using mechanical energy from an electric motor or a diesel engine.

Both configurations operate at low temperature difference between the boiling and the condensing water, thus minimizing the system's energy consumption.

The first VC units employed diesel engines to drive the compressor and operated slightly above atmospheric pressure. Though these units met the urgent need of the military a great deal of maintenance (scale removal, and maintenance of the diesel engines) was required to maintain the desired performance. Diesel units were replaced by electrically driven ones because of their short life under continuous operation conditions. In this way the maintenance needs were reduced, but scale was still affecting the operation of the systems. This problem was overcome with the development of units operating under vacuum. Hence, the operation at lower temperature was possible as it is in most modern vapour compression and multi-effect systems.

Mechanical vapour compression is especially for applications where heat/steam is not readily available, and has so far been used in relatively small units - up to about 1,500 m^3 per day [17].

The mechanical vapour compression (MVC) process is dealt with in more detail in the next section.

1.3.3.2 Basic Functioning Principle of MVC

The basic principle of mechanical vapour compression (MVC) technology is depicted in figure 1.3. Vapour from heated saline water flowing in a thin film on a tube's surface, is compressed by a compressor to a saturation temperature that is 2 to 3°C above the evaporation temperature. This is done to offset the boiling point elevation on the evaporating side and to provide the required small temperature difference for the heat

transfer process [7].

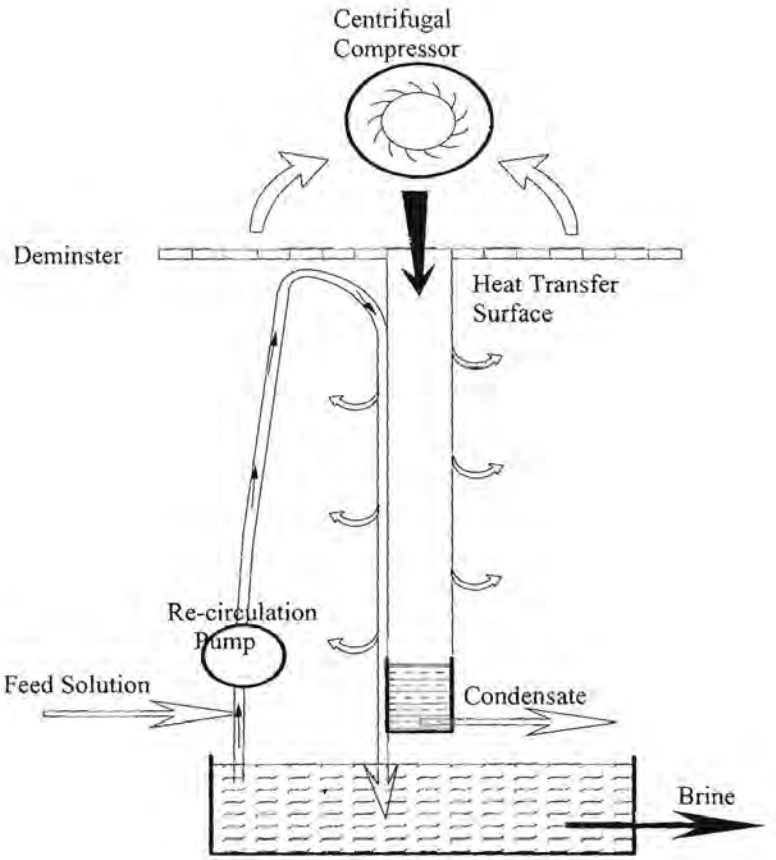

Fig.1.3 Basic principle of vapour compression

The compressed vapour is introduced on the other side of the tubes, where it condenses. The heat of condensation is conducted through the tube wall to the evaporating side, where it provides the heat of evaporation for saline water. The condensate flows downwards and is discharged as distillate. The brine (concentrated saline water) is partly discharged for disposal and the balance mixed with the feed solution. The mixture is pumped again onto the tube surface for further evaporation.

1.3.3.3 Temperature - Entropy Chart

An approximation of the vapour compression process can be represented on the temperature-entropy diagram, depicted in figure 1.4. According to the diagram, evaporation of portion of the feed occurs at constant temperature represented by the line $1' \rightarrowtail 1$.

The obtained vapour is compressed from state point 1 to 2 before condensing along the isobar $2 \rightarrowtail 3$. As a result, distillate is produced along the horizontal line which ends at

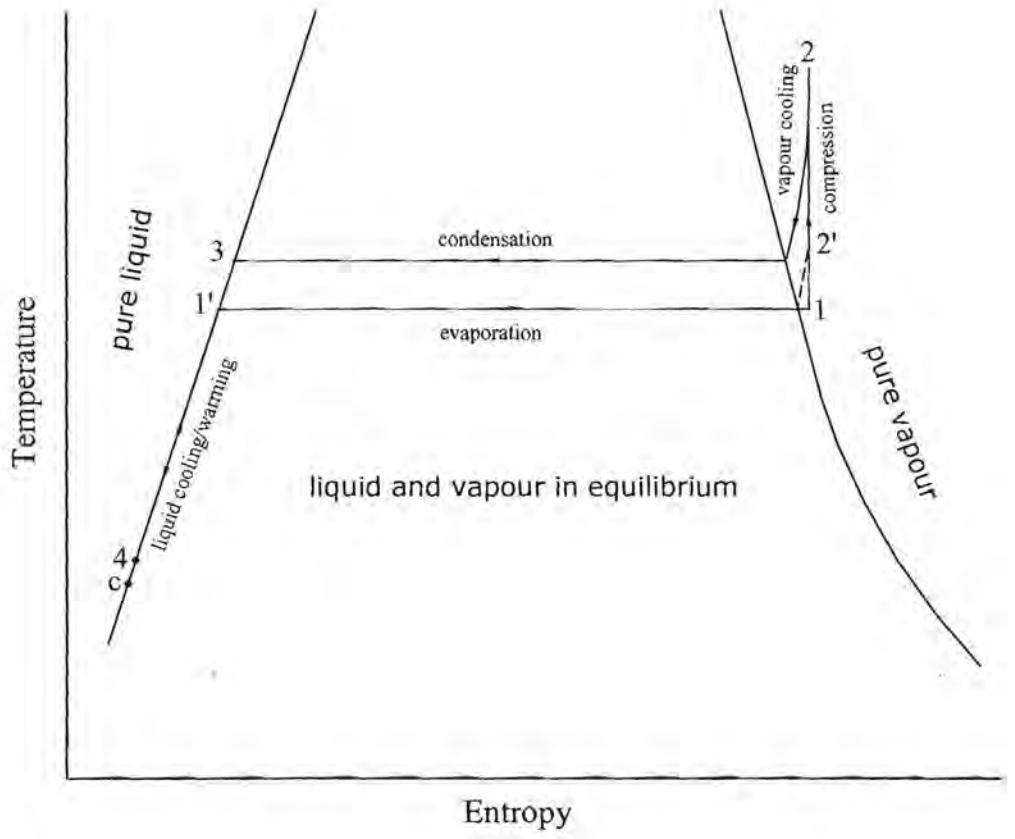

Fig. 1.4 Temperature - entropy chart of vapour compression process [7].

state point 3. The distillate is cooled by passing through a liquid-liquid heat exchanger and discharged at 4. The brine (non-evaporated portion of the feed) passes also through the heat exchanger, thus being cooled in the process, from 1' to 4, and discharged at this temperature. The feed solution enters the heat exchanger at a temperature t_c below that at 4 and is heated to a temperature slightly less than at 1'. The additional temperature required for evaporation (at 1') is provided by the condensation of compressed vapour from the compressor.

The processes are described below using equations and the following is assumed:

(a) the temperature of the feed solution at the evaporator is exactly at 1', instead of being

slightly less than that at 1',

(b) the compression is isentropic,

Then the heat balance on the evaporator is

$$\dot{m}(h_2 - h_3) = \dot{m}(h_1 - h_1') \tag{1.1}$$

where $\dot{m}$ is the production rate and h the specific enthalpy (enthalpy per unit mass).

On the liquid-liquid heat exchanger the heat balance is given by

$$\dot{m}_f c(t_1 - t_c) = \dot{m}c(t_3 - t_4) + \dot{m}(\frac{\dot{m}f}{\dot{m}} - 1)c(t_1 - t_4) \tag{1.2}$$

where $\dot{m}_f$ is the feed supply rate, t the temperature, and c the specific heat. The heat transfer in the evaporator is given by

$$\dot{m}(h_2 - h_3) = UA\Delta t_m = UA(t_3 - t_1) \tag{1.3}$$

where U is the overall heat transfer coefficient, A the area, and Δt_m the mean temperature difference for heat transfer.

The heat transfer in the heat exchanger is

$$\dot{m}_f c(t_1 - t_c) = U_1 A' \Delta t_m' \tag{1.4}$$

Solving the equation (1.2) and assuming that the specific heats are equal, thus

$$t_4 = t_c + (\frac{\dot{m}}{\dot{m}_f})(t_3 - t_1) \tag{1.5}$$

and from the equation (1.3)

$$t_4 = t_c + (\frac{h_2 - h_1}{c}) \tag{1.6}$$

Comparing both equations the relationships

$$c(t_3 - t_1) = h_2 - h_1 \tag{1.7}$$

is obtained. This result certifies that the energy input must equal the sensible heat involved in changing the temperature of water from that of evaporation to that of condensation.

1.4 Implementation of Results

The output of the research will be valuable for the efficient production of fresh water from seawater or brackish water needed in remote communities which experience problems with drinking water supply, such as the Northern Cape, Limpopo, Botswana, Namibia and Mozambique. The improved technology may also be applied in the process of concentrating industrial effluents.

1.5 Summary

Human development and civilization in general require the availability of fresh water at an affordable price. Traditional water supply sources cannot alone satisfy the increasing demand for potable water.

Desalination can supplement the need for fresh water. As a result of wide experience accumulated over many years different desalination processes were developed. Some of the processes are undergoing major improvements required for efficient large scale production of potable water competitively compared with that obtained from the traditional sources. The improvement of the existing designs and the use of better and inexpensive materials can contribute to the reduction of the cost of desalted water which is obstructing the widespread use of desalination. This is where this thesis makes a contribution.

1.6 References

1. M.K. Darwish and Al Gobaisi, *Sustainable Augmentation of Fresh Water Resources through Appropriate Energy and Desalination Technologies*, Proceedings of IDA conference, Madrid, Spain, 1997.

2. H.G. Heitman, *Saline Water Processing: Desaliantion and Treatment of Seawater, Brackish Water, and Industrial Waste Water*, VCH, Weinheim, 1990.

3. Abu Qdyas H. A., *Environmental Impacts of Desalination Plants on the Arabian Gulf"*, Proceedings of IDA conference, Manama, Bahrain, 2002.

4. R Wiseman, *IDA Desalination Inventory: Installed Capacity Doubles in less than two years*, Desalination & Water Re-use 12/3 (2002), p10 – 13, based on the report 17 compiled by K. Wangnick.

5. K. S. Spiegler, *Salt-water Purification*, Plenum Press, New York, 1977.

6. R. S. Silver, *Seawater Desalination*, In: Desalination Technology Ed A Porteous Applied Science Publishers.

7. E. D. Howe, *Fundamentals of Water Desalination*, Marcel Dekker, New York, 1974.

8. A. F. Mills, *Heat and Mass Transfer*, Irwin, Chicago, 1995.

9. C. F. Schutte, *Desalination – a South African Perspective*, Water Research Commission, 1983.

10. A. Porteous, *Saline Water Distillation Process*, Longman, Norfolk, 1975.

11. Hadwaco Brochure, *A Quantum Leap toward Effluent-Free Industrial Plants*.

12. K. S. Spiegler, *Principles of Desalination*, Academic Press, New York, 1980.

13. J. R. Howarth, *Vapour Compression,* In: Desalinaton Technology, A. Porteous, Applied Science Publishers LTD, 1983.

14. H. Glade, *The Carbonate System in MSF Distillers*, Proceedings of IDA conference, Manama, Bahrain, 2002.

15. E. Ghiazza and A. M. Ferro, *The Scaling of Tubes in MSF Evaporators: A Critical Review across 20 Years of Operation Experience,* Proceedings of IDA conference, Manama, Bahrain, 2002.

16. D.I. Dykstra, *Sea Water Desalination by Falling Film Process*, In: Desalination and Ocean Technology, S.N. Levine, Dover publications INC., New York.

17. N. M. Wade, Technical and Economic Evaluation of Distillation and Reverse Osmosis Desalination Process, Desalination 93(1993) 343 - 3633.

List of Symbols

A : heat transfer surface area (m^2)

c : specific heat (J/kgK)

h : enthalpy (J/m)

$\dot{m}$: production rate (kg/s)

$\dot{m}_f$: feed supply rate (kg/s)

t : temperature (C)

U : overall heat transfer coefficient (W/m^2K)

Δt_m : mean temperature difference for heat transfer (K)

2 Reducing the Cost of Desalinated Water: Polymer Film Heat Transfer Elements

2.1 Introduction

In the last decade the use of desalination to provide potable water – competitive in many situations with that supplied by conventional means – has witnessed an astonishing growth. Thus the world capacity increased more than 100% in the 24 months from 1 January 2000 to 31 December 2001 [1]. Over a longer term, the growth of the desalination industry (at about 12% per annum) is still far above the growth in the world economy (about 2.3%) [11].

Distillation technologies (MSF, MED and VCD) have been improved significantly for durability and availability [2, 3, 4, 6]. These technical improvements, as well as new modes of delivering systems (BOO and BOOT – build, own, operate and transfer) have significantly reduced the cost of desalinated water.

To lower the cost of desalination systems, desalination activities in progress in the last years have focussed on system optimization, larger unit sizes, improved construction methods, and use of more suitable materials. The basic processes and the heat transfer mechanisms have remained unaltered.

The total cost of desalinated water are the *capital* and *operational* costs. The capital cost (per m^3 of distillate) depends on the total capital cost/unit capacity and the system life-time. The latter is confidently predicted [2, 6] to be about 40 years for currently installed state-of-the-art systems with shells of solid duplex stainless steel. The operating cost comprises energy, maintenance and parts, consumables (mainly antiscalant chemicals), and labour. *The major costs are the capital and the energy costs.* Of the capital, the major parts are 40% for the heat transfer surface and another 40% for the shell [7]. Reference [6] gives 25-35% for the heat transfer surface.

Figure 2.1 shows the qualitative relationship between the installed *thermal conductance*

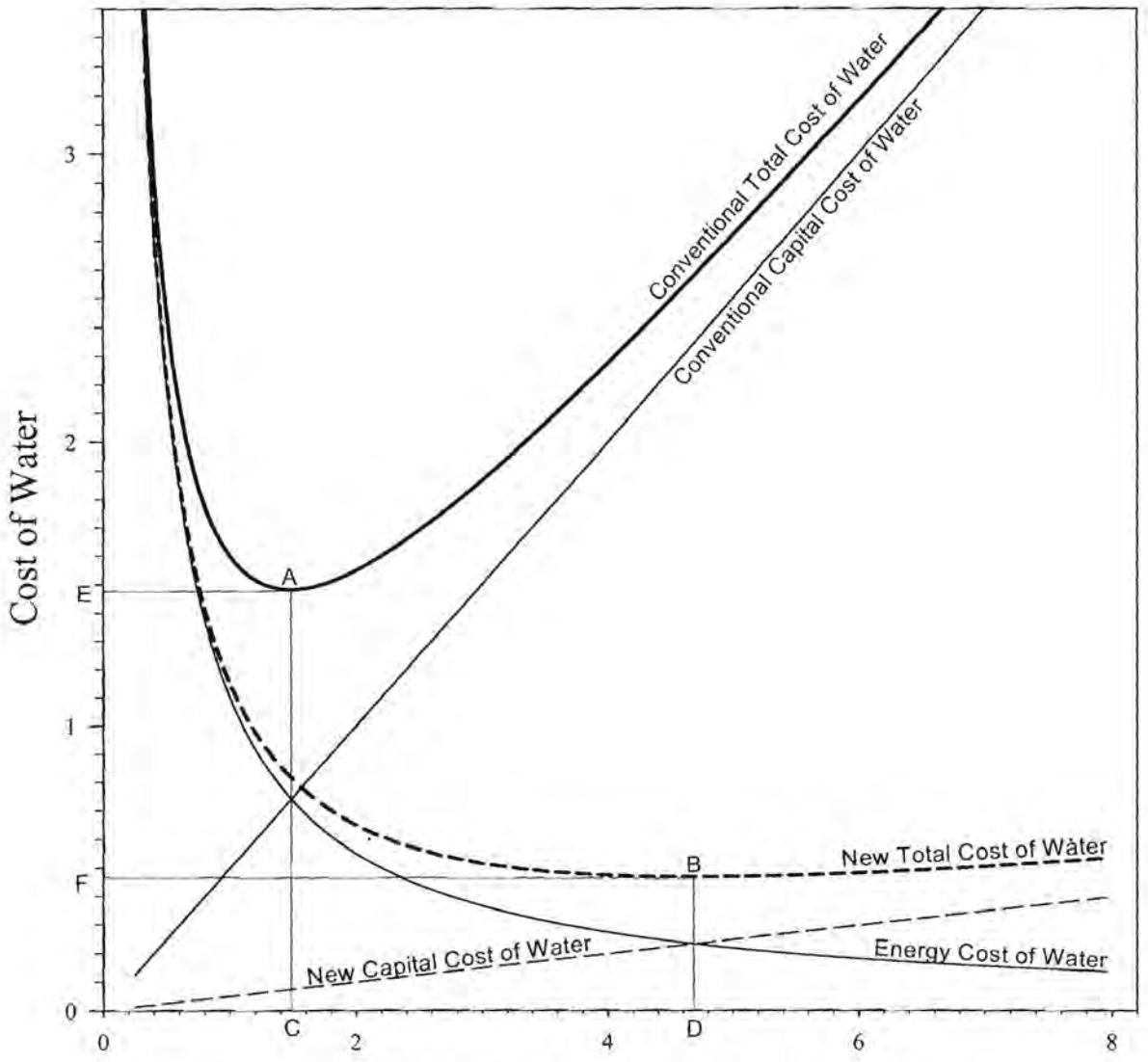

Fig 2.1 Variation of the capital, energy and total cost of desalinated water with the total installed thermal conductance UA. The optimal amount of conductance (point C for the total cost solid curve, and D for dotted one) is that which minimizes the total cost of water. Solid lines are for conventional heat transfer surfaces (high cost per unit conductance). Dashed lines are for thin polymer heat transfer surfaces, where the cost per unit of thermal conductance UA is decreased by more than an order of magnitude. (Of course the cost of the shell will *initially* not show such a dramatic decrease.)

As the unit cost of the conductance decreases, the optimum point A moves down and to the right, to B. More conductance is installed - point C moves to D. The energy consumption and cost decreases, as does the *total* capital cost and the water cost (point E moves to F). In the simplest model: if the *total* capital cost per unit conductance should *decrease* by a factor 10, the energy use, the total capital cost and the cost of water will all *decrease* by a factor of about 3 (=$\sqrt{10}$). The optimal *amount* of conductance will *increase* by this factor (but its *cost will decrease* by the same factor).

We believe that - with a suitable decrease in the cost of the vacuum vessel (shell) - such a decrease is possible. The *decreased cost of the shell* is expected to be the result of further technological improvements due to the sustained growth of the desalination industry, which itself is (and will remain to be) the result of the sustained growth in the demand for potable water.

(UA value) and the energy, capital and total cost of water from a seawater desalination plant after Howe [5]. With increasing conductance UA the energy cost decreases, while the capital cost increases. The *optimum conductance* is where the *total water cost* is a minimum.

Conventional aluminium brass and cupronickel are expensive materials. Yet an annual corrosion allowance of about 25-50μ must be made for these materials [2], even when flow velocities are *below* 2.1 m/s for AlBr, and *below* 4.0 m/s for 70/30 CuNi. Titanium is even more expensive (about $25/kg), but due to the absence of measurable corrosion or erosion in heat transfer or desalination service [2], it can be used in thinner walls. It is also used in erosive flows – e g in flashing flow, and in the top rows of a horizontal tube MED or VCD, where impingement on CuNi and AlBr causes erosive corrosion.

Both high density polyethylene (HDPE) and polypropylene (PP) resist *ionic corrosion* [12] as well as titanium does, and are commonly used to store and transport the most corrosive chemicals – including strong acids, bases and salts. They also show many times the *abrasion resistance* of steel in a Taber abrasion test [12], and may therefore be expected to have excellent resistance against erosive flows.

Their flexibility and elasticity can be used to counter the *adherence of scale* on surfaces treated for wettability. Untreated surfaces possess a well-known anti-stick property [13] which unfortunately is lost when the surface is made wettable.

The *upper brine temperature* of VCD and MED stills have been decreased in the last 2 decades, to reduce the scaling potential. At these lower temperatures (generally below 65°C) the polyolefins (HDPE and especially PP) retain sufficient strength. Also, when they are suitably stabilized, their free radical mediated oxidation does not present a too serious problem at these temperatures.

Heat transfer elements made from *thin* HDPE or PP film (below 60μ) have a calculated *overall heat transfer coefficient* (U value) that is comparable to that of CuNi or Ti metal tubes, but cost far less. See figure 2.2. Thus the material cost per unit conductance is 3 orders of magnitude below that of 0.6 mm titanium. Such low cost per unit conductance

allows the use of more conductance, which reduces the energy consumption, and the total water cost at the optimal point A. Figure 2.1 also shows the effect of reducing the capital (thermal conductance plus accompanying shell) cost – on both the vertical and horizontal position of the optimum (minimum of the total water cost). And on the energy use at this optimal point A, which now moves to B.

Vapour compression stills using heat transfer elements made from such thin polymer film has been used successfully for a decade in VCD units in several countries for the treatment of chemically aggressive industrial effluent and landfill leachate [8]. Their energy consumption is about 9 kWh/m^3 of distillate [8], against about 24 kWh/m^3 for a comparably sized VCD with titanium heat transfer tubes.

The design of these novel units exhibit much ingenuity. Yet with such a new type of technology, we have reason to believe that this design can be further improved on, to give an even lower water cost and energy consumption [10].

The objective of this thesis is a very ambitious one – to design, build and test such an improved distillation system, that would reduce both energy use and capital cost. To understand the scope of the challenge, it should be taken into account that our budget – below €100 000 – was truly modest compared to the €20 million grant that the developers of the competing system received [15]. Thus we had to undertake many tasks which otherwise might have been out sourced. Without support from the Mechanical and Electrical Workshops of the Physics Department, this would not have been possible

We:

(a) conducted an extensive patent search, in which over 3000 (mainly US) patents were briefly examined (abstracts), about 500 with their drawings, and a smaller number in detail.

(b) identified where the existing thin polymer film desalination technology can be improved on (vapour flow resistance).

(c) designed suitable novel polymer heat transfer elements (hte's).

(d) designed vapour flow manifolds, and the mode of affixing the hte's to them. Had the needed manifolds etc specially made.

(e) designed and built saline water distributing and distillate collecting manifolds.

(f) designed, built, tested and improved many apparatuses for fabricating the polymer film heat transfer elements by welding

(g) designed, contracted, tested and refurbished the sealing surfaces of a 400 mm diameter, 3 m tall vertical vacuum shell of 3 mm carbon steel, with external steel ring reinforcement welded on. With 5 large windows to check the wetting of the originally *hydrophobic* polymer film hte's. Despite the dire warnings of an engineer, it has not collapsed when evacuated. However, the sump (from 20mm PVC) imploded, and was replaced with one made of stainless steel. Thermally insulated this vessel.

(h) specified, co-designed, contracted, waited 2 years for and – after many trials and tribulations – and design changes – eventually successfully tested a turbo-compressor, with a specially made high speed water cooled rotary vacuum seal, specially made (in Germany) high speed ceramic bearings and a special high speed belt drive.

(i) had the hydrophobic polymer film hte's treated for wettability *via* oxyfluorination and through a process of sulfonation of which we were the initiators in South Africa (where others are now also using this process for the surface treatment of polymers). Test rigs were built to evaluate the suitability of the treated film for desalination, which requires a *water film* to cover the entire outer surface of the *polymer* film heat transfer element. The results from this testing were correlated with those from contact angle measurement.

(j) assembled the VCD, and successfully tested the integrity of the vacuum system. In addition to the items already mentioned, this required a specially designed and built feedwater heater, pneumatically operated diaphragm pumps for brine recirculation and for distillate extraction, a vacuum pump, and a small plate heat exchanger serving as condenser (cooled with ice water) to protect the vacuum pump from excessive moisture.

2.2 Polymer Heat Transfer Elements

Figure 2.2 shows the calculated variation of overall heat transfer coefficient U in multi-effect distillation with the wall thickness t for a variety of metals and polymers.

The combined effect of evaporative and condensing heat transfer coefficients (plus fouling) was estimated to be about 4400 W/m^{2}K. Despite being poor thermal conductors, polymers of 15-50μ thickness show U-values that are about 60-100% of the value for

titanium or cupronickel used at their traditional thickness (dictated by their rate of corrosion).

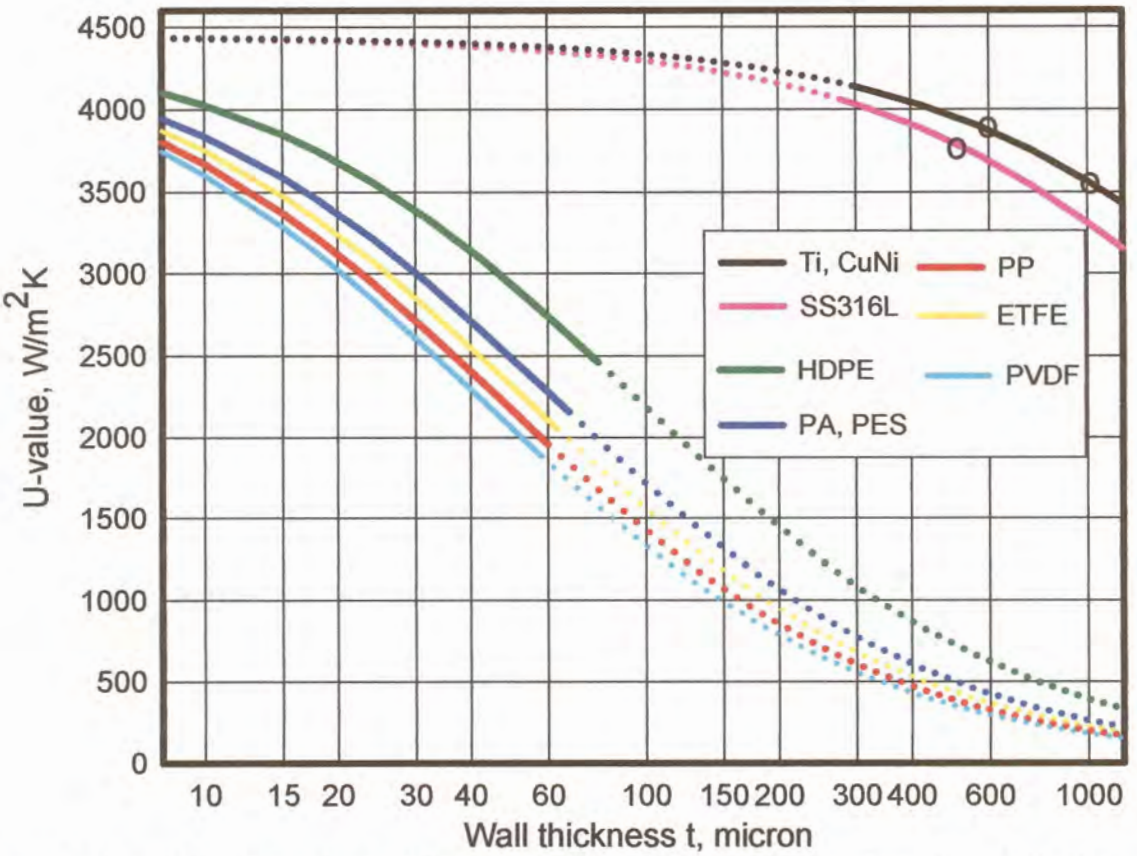

Fig. 2.2 Overall heat transfer coefficients U in MED or VCD as function of wall thickness t for some metallic and polymeric materials. Calculated from $1/U = 1/h_c + 1/h_e + f + t/k$, with the sum of the first 3 terms on the right = 1/(4400) m^2K/W. PA = polyamide, PES = polyester, PVDF = poly(vinylidene fluoride), ETFE = poly(ethylene-tetrafluorethylene).

Thus titanium has normally been used 0.6mm thick, cupro-nickel 1-1.2mm and the rarely used 316L stainless steel 0.5mm. Polyolefins can be used below 30µ. Thus 40µ polyethylene (HDPE) or 20µ polypropylene (PP) give U-values of 3150 – 82 % of the value of 600µ titanium (Ti – 3850 W/m^2K). The material cost of 20µPP is a factor 1000 below that of 600µ titanium. This allows lower energy, capital and maintenance (corrosion & scale) cost. 14µ HDPE gives a U-value *equal to* the value of 600µ titanium.

2.3 Coaxial Helical Polymer Tube Condenser for Multi-stage Flash Distillation – an early project

Multistage flash distillation (MSF) has been the most used distillation process in large scale seawater desalination. For best energy efficiency and best heat exchange efficiency, among others, the number of stages required has to be very high (about 200 stages). Such

a large number of stages required for best energy efficiency presents a limitation to the application of MSF.

Therefore we proposed a modification to conventional MSF. Thin walled (0.5 mm) extruded HDPE tubes were to be used instead of metals as heat transfer surface. The number of stages was to be drastically reduced without sacrifice of the energy or heat exchange efficiency by creating a continuous controllable counterflow temperature gradient within each condenser stage. The vapour flow resistance in each condenser was to be adapted for establishing and maintaining a continuous gradient of saturated vapour pressure, and hence of vapour temperature. Thus, the stage to stage vapour temperature was to be eliminated.

A series of (vertical axis) coaxial helices of HDPE/PP tubing was to form the counter flow condenser. The brine was to flow inside each tube in an upward helical path, while the water vapour and the condensate were to flow outside the tube in a downward direction. With this arrangement, the counter flow nature of the overall flow between the brine and the water was combined with the cross flow nature at local level. The former effect was to maintain an approximately constant temperature difference thus promoting an even and efficient use of the heat transfer surface. The latter effect enhanced the vapour-to-tube heat transfer by generating frequent changes in the vapour flow direction around the tubes.

Using well known formulae from the literature for flow across tube banks the flow resistance in the vapour phase was engineered. The optimal inter-tube spacing and the pressure drop in different parts of the condenser as function of various parameters were determined.

The obtained inter-tube spacing was extremely small and varied along the length of a helix – being smallest (±2.8μ) at the high temperature end and much larger (±40μ) at the low temperature end. This was because of the higher required per stage saturated vapour pressure drop at high temperature, and the higher specific vapour volume at low temperature.

The extreme smallness of the needed inter-tube spacing coupled with the much larger thermal expansion of the diameter of the used tubes caused us to abandon this approach.

2.4 Summary

To further reduce the cost of desalinated water, we develop a vapour compression still with thin film polyolefin (HDPE or PP) heat transfer elements. This will dramatically

reduce the cost of the heat transfer surface – per unit area A, and per unit of conductance. The much lower cost per unit of conductance UA enables the use of more thereof, whereby both the capital and the energy cost of desalinated water will be reduced substantially.

2.5 References

1. K. Wangnick, *2002 IDA Worldwide desalination plants inventory*, Report no. 17.

2. E. Ghiazza and P. Peluffo, *A new design approach to reduce water cost in MSF Evaporators*, Proceedings of IDA conference, Paradise Island, Bahamas, 2003.

3. V. Baujat and T. Bukato, *Research and development towards the increase of MED units capacity,* Proceedings of IDA conference, Paradise Island, Bahamas, 2003.

4. H. Glade, The Carbonate System in MSF Distillers, Proceedings of IDA conference, Manama, Bahrain, 2002.

5. E. D. Howe, *Fundamentals of water desalination*, Marcel Dekker, New York, 1974.

6. C. Sommariva, H. Hogg, and K. Callister, *Forty-year design life: the next target material selection and operating condition in thermal desalination plants*, Desalination 136 (2001) 169-179.

   Also (same authors), *Cost reduction and design lifetime increase in thermal desalination plants: thermodynamic and corrosion resistance combined analysis for heat exchange tube material selection,* Desalination 158 (2003) 17-21.

7. A. Porteus , *Saline Water Distillation Processes*, Longman, London, 1975.

8. Hadwaco brochure, *A quantum leap toward Effluent-Free Industrial Plants*.

9. A. F. Mills, *Heat and Mass Transfer*, Irwin, Chicago, 1995.

10. T B Scheffler, *A cost-effective multi-effect desalinator*, Proceedings of IDA conference, Paradise Island, Bahamas, 2003.

11. A. Macoun, *Alleviating Water Shortages - Lessons from the Middle East*, Desalination & Water Re-use 10/2 (2000) 14 - 20.

12. Hoechst Plastics, *Hostalen*, June 1976.

13. C. Maier and T. Calafut, *Polypropylene: The definitive user's guide and databook*, PDL, New York, 1998.

14. R.S. Silver, *Seawater Desalination:* In Desalination Technology : Developments and Practice, Edited by A. Proteous, Applied Science Publishers, London, 1983.

15. P.R. Koistinen, *Treatment of Industrial Effluents and Landfill Leachates using new low cost Evaporation Technology with Polymeric Heat Transfer Surfaces,* Proc WAT98 - Advanced Wastwater Treatment, Recycling & Reuse. Milan 14-16 September 1998.

3 Flow in a Thin-walled Polymer Tube

3.1 Introduction

In previous chapters we discussed the use of air mattress-like heat transfer elements fabricated from thin flexible high density polyethene (HDPE) and polypropene (PP) film.

In this chapter we show how one may calculate an important design parameter – the diameter of the tubes – as a function of the *fractional* drop $\Delta T_f/\Delta T_1 \equiv 1/R_T$ of the temperature difference along the length of the tubes due to the *frictional* drop Δp_f of the vapour pressure.

We determine the tensile stress in a tube resulting from a pressure difference between the inside and outside of an air mattress-like element, and compare the results with polymer material data [3,4,12].

3.2 Polyolefins (HDPE and PP)

A polymer comprises large molecules – so-called macromolecules. Each of these contains a large number of the same repeating units (monomers) joined by covalent bonds. Synthetic polymers are prepared by polymerization of monomers – which can be by addition or by condensation. The polymerization reaction is mediated by a catalyst [11] and comprises the following stages: initiation, propagation, and termination.

The number n of repeating units is called the *degree of polymerization* (DP).

3.2.1 Polypropene (PP)

Polyprop(yl)ene is a semi-crystalline polymer made by addition polymerization. In the polymerization reaction – in the presence of Ziegler-Natta catalysts – propene molecules are joined together forming a large molecule of polypropene.

$$n CH_2 = CHCH_3 \rightarrow \cdots - [CH_2 - CHCH_3]_n - \cdots$$

Depending on the position of the methyl ($-CH_3$) group on the polymer backbone [9], three possible structures (*stereoisomers*) of PP can be defined:

a) **Isotactic PP:** All methyl groups are located on the same side of the polymer backbone. This is the useful form, which crystallizes in a regular structure, where the pendant methyl groups link adjacent linear chains and imparts good tensile strength and modulus – even at temperatures up to about 100°C. Melting point about 170°C.

b) **Syndiotactic PP:** The methyl groups are alternated regularly between both sides of polymer chain [11].

c) **Atactic PP:** The methyl groups are located randomly with respect to the polymer chain. No crystallinity – an amorphous tarry material.

The catalyst used and the polymerization conditions determine the amounts of isotactic, atactic, and syndiotactic segments in the formulation.

Typical properties of PP are the following:

- low density (about 0.9 g/cm^3)
- good flexibility,
- high stiffness, hardness, and mechanical strength,
- excellent resistance to electrolytes, acids and alkalis.

At high temperatures, in the presence of ultraviolet and ionizing radiation PP decomposes and oxidizes via a free radical chain reaction. The pendant methyl group is especially vulnerable, and is the site of first attack. Stabilizers are added to the melt to counter this degradation. Most are anti-oxidants which act by absorbing free radicals.

3.2.2 High Density Polyethene (HDPE)

High density polyeth(yl)ene is a semi-crystalline plastic developed by Ziegler using low-pressure polymerization. It has a linear molecular structure – with either no branches or a small number of branches – and thus stronger intermolecular forces and more strength than the more branched low density polyeth(yl)ene. In the polymerization process of ethene the double bonds are broken to allow single bonds among the carbon atoms, thus creating a macromolecule – polyethene.

$$n.CH_2 = CH_2 \rightarrow \cdots - [CH_2 - CH_2]_n - \cdots$$

Typical properties of HDPE are:

- low density (0.93 – 0.955 g/cm^3)
- high toughness and tensile strength
- low water absorption
- easily processed and fabricated
- resistant to acids, alkalis, salt solutions, and water
- resistance to temperatures from -50 to 80°C

Special ultra-high molecular mass forms also show resistance to non-polar materials – oils and petrol.

3.3 Optimal Tube Diameter

The diameter of the individual film tubes in an air mattress-like heat transfer element must be carefully chosen, as this choice has important implications for both the capital and the energy cost of a multi-effect or vapour compression desalinator. Thus the choice affects:

(a) the hardware for fabricating the heat transfer elements by multiple line welding.

(b) the design and construction – and cost – of the *entry manifolds for vapour* into the heat transfer elements. A *low vapour flow resistance* is essential for good energy efficiency, and is the primary reason why the existing polymer film desalination technology has only *partly* realized its energy- and capital saving potential.

(c) the *length* of the heat transfer elements that are possible before inner flow resistance to vapour flow in the tubes degrades the energy efficiency. Longer elements will save substantially on the capital cost of the manifolding and of the chambers.

(d) the total size and cost of the *vacuum vessel.* These will be smaller for smaller diameter tubes, which give a higher heat transfer area to vessel volume ratio.

What is needed is a careful balancing/optimization of the capital cost of a smaller vessel, and of longer elements, and of the energy cost benefits of lower flow resistance. For this one needs the pressure drop Δp_f due to the flow as function of:– tube diameter d and length l, temperature difference for heat transfer $\Delta T_1 = \Delta T_0 - \alpha$, overall heat transfer coefficient U; and the density ρ, viscosity μ and enthalpy of condensation L of the vapour.

We now give a simplified derivation of this relation for the case of laminar flow:

Assume

1. *Steady state* operation.
2. The superheat in the vapour is removed. *Saturation* holds inside, and condensation starts at axial position x = 0.
3. *Temperature.* The *outside* temperature T_o is independent of x. *Inside* saturation holds:– the temperature will depend on the vapour pressure p_v, and will decrease when flow resistance causes a decrease in p_v. The temperature difference $\Delta T_1 = T_i(x) - T_o$ between the inside and outside of the tube will also decrease when flow resistance causes a decrease in p_v.
4. The specific volume of the liquid (condensate) is negligible when compared to the vapour. For water at 50°C the respective values are 0.001 and 12 m^3/kg – a ratio of 1 to 12 000. Consequently, for vapour flow we ignore the additional flow resistance due to the presence of the condensate.
5. *Film condensation* inside (as the polymer grade – with a minimum of waxy additives and oligomers – is not *sufficiently* hydrophobic to ensure drop condensation. Dropwise condensation will also not lead to nearly *as* high condensation coefficients with thin polymer film tubes as for metal tubes, where sideways conduction in the wall plays a key role). *Film evaporation* on the outside of the tube, where the surface is treated to make it wettable.
6. The tube *wall thickness t is small* compared to its diameter d: t/d « 1 (3.1a)

   $$\Rightarrow \frac{1}{U} = \frac{1}{h_o} + \frac{1}{h_i} + \frac{t}{k} \qquad (3.1b)$$
7. Because of (3.1a) and the low conductivity of the thin tube wall, we consider only *radial heat conduction* through the tube wall. Also, the very *low axial temperature gradient* further permits us to ignore axial conduction in the wall, in the vapour and in the condensate.
8. All the vapour condenses in a length *l* of tube where the *temperature varies by only 0.1-.5°C.* Therefore the *latent heat* L of condensation, and the *viscosity* μ and *density* ρ of the vapour do not depend on x. Likewise, $\frac{dp_{sat}}{dT}$. The salinity of the brine on the outside tube wall is independent of x.
9. $p_v = p$: *no non-condensibles.*
10. Laminar flow.

A reasonable first approximation is to assume a heat flux and a condensation rate independent of the axial position x. The vapour mass flowrate $\dot{m} = \rho \dot{V}$ will then be a linearly decreasing function of x. From the Poiseuille equation, so will the pressure gradient be. But to simplify the derivation, we first calculated with an $\dot{m}$ that is independent of x, and finally compensated by using (as the mean value) half the value at entrance. The linearity of the Poiseuille equation ensures the correct result from such a simplified procedure.

Heat rate & condensation/evaporation rate

$$\dot{Q} = \mathrm{U}\,\mathrm{A_h}\,\Delta\mathrm{T_l} = U l \pi d \Delta\mathrm{T_l} = \dot{m} L = \rho \dot{V} L \quad \Rightarrow \quad \dot{V} = \frac{U l \pi d \Delta\mathrm{T_l}}{\rho L} \tag{3.2}$$

Poiseuille $$\dot{V} = \frac{\pi R^4}{8\mu}\frac{\Delta p_f}{l} = \frac{\pi d^4}{128 \mu l}\Delta p_f \tag{3.3}$$

Solve (3.3) for Δp_f, and substitute $\dot{V}$ from (3.2): $$\Delta p_f = \frac{128\, U l^2 \Delta\mathrm{T_l}\,\mu}{\rho L\, d^3} \tag{3.4}$$

For U = 2500W/m²K, l = 4m, ΔT_l = 1K, d = .01m, μ from [8] table A4, p702, (3.5)

$$\Delta p_f = \frac{128\times 2500\times 16\times 1\times 1.02\times 10^{-5}}{\rho\times 2.3\times 10^6\times 10^{-6}}\left(\frac{T+273}{293}\right)^{1.15} = \frac{22.7}{\rho}\left(\frac{T+273}{293}\right)^{1.15} \tag{3.4a}$$

Reynolds $$Re = \frac{\rho d v}{\mu} = \frac{\rho d\, 4\dot{V}}{\mu \pi d^2} \overset{(3.2)}{=} \frac{4\, U l \Delta\mathrm{T_l}}{L\mu} = \frac{4\, U l \Delta\mathrm{T_l}}{L\times 1.02\times 10^{-5}}\left(\frac{293}{273+T}\right)^{1.15} \tag{3.6}$$

For the values in (3.4a)& (3.5), $Re = 1705\left(\frac{293}{273+T}\right)^{1.15}$ and the flow is laminar, so that use of Poiseuille's eq (3.3) may be justified. But if $U l \Delta T_l$ should increase more than 35%, this will be a dubious assumption, as the nature of the flow *at the entry to the tube* will then be uncertain (the flow velocity v, like the mass flowrate, will decrease linearly with x).

Let $\Delta p_f = \frac{dp_{sat}}{dT}\cdot\Delta\mathrm{T_f} \equiv p'_{sat}(\mathrm{T})\,\Delta\mathrm{T_f}$, where ΔT_f is the drop in saturation temperature due to the pressure drop Δp_f. With this into eq (3.4),

$$d^3 = \frac{64\, U l^2 \Delta\mathrm{T_l}\,\mu}{\rho L\,\Delta p_f} = \frac{64\,\mu\, U l^2\,\Delta\mathrm{T_l}}{\rho L\; p'_{sat}(\mathrm{T})\;\Delta\mathrm{T_f}} \tag{3.7}$$

will give the design diameter as a function of the parameters mentioned at the outset. To include the linear decrease (to 0) of $\dot{m}$, the factor 128 has been halved. An independent derivation of (3.7) (or of (3.4) with 128 halved) can also be given. It is more complex, and will not be included here.

It appears from the important result (3.7) that the optimal tube diameter depends on the *fractional drop* $\Delta T_f/\Delta T_l$, the ratio between the temperature difference along the length of the tubes due to the *frictional* drop $\Delta p = \Delta p_f$ of the vapour pressure, and the temperature difference between the inside and the outside of the tubes. The derivation (in which ΔT_l is treated as independent of x) is valid as long as this fraction is small. That is, as long as its inverse, the *ratio*

$$R_T = \Delta T_l/\Delta T_f \text{ is } >>1. \tag{3.8}$$

Figures 3.1 - 3.6 show the diameter d calculated from (3.7) for 2, 4 and 8m long 50μ thick polypropene (PP), where according to fig 2.2, U = 2500 W/m² K. Also for similar lengths of 39μ thick polyethene (HDPE), where U = 3200 W/m² K. For values 3, 4, 5, 6, 8 and 10 of the ratio R_T (i.e. for a fractional pressure drop $\Delta p_f/\Delta p_l$ of 1/3, 1/4, 1/5, 1/6, 1/8 and 1/10). For the temperature range (35 - 90°C) relevant for polyolefin film heat transfer elements.

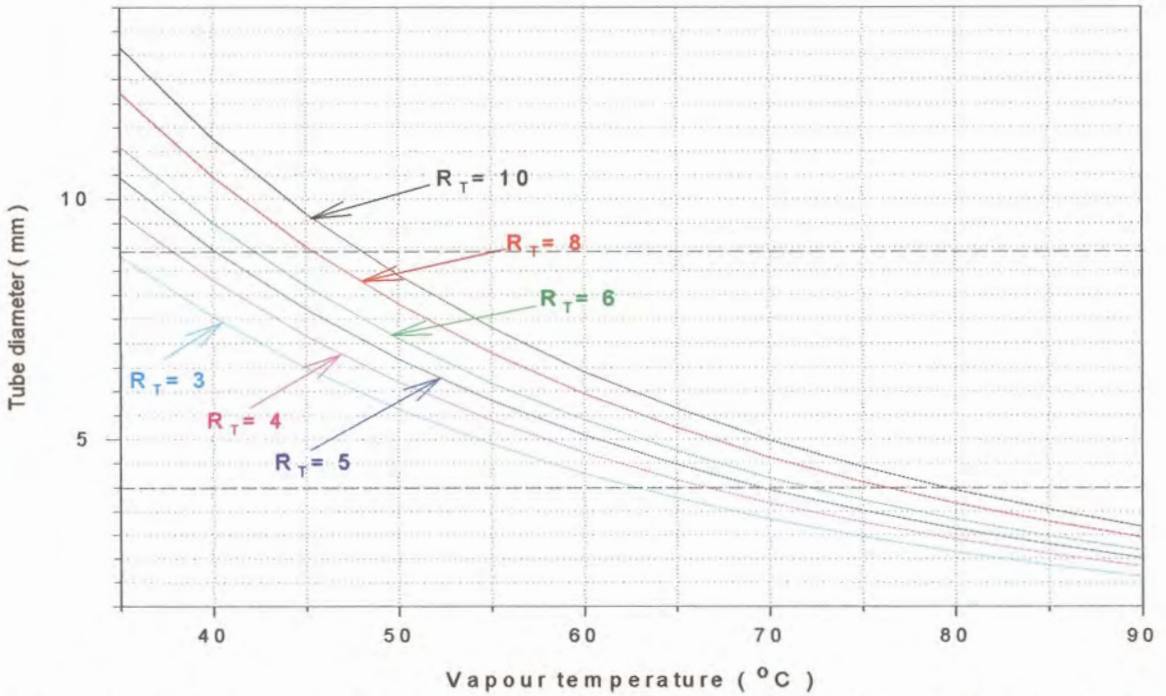

Fig. 3.1 Tube diameter as function of temperature for given ratios R_T (eq.(3.8)). For 2 m long tubes of 50μ thick PP film (U value 2500W/m^{2}K). The dashed horizontal lines indicate tube diameters that can be readily produced by our film welding apparatus.

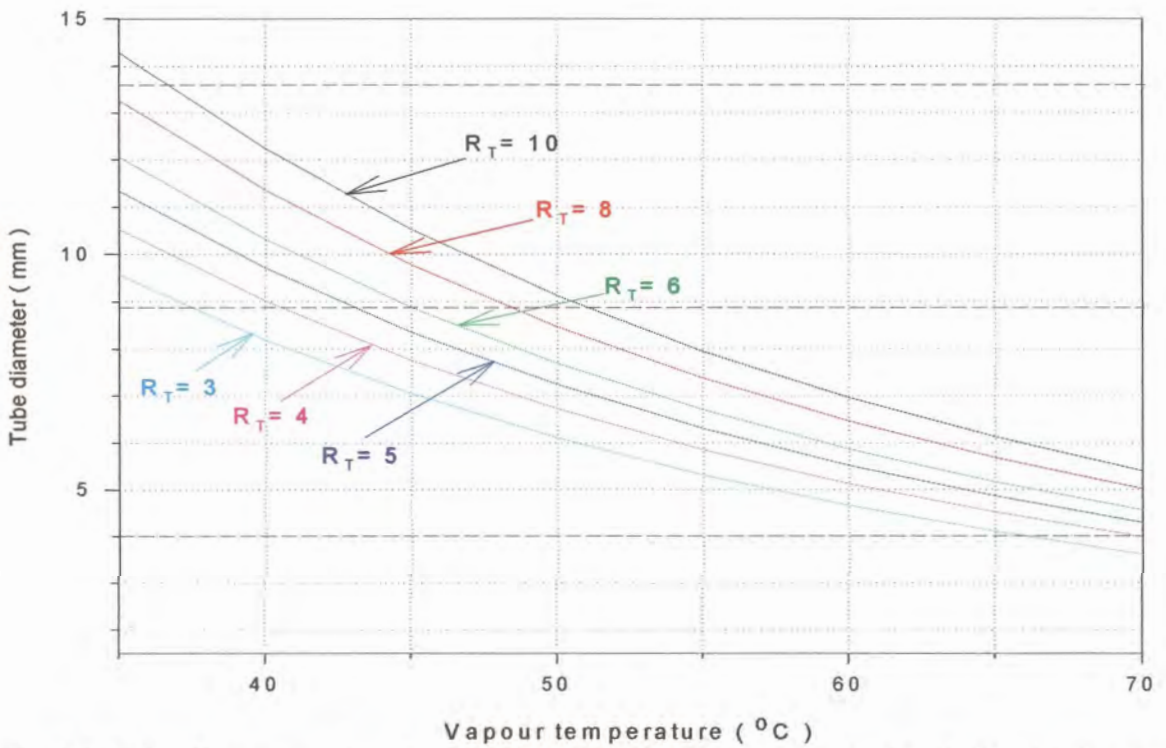

Fig. 3.2 Tube diameter as function of temperature for given ratios R_T (eq.(3.8)). For 2 m long tubes of 39μ thick HDPE film (U value 3200W/m^{2}K).

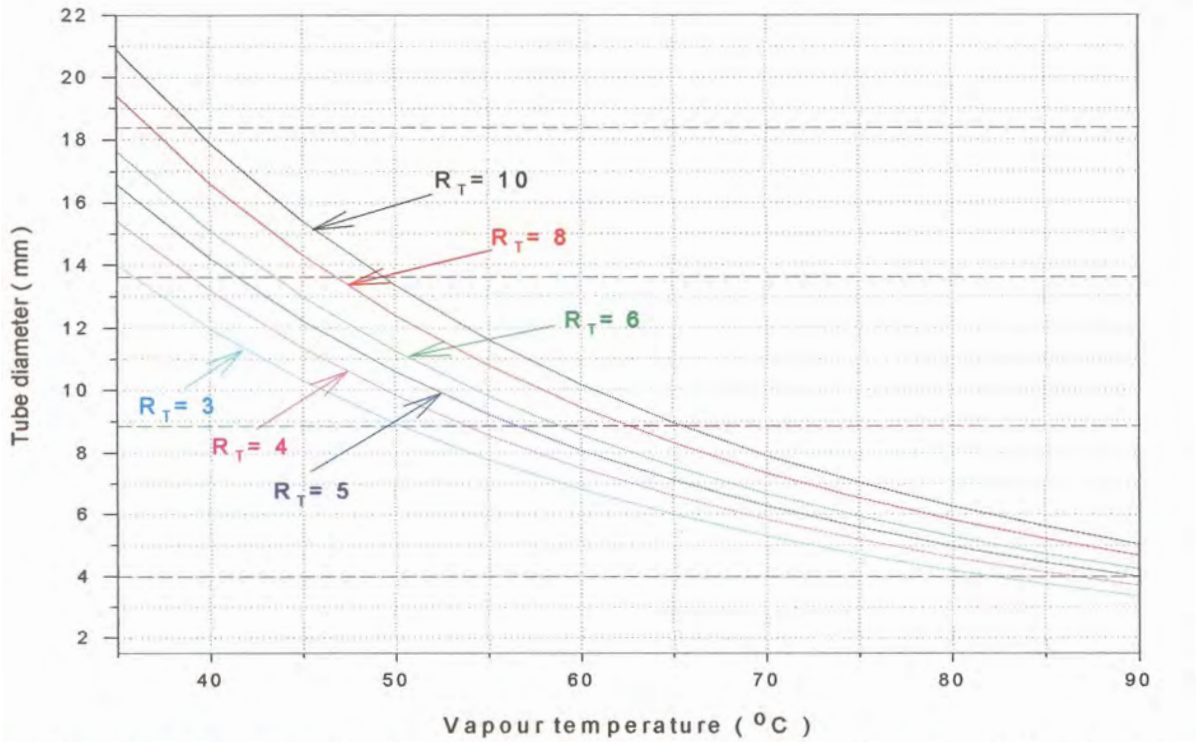

Fig. 3.3 Tube diameter as function of temperature for given ratios R_T (eq.(3.8)). For 4 m long tubes of 50μ thick PP film (U value 2500W/m^{2}K).

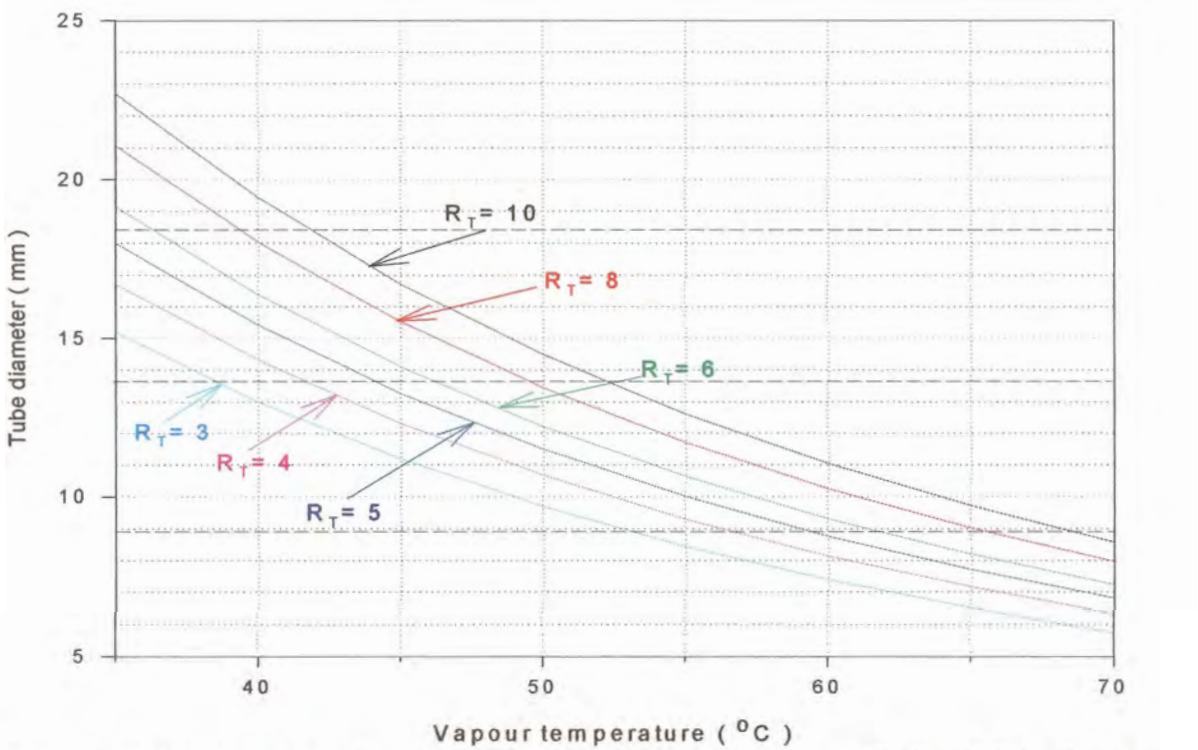

Fig. 3.4 Tube diameter as function of temperature for given ratios R_T (eq.(3.8)). For 4 m long tubes of 39μ thick HDPE film (U value 3200W/m^{2}K).

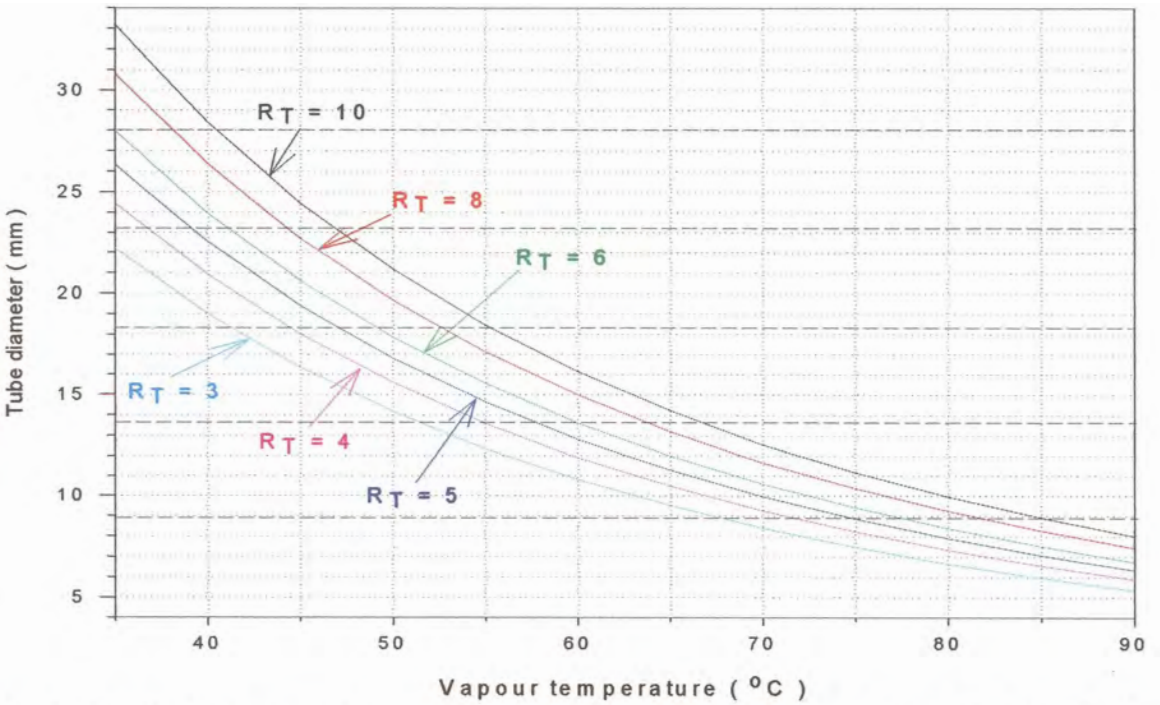

Fig. 3.5 Tube diameter as function of temperature for given ratios R_T (eq.(3.8)). For 8 m long tubes of 50μ thick PP film (U value 2500W/m^{2}K).

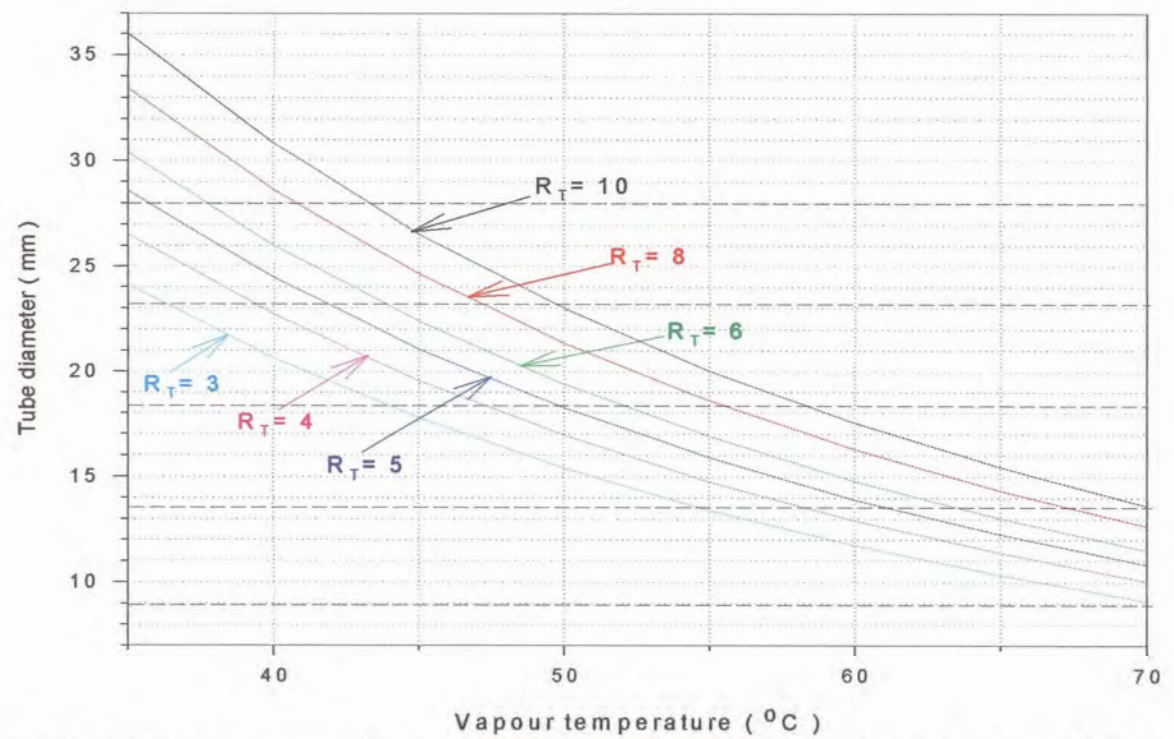

Fig. 3.6 Tube diameter as function of temperature for given ratios R_T (eq.(3.8)). For 8 m long tubes of 39μ thick HDPE film (U value 3200W/m^{2}K).

As seen from these figures, the tube diameter d decreases with increasing temperature T. In eq (3.7) this follows from the dependence $\rho(T)\, p'_{sat}(T)$. The reduction is steeper at lower temperatures. For given T, d decreases with increasing fractional drop in temperature difference, and increases with its inverse – R_T.

3.4 Tensile Stress in Polymer Film Tubes. Creep

Polymers are *visco-elastic* materials. When subjected to an applied stress, they behave partly as fluids of very high viscosity and partly as elastic solids. Thermoplastics, in particular, exhibit a behavior known as *creep* which is the deformation of the material in the course of time under constant load. In all thermoplastics, creep rupture strength falls off as the duration of the applied stress is lengthened. This can happen even at room temperature and under relatively slight load stress.

In quantitative design involving polymers the visco-elastic effects must be considered [8]. In the present case the plastic tube is subjected to a tensile stress σ due to the pressure difference between the saturated vapour (inside) and the lower pressure vapour on the tube's outside surface. This stress acts uniformly in the directions orthogonal to the wall. It induces a tensile strain which depends on the stress as well as the applied time. The tensile stress in a tube of diameter d and wall thickness t under pressure difference Δp is given by

$$\sigma = \frac{\Delta p d}{2t} . \qquad (3.9)$$

The vapour pressure difference Δp between the inside and outside of the polymer film tube includes a term $\Delta p_1 = p'_{sat}(T)\, \Delta T_1$ for the pressure difference needed to create a temperature difference ΔT_1 for heat flow. And another term $\Delta p_{saline} = p'_{sat}(T)\, \alpha$ representing the reduced pressure outside the tube due to the salinity of the evaporating brine. Here α is the boiling point elevation due to the salinity of the evaporating brine. Therefore the total pressure difference Δp in (3.9) is

$$\Delta p = \Delta p_1 + \Delta p_{saline} = p'_{sat}(T)\, \Delta T_0 \qquad (3.10)$$

where $\Delta T_0 = \Delta T_1 + \alpha$ is the per effect temperature difference in a multi-effect plant. In a vapour compression plant Δp is the pressure difference created by the compressor.

The tensile stresses were calculated for the tube diameters corresponding to $R_T = 8$ (a fractional drop in temperature difference of 1/8) – for $\Delta T_0 = 2K$ with 2, 4 and 8 m long 50μ thick PP and 39μ thick HDPE film tubes. According to equations (3.9) and (3.10) the tensile stress – plotted in figure 3.7 – increases with the temperature. This is because the slope p' of the vapour pressure curve increases steeply with T – more than offsetting the reduction of d with increase in T.

The tensile stress values shown in fig 3.7 are below 0.4 MPa. For (a suitable grade of)

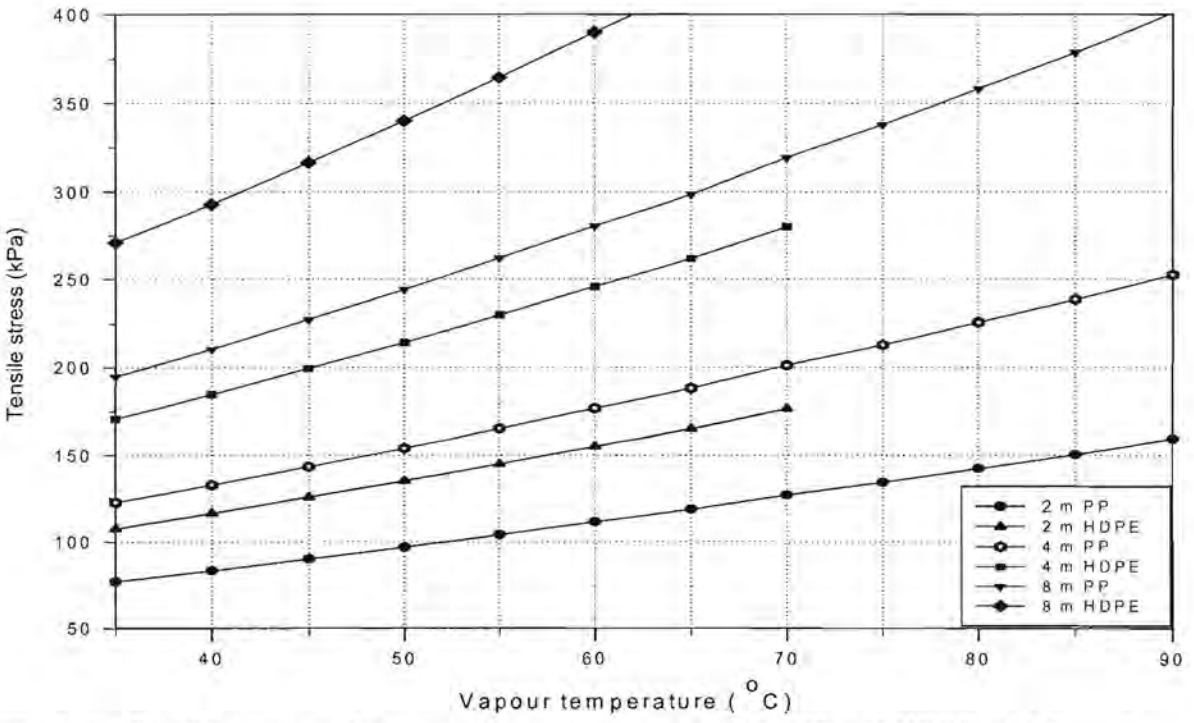

Fig. 3. 7 Tensile stress as function of vapour temperature for PP and HDPE with $R_T = 8$.

polypropylene the creep data [3,12] show that it can handle – with minimal (~ 1%) creep – a tensile stress of 7.7 MPa at 40°C, 5 MPa at 60°C, and about 2MPa at 80°C – for 10 years. At 95 - 100°C it can likewise handle ~ 2 MPa for 1 year. Therefore, polypropylene appears to have sufficient tensile creep strength to be used as film tube material in thicknesses far below the 50μ we have so far considered. Indeed, at 10 or 15μ it would still probably have sufficient creep strength (and a much better U value than at 50μ), if at this low thickness it can still be suitably welded and made wettable. Polyethylene [4] appears able to handle a tensile stress of 3.5 MPa at 40°C for 10 years, and 2.2 MPa at 60°C for 1 year. Extrapolation suggests 0.5 MPa at 60°C for over 10 years.

A good choice will be to choose PP over HDPE above about 60 - 65°C (higher for shorter film tubes, lower for longer ones). If it is deemed best to go to temperatures above 90°C, then it will be best to use a fluoropolymer such as ethylene-tetrafluor-ethylene (ETFE), poly-(vinyl fluoride) (PVF) or poly-(vinylidene fluoride) (PVDF).

An advantage of going above 90°C would be to operate close to atmospheric pressure, which will save on the considerable cost of a vacuum vessel and of vacuum pumps and vacuum pumping. However, one needs also to consider the very substantial extra cost of the more expensive polymers, and of their more expensive wettability treatment.

3.5 Summary

Equation (3.7) (and the figures (3.1) to (3.5)) relate the tube diameter d to temperature and the fractional drop $1/R_T$ in temperature (due to frictional pressure drop). This relation is essential for optimizing the film tube dimensions (length, diameter and thickness) for the air mattress-like heat transfer elements.

The tensile stresses for $R_T = 8$ are below 0.5 MPa for polypropylene (PP), and for HDPE below 65°C . Up to about 60 - 65°C high density polyetylene (HDPE) has sufficient creep strength, and up to about 95°C, PP also has sufficient creep strength to be used as film tube material as described herein.

3.6 References

1. K Wangnick, *Present status of thermal seawater desalination techniques*, Desalination and water Re-use 10/1 (2000) p14-21.
2. C. Hall, *Polymer Materials: An Introduction for Technologist and Scientists*, Macmillan, 1986.
3. Hoechst Plastics, *Hostalen PP*, July 1976, fig. 8.
4. Hoechst Plastics, *Hostalen*, June 1976, fig. 7.
5. A. F. Mills, *Basic Heat and Mass Transfer*, Irwin, Chicago, 1995.
6. S.P. Sukhatme , *A textbook on Heat Transfer*, Orient Longman, Hyderabad India, 1989.
7. R. S. Silver, *Seawater desalination,* In: Desalination Technology Ed A Porteous Applied Science Publishers, 1983.
8. N. G. McCrum, C. P. Buckley, and C. B. Bucknall, *Principles of Polymer Engineering*, Oxford University Press, New York, 1997.
9. F. M. White, *Fluid Mechanics*, McGraw–Hill, New York, 1994.
10. Kirk-Othmer, *Encyclopedia of chemical technology – Nickel and Nickel Alloy to paint*, 4th edition, Volume 17, John Willey & Sons, New York.
11. O. Schwarz, *Polymer Material Handbook*, Translated from German by F.-W Ebeling,

H. Schirber, H. Huberth and N. Schlör, for the Plastics Industry Training Board (PITB), South Africa, 1995.

12. C. Maier and T. Calafut, *Polypropylene: The definitive user's guide and databook*, PDL, New York, 1998.

List of Symbols

A_h : total area for heat transfer (m^2)

d : diameter of heat transfer tube (m)

h_i : condensation coefficient inside film tubes (W/m^2K)

h_o : evaporation coefficient outside film tubes (W/m^2K)

k : conductivity of polymer film heat transfer material (W/mk)

L : enthalpy of evaporation (J/kg)

$\dot{m}$: mass flow rate of vapour (kg/s)

p : pressure of vapour + non-condensible gases (Pa)

p_v : vapour pressure (Pa)

q : heat flux (W/m^2)

$\dot{Q}$: outward heat flow rate through tube wall (W)

R_T : ratio between the temperature difference between the inside and the outside of the tubes, and temperature difference along the length of the tubes due to the *frictional* drop Δp_f of the vapour pressure (-)

t : thickness of polymer film tube wall (m)

T : temperature (K or C)

U : overall heat transfer coefficient (W/m^2K)

v : vapour flow velocity (m/s)

$\dot{V}$: vapour volume flowrate (m^3/s)

x : axial position along tube (m)

α : boiling point elevation of evaporating saline water on outside of tubes (K or C)

Δp : pressure difference between inside and outside of polymer film tubes (Pa)

Δp_f : pressure drop due to friction inside tubes (Pa)

Δp_i : pressure difference needed to create a temperature difference ΔT_i (Pa)

Δp_{saline}: reduced pressure outside the tube due to the salinity of evaporating brine (Pa)

ΔT_1 : temperature difference for heat transfer between condensing vapour and evaporating saline water In- and outside film tubes (K or C)

ΔT_f : decrease in saturation temperature due to vapour flow resistance (K or C)

$\Delta T_o = \Delta T_1 + \alpha$: temperature difference per effect (K or C)

μ : dynamic viscosity of vapour (kg/ms)

ρ : mass density of vapour (kg/m^3)

σ : tensile stress (Pa)

4 Fabrication of Polymer Film Heat Transfer Elements

4.1 Introduction

The use of inexpensive thin corrosion resistant plastic films as heat transfer elements can reduce both the capital costs and the energy requirement of a distillation system [1, 2]. For the film to be able to withstand the vapour pressure difference between the condensing and evaporating sides we fabricated "air mattress" elements – by welding two superposed plastic films (or 2 parts of a folded single film) together along parallel weld lines.

The process of joining thermoplastics using heat and force is named plastic welding [3]. All welding methods have in common three steps – plasticising, joining and cooling. The quality and strength [3] of a thermal weld are determined by an accurate selection of the welding parameters – welding temperature, welding pressure and temperature effect time. The welding temperature permits the plastic to reach the plasticised state. The welding pressure ensures a close bonding of the joining surfaces, and the correct temperature effect time ensures that the heat reaches a sufficient depth in the parts to be joined.

In this chapter we describe the design, building and testing of the welding apparatus.

4.2 Welding Apparatus (Design)

The final version of the thermal impulse indirect welding [3] apparatus used to weld polymer films is shown in figure 4.1. It comprises a smooth and flat block of polished granite (1100 mm x 320 mm x 30 mm) placed on a table. Two layers of a mica composite material were laid on top of the granite block to reduce heat loss to the granite during welding. At each end of the granite is a block of nylon (320 mm x 30 mm x 30 mm) fitted with 40 brass studs of 8mm diameter. Each stud is designed to clamp and hold the end of a flat nichrome ribbon of the type used as heating elements. In the first configuration, as seen in figure 4.2, the welding apparatus had 40 parallel ribbons – each 1140mm long – used as heating elements. They were placed on a sheet of polytetrafluorethylene impregnated fibreglass cloth on top of the mica layers. In the transverse direction the

ribbons were spaced 7.5 mm centre to centre. When assuming perfect flexibility of the film, this setup permits the fabrication of "air mattresses" with tubes of 4.0 mm diameter.

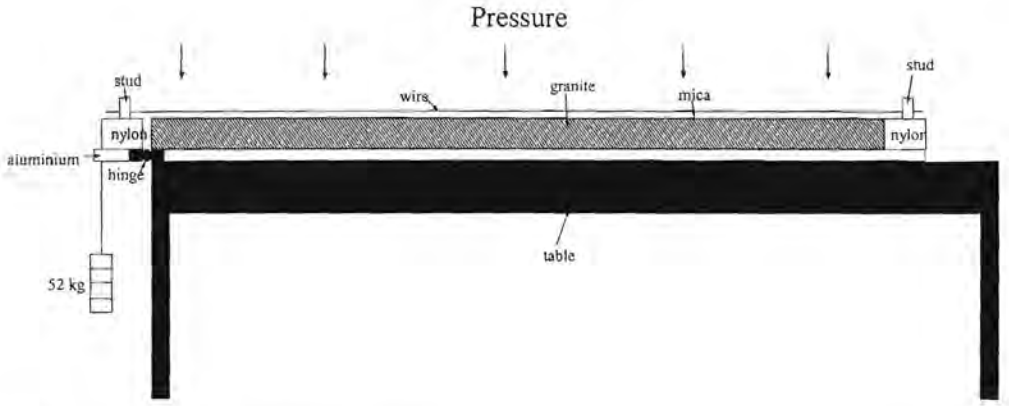

Fig. 4.1 Side view of the welding apparatus.

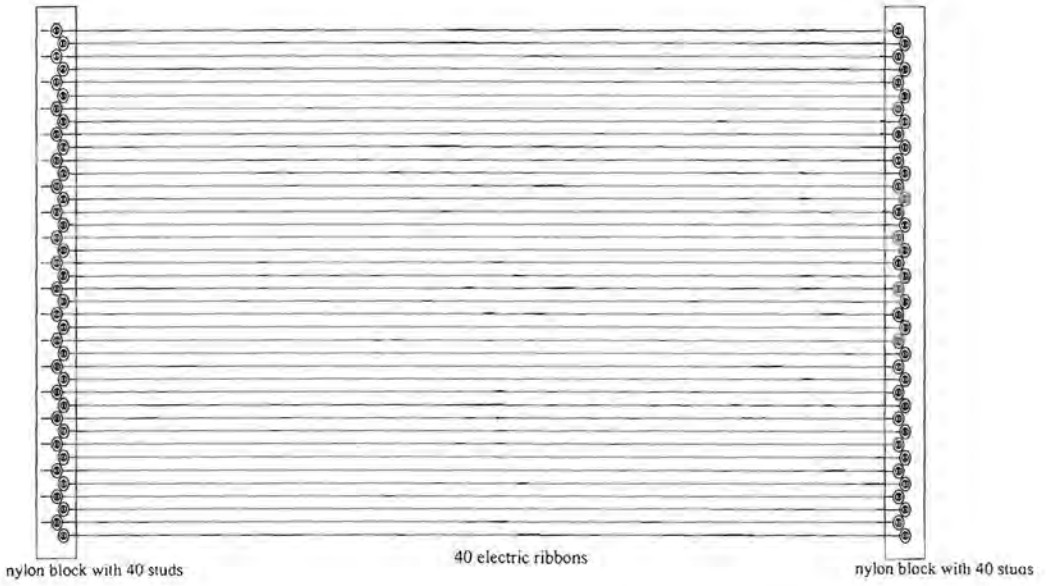

Fig. 4.2 Schematic overview of the first configuration of the welding apparatus with 40 electric heating ribbons. In a later version, only every 4th ribbon was retained.

In later versions the number of ribbons in the apparatus was reduced to 7, 8 or 10. Only every 4th stud was used, so that the new centre to centre spacing was 30 mm, corresponding to "air mattress" tubes of 18.4 mm diameter.

An adapted pocket scale (with its hook replaced by a ribbon clamp) was used to put all ribbons under the same initial tension of 25 N. This procedure was repeated every day welding was carried out.

4.2.1 Heating Elements

For the identification of suitable heating elements to be used in the welding apparatus, round (295, 355 and 560 μ diameter) and flat (794 μ x 254 μ) nichrome wires were tested. Nichrome is a Nickel/Chromium alloy (Ni80%/Cr20%) with a "normal" coefficient of thermal expansion:– $\alpha = 14 \times 10^{-6} K^{-1}$ at 20 - 100°C [8].

The wires – each 1140mm long – were put under variable electrical load in the welding machine to test their weld capability on polypropylene (PP) films of different thicknesses. However the obtained weld lines on the PP films using the round wires were weak. Due to the round shape during welding molten material was squeezed out from the welding zone under the applied pressure. The round wires were therefore excluded and the ribbons were instead adopted as the electrical heating elements for the welding apparatus.

The thermal expansion of the ribbons was of real concern. Thus a practical way to offset the expansion, thereby preventing the ribbons to move sideways and touch one another during welding had to be found. The ribbons were heated with electrical currents from 1 to 5 A. Initially a single ribbon and gradually the number was increased to 3. This was done to establish the effect of the increase of the number of ribbons on the thermal expansion.

Figure 4.3 shows the dependence of the thermal expansion (the mean of two measurements) on the applied power per unit length for the ribbons. As seen from the graph, the thermal expansion increases with the growing electrical heating power. This increase is slightly steeper with a larger number of ribbons. Then the generated heat in a wire contributes not only to its own temperature increase and expansion but also to the temperature increase and thermal expansion of the neighboring ribbons.

In an attempt to use elements with lower coefficient of thermal expansion than nichrome, invar was tested. Invar is a ferromagnetic iron-nickel alloy (64%Fe and 36%Ni) with the

lowest thermal expansion coefficient of its kind (α = 1.7 - 2.0 x $10^{-6}K^{-1}$at 20 - 90°C [8]).

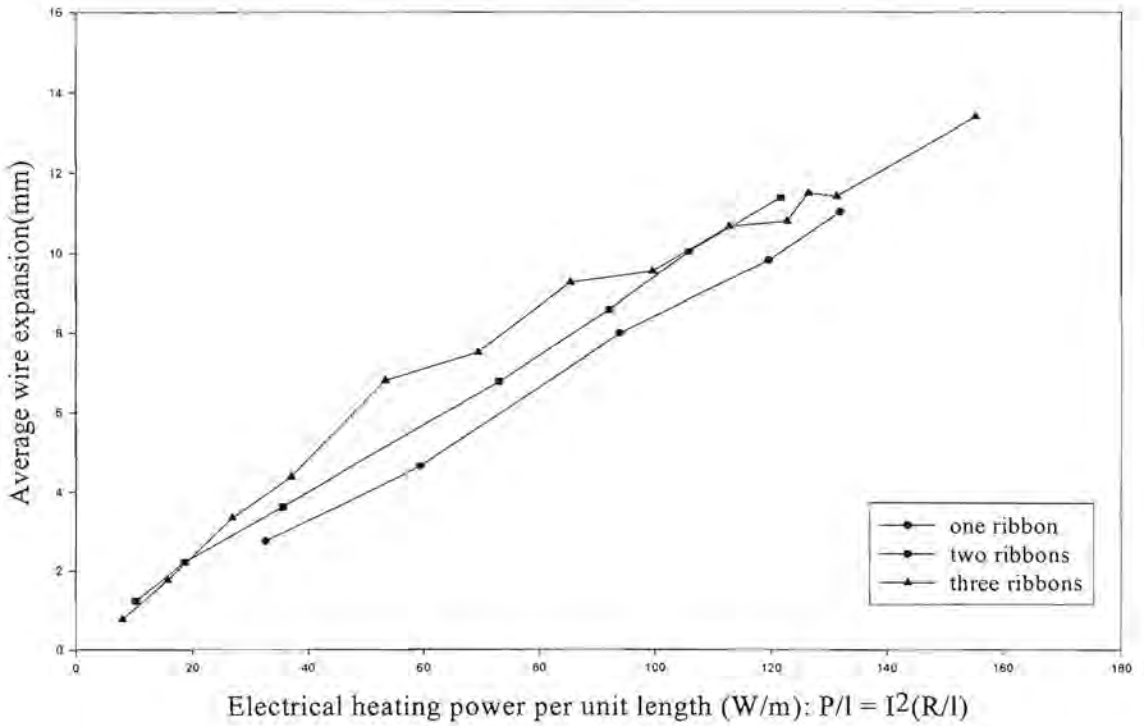

Fig. 4.3 Dependence of thermal ribbon's expansion to the electrical heating power per unit length.

As shown in figure 4.4 invar exhibits a uniform expansion up to near the inflection point – which increases with nickel content. The inflection point is associated with the Curie temperature. Above this temperature the magnetic properties in the material are lost, therefore it expands as much as other metals (slightly more than pure iron – its main constituent).

For welding plastics heat must be transferred from the ribbon to the plastic therefore the ribbons' temperature should be higher than the welding temperature – plasticised state. The used invar ribbons (150μ x.600μ) – specially manufactured for the project – displayed nearly as large thermal expansion as that of nichrome. At a welding current of 2.50A they changed colour due to oxidation. Further attempts at using the oxidized ribbon caused breakage due to embrittlement.

We also thought to use other metals such as molybdenum ($\alpha = 5.1x10^{-6}K^{-1}$) and tungsten

($\alpha = 4.5 \times 10^{-6} K^{-1}$) which have lower thermal expansion than nichrome. However within our budget we could not find ribbons in these materials.

Different approaches were tested to compensate the thermal expansion experienced by the adopted nichrome ribbons. Initially – as shown in figure 4.5 – springs of different strengths were attached to a movable nylon block. The block could slide longitudinally

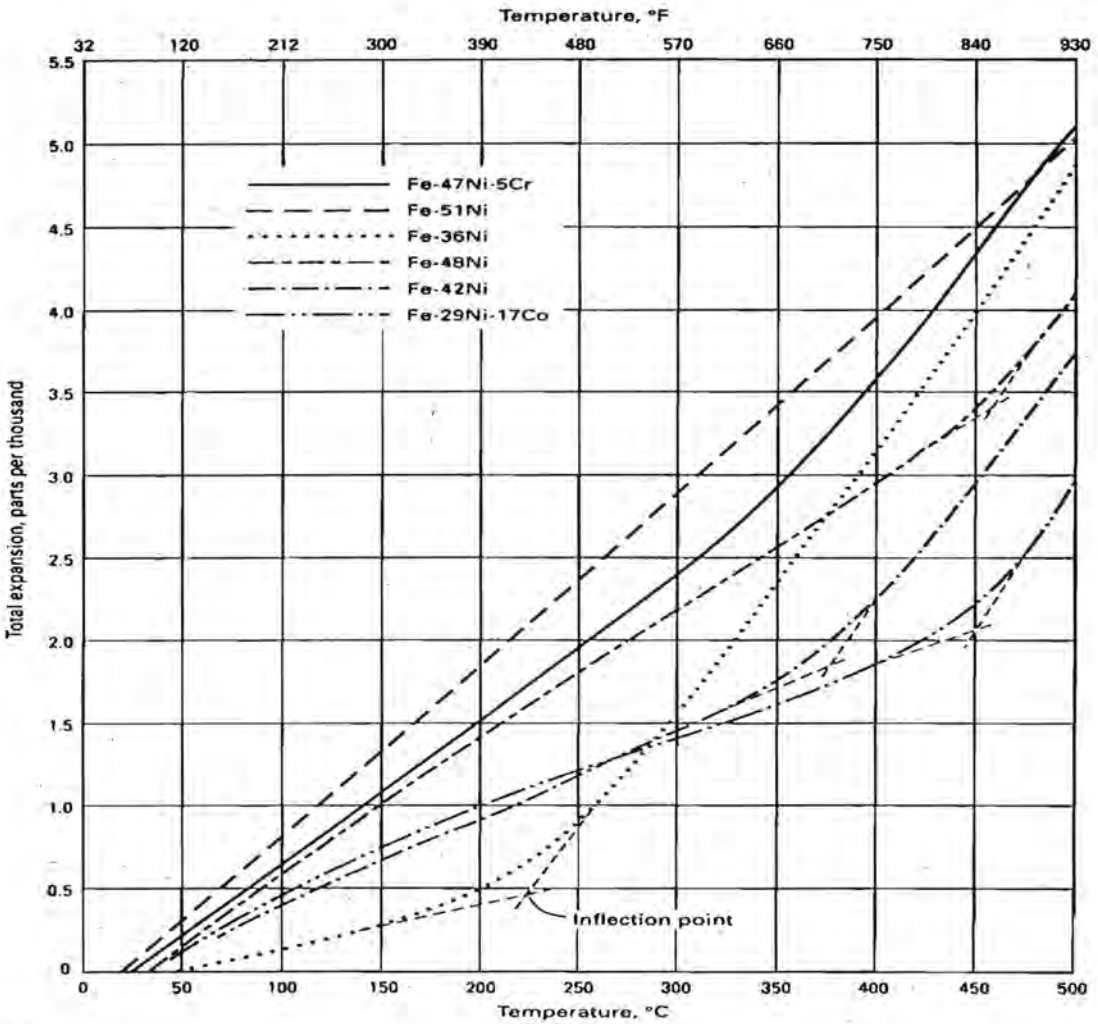

Fig. 4.4 Total thermal expansion of iron-nickel alloys showing the effect of third elements [6].

over 3 brass rods imbedded in the granite slab. During welding the ribbons – attached to the nylon block through studs – expanded thermally. With the help of the springs the nylon block was pulled and in this way the ribbons' expansion was offset. However, friction between the nylon block and brass rods hampered the effective compensation of the thermal expansion.

In another setup – as illustrated in figure 4.1 – weights totaling 52 kg were attached to a thick hinged aluminum plate on top of which a block of nylon was fixed. Three strong door hinges were used to connect the moving part to the granite block. During welding

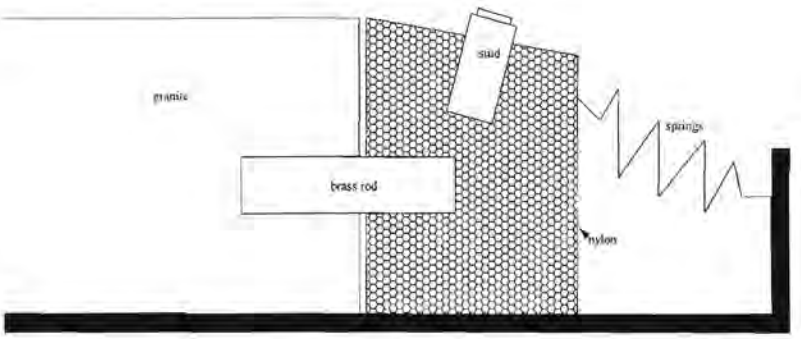

Fig. 4.5 Schematic setup using springs to offset thermal expansion of the used ribbons.

the ribbons' thermal expansion was compensated using the weights for straightening the ribbons. This option was so far the best alternative and was therefore adopted.

4.2.2 Welding Pressure

As mentioned, the weld pressure is an important welding parameter. We built and tested various devices to apply the needed uniform pressure during welding.

The first comprised commercially available sheets of molded foamed silicone rubber (300 x 300 x 10 mm). These were precisely cut and glued on to a piece of flat plywood. Due to the non-uniformity of the thickness and modulus in the silicone sheets the application of a uniform pressure on the welding area was not possible.

In other development a pneumatically inflated thin-walled silicone rubber tube was tested without success. As shown in figure 4.6, fabricated silicone rubber tubes of different wall thickness were confined on 3 sides inside a large rectangular aluminum channel and inflated with compressed air. Weights were placed on top of the frame to exert the pressure during welding.

Yet another pressure device was tested. It comprised a layer of polyether foam rubber glued on to one side of a piece of a flat chipboard. Three 25 kg slabs of granite – placed

on the top side of the chipboard – were used to exert the pressure during welding. With

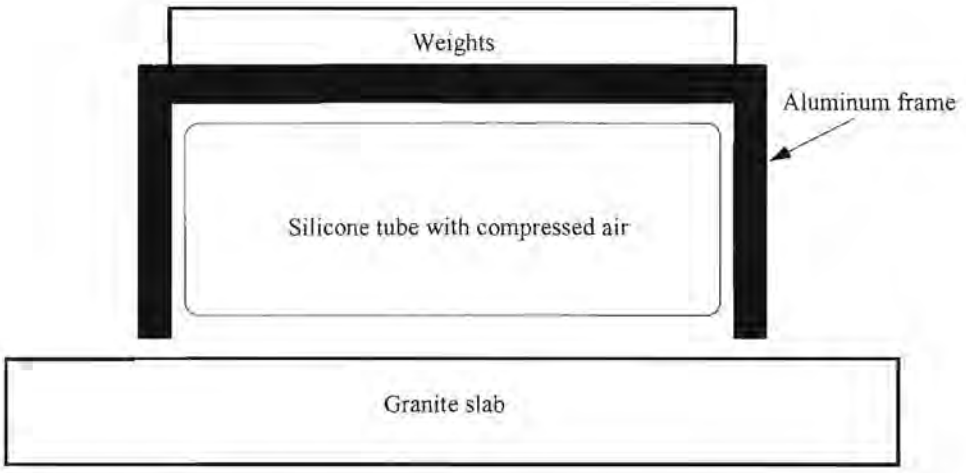

Fig. 4.6 Drawing visualizing the application of weld pressure using pneumatically inflated thin-walled silicone rubber tube.

this option better welds were attained. This alternative was unpleasant due to the need to lift and replace heavy slabs each time a welding had to be carried out.

Financial constraints prevented the use of a more convenient option.

The welding pressure obtained with the adopted option – as seen in table 4.1 – is low

Process	**Welding Pressure (kPa)**
Heated tool [7]	100 - 350
High frequency [7]	500 - 2000
Spin [7]	1000 - 7000
Induction [7]	100 - 300
Resistance implantation [7]	62
Commercial impulse heat sealer (our measurement)	24
Our impulse method	2.3

Table 4.1 Welding pressure for polypropylene used in different technologies.

compared with the pressures proposed in the literature for other techniques. As a result,

a relatively high welding current was used. However, an increase of the welding pressure would lead to higher friction between the ribbons and the films. This could cause the breakage of the films.

4.3 Fabrication of "Air Mattresses"

Commercially available 20, 30 and 50μ thick polypropylene (PP), and later specially made 39μ high density polyethylene (HDPE) films were used to build tubelike elements – the "air mattresses" – to be employed as heat transfer unit in a mechanical vapour compression desalination prototype plant (MVC). The films were welded using the thermal impulse indirect welding process [3].

The welding process started with an electrical circuit comprising 10 ribbons. Several welds were done, using 20, 30 and 50μ thick polypropylene films of different lengths. The welding with 20 and 30 μ films was not satisfactory – especially for films of 1 m long. They were, therefore, abandoned. Thus the 50μ PP films were adopted as the first material to used for the fabrication of the "air mattresses".

The electrical circuit was increased – in steps – from 10 to 40 ribbons. This permitted the fabrication of "air mattresses" with 40 vertical weld lines (1000 mm x 1 mm) spaced 7.5 mm centre-to-centre. Parameters such as current, time, and pressure were deliberately changed – one at a time – until strong welds were attained.

The attainment of suitable welding parameters was a difficult task. It required some patience from the welder. During welding, the current and welding time were recorded against the weld quality. This information served as basis for further tests to improve the welding. The optimal welding parameters found for the 50 μ PP film were 7 seconds weld current time, 3.95 A weld current in each ribbon, and 2.3 kPa weld pressure.

The alternating current electrical power supply to the system was provided by four independent 15A, 230V electrical circuits. Each circuit comprises a variable transformer for the adjustment of the welding current, a multi meter for current or voltage measurement, and two equal resistors in parallel. Each resistor comprises five ribbons – heating elements – connected in series. The four circuits were coupled to a timer used to

set the temperature effect time.

As mentioned in section 4.2, due to practical reasons the configurations of the "air mattresses" was changed. The number of tubes was reduced from 40 to 7 or 10 tubes of bigger diameter. The used electrical circuit in the final version of the welding machine is shown in figure 4.7. Each resistor comprises four ribbons – instead of five – connected in series.

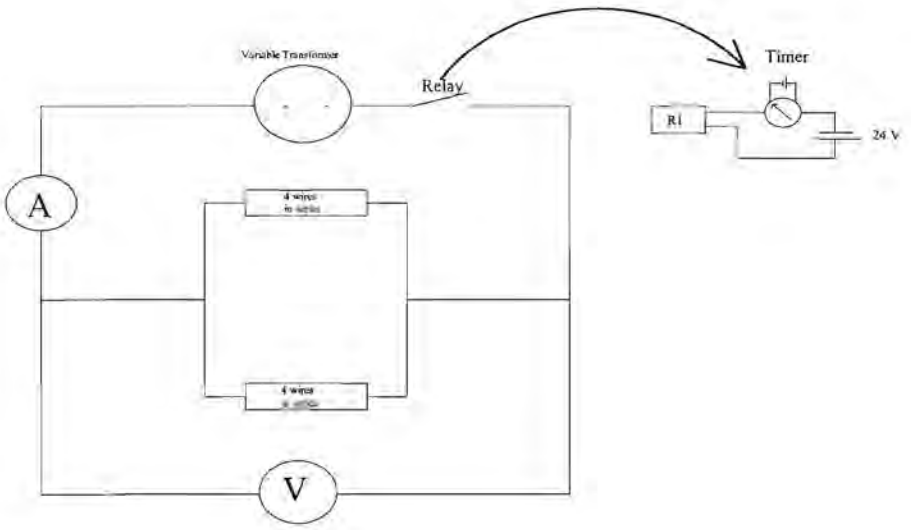

Fig. 4.7 Diagram of the electrical circuit used in the final version of the welding apparatus.

Later, the 39μ HDPE film from a special grade suitable for wettability treatment (see next chapter) was adopted as heat transfer material for the desalinator. It has the advantages of a lower wall thickness and higher thermal conductivity than the 50μ PP film. For this the welding parameters were 3 seconds, 3.9 A and 2.3 kPa.

4.4 Pressure and Leakage Tests

The "air mattresses" produced with the welder showed sound welds. This was confirmed by visual inspection against back light and by inspection with a Nikon 6C-2 profile projector. The strength of the welds in the "air mattresses" with eight tubes were checked using compressed air.

Initially a single tube was inflated with compressed air and gradually the entire "air mattress". Maximum air pressures of 400 kPa for a single tube and 350 kPa for the entire "air mattress" were recorded for the 7.5 mm PP film tube mattresses. In use the pressure difference between the inside and outside of the desalinator will be below 5 kPa. However, at temperatures above room temperature the plastic films become weaker.

For leakage detection some inflated "air mattresses" were introduced inside a container filled with water. The "air mattresses" experiencing air leakages – due to discontinuities on the weld lines – were repaired with a tool built specially for this purpose.

The device – as shown in figure 4.8 – comprises a disk of approximately 40 mm diameter and 16mm thick made of "vesconite" polyester. The round surface is covered with a small sheet of polytetrafluoroethylene impregnated fiberglass cloth. On top of the cloth – in the middle of the disk – a short piece of nichrome ribbon was attached. Both ends of the ribbon were connected to a power supply used to heat the element. A metal rod covered with insulation tape is used as a handle for applying the weld pressure. The electrical power and the weld pressure are manually adjusted for welding weak spots or places with discontinuities in the films.

4.5 Summary

The design and building of the welding apparatus was successful. However, the welding apparatus still needs further improvements to facilitate the process of mass production of the "air mattresses". Thus, the following considerations need to be attended to for the improvement of the apparatus:

(a) The adjustment of the welding current with the adopted electrical setup – in the case where 40 ribbons were used – was done independently in each circuit. With this procedure the application of the same values of current in each circuit was difficult. This resulted in the production of "air mattress" with tubes of different strengths. For safety reasons the electrical setup needs to be compact and well insulated.

(b) The manual procedure for the application of the pressure during welding was arduous. It did not ensure the needed uniformity in the application of pressure across the

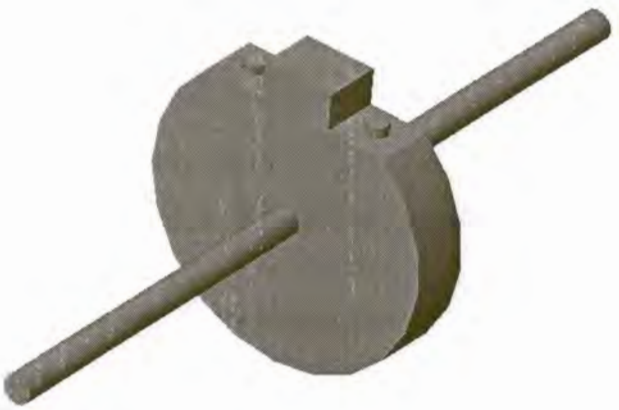

Fig. 4.8 Device used to repair "air mattresses" with discontinuities in the weld lines.

entire film to be welded. Thus, a mechanized setup is recommended for exerting the weld pressure.

(c) The use of ribbons with low coefficient of thermal expansion at the welding temperature of the adopted film is vital to obtain good, strong and uniform weld lines.

The fabricated "air mattresses" from PP and HDPE films are strong enough to be used successfully as heat transfer elements.

4.6 References

1. Hadwaco brochure, *A Quantum Leap toward Effluent-Free Industrial Plants*.

2. T. B. Scheffler, *A cost-effective multi-effect desalinator*, proceedings of IDA conference, Paradise Island, Bahamas, 2003.

3. O. Schwarz , W. Ebeling and G. Lüpke, *Plastics processing,* Translated from German

by O. C. Vorster and W. P. J. Rabé, for the Plastics Industry Training Board (PITB) South Africa, 1996.

4. O. Schwarz, *Polymer Material Handbook*, Translated from German by F-W Ebeling, H. Schirber, H. Huberth and N. Schlör, for the Plastics Industry Training Board (PITB), South Africa, 1995.

5. A.F. Mills, *Heat and Mass Transfer*, Irwin, Chicago, 1995.

6. Materials Handbook, *Properties and selection: nonferrous alloy and special purpose materials*, Volume 2, 10th edition, ASM, USA, 1990.

7. C. Maier and T. Calafut, *Polypropylene: The definitive user's guide and databook*, PDL, New York, 1998.

8. Goodfellow Catalogue, 2000

5 Assembly

5.1 Introduction

The previous chapter discussed the fabrication of polymer film heat transfer elements (HTE's). This chapter deals with the assembly of such air mattress shaped elements to form a heat transfer unit. This unit is inserted and suitably mounted into the larger, lower compartment of a vertical vacuum vessel which has a turbo centrifugal vapour compressor in the upper compartment.

The vacuum vessel and its auxiliary water pumps, feedwater heater, vacuum pump with protecting condenser, high speed rotary vacuum seal and (ceramic) bearings for the compressor, with valves, windows . . . form the desalinator. They are described in this chapter.

5.2 Heat Transfer Unit

A heat transfer module for the desalinator comprises welded air mattress-like plastic films joined together in a single unit with 3 manifolds:– for vapour inlet, saline water distribution, and distillate collection. After ambitious, expensive and time-consuming earlier trials attempting to manifold smaller diameter air mattress-like elements, we decided to build up the vapour inlet manifold - for introducing compressed vapour into the air mattress shaped heat transfer elements for condensation - of pieces as shown in plan in figure 5.1a. The weld line parts of the heat transfer elements are clamped between the short straight line sections of adjacent elements. To avoid the flow resistance on entry due to the *vena contracta* phenomenon, it was decided to round the entry ports. Thus a side view of an entry hole appears as in figure 5.1b [2,3]. This is built into the shape of the manifold pieces, of which 5.1b is therefore an illustration.

Initially the idea was to drape the welded film over the top of the manifold pieces, and to use smaller diameter film tubes. Manifold pieces designed with this in mind are shown in figures 5.2a-d, and were made directly from electronic versions of our 3 dimensional CAD (computer aided drawing) drawings.

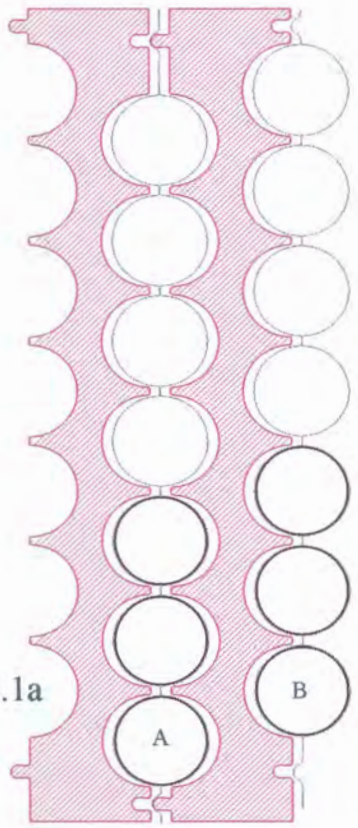

Fig 5.1a

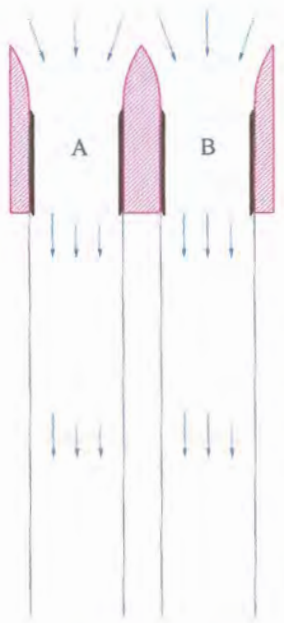

Fig 5.1b

Fig. 5.1 (a) Top view of part of a manifold, showing air mattress shaped film elements (thin blue lines) to be clamped between manifold pieces. The lowermost 3 film tubes also show short thin-walled tubular inserts (thicker black lines) that will press them against the manifold pieces when these are clamped. The friction of this clamping and pressing is what hold the film elements in place. (b) Side view of entry ports into adjacent film tubes like A and B (see fig 5.1a). The entry flow paths are rounded to avoid *vena contracta* type flow resistance. The thin-walled closely fitting tubular inserts – with one end tapered to facilitate insertion – offer only a minimal flow resistance.

[We used Allycad for 2 dimensional, and Solid Works for 3D drawings]. The pieces were for HTE's with 40 polymer film tubes of 4mm diameter. This version was manufactured by a stereo lithography process. Despite the poor results from this process at the required high resolution, they clearly showed that (even if the parts had been manufactured perfectly), the relatively stiff 50μ welded polypropylene film would not drape as desired over the top of the finely sculpted three dimensional manifolds.

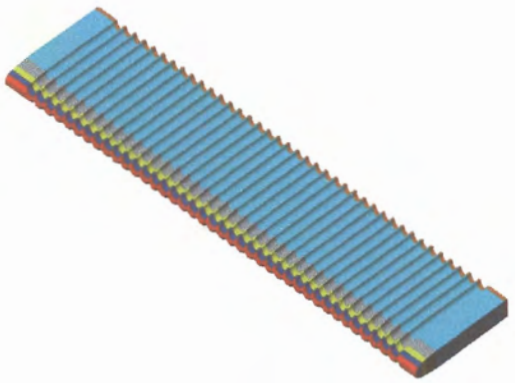

Fig. 5.2a

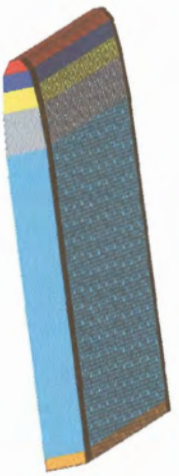

Fig.5.2b

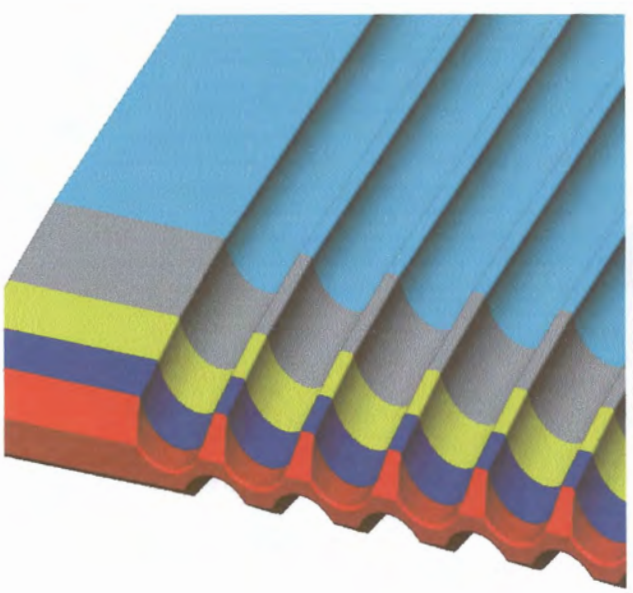

Fig.5.2c

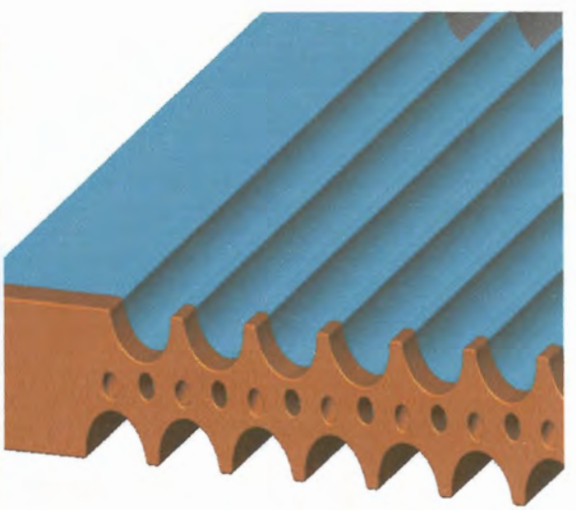

Fig.5.2d

Fig 5.2 Initial design for a vapour manifold piece – intended for use with 4mm diameter polymer film tubes:– (a) isometric view; (b) side view; (c) close-up top view; (d) close-up bottom view, showing the small holes for distributing saline water to each individual film tube on each side of this part, which was also intended to serve as saline water distributor. The saline flow per hole would, however, be so low that blockages due to dirt particles or scale would be likely.

Therefore a HTE with seven film tubes of 18.4mm diameter was designed and fabricated, along with new vapour manifold pieces (see figure 5.1) to fit them. Instead of trying to drape the film over the top of the manifold pieces, we had thin walled tubular pieces made to tightly fit into the upper parts (the *necks*) of the film tubes, to hold the tube entrances open. Also - by pressing them onto the concave semi-cylindrical parts of the manifold pieces - to help hold them by friction.

Figures 5.3 a - b show an assembled vapour manifold.

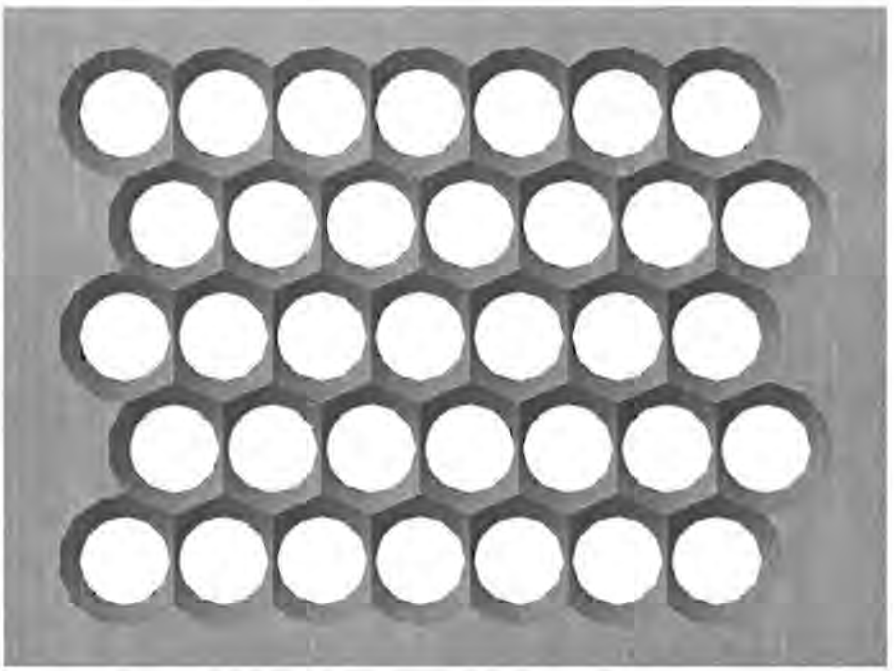

Fig 5.3a Vapour manifold entry for 35 film tubes of 18.4mm diameter, with rounded (anti-*vena contracta*) inlets as shown in fig 5.1b.

The insertion of the thin-walled tubes into the films requires care to avoid damaging the films. In order to obtain the necessary tight fit – and to establish which insert diameter would give the best round shape in the tubes of the HTE – thin walled tubes of outside diameters 18.1, 18.2, 18.3 and 18.4mm were separately inserted inside each tube of a HTE. The manifold pieces were then clamped on. The tests indicated that the 18.1mm inserts – apart from being easiest to insert, and having the smallest risk of damaging of the film tubes – also gave the roundest film tubes on assembly with the PP HTE's.

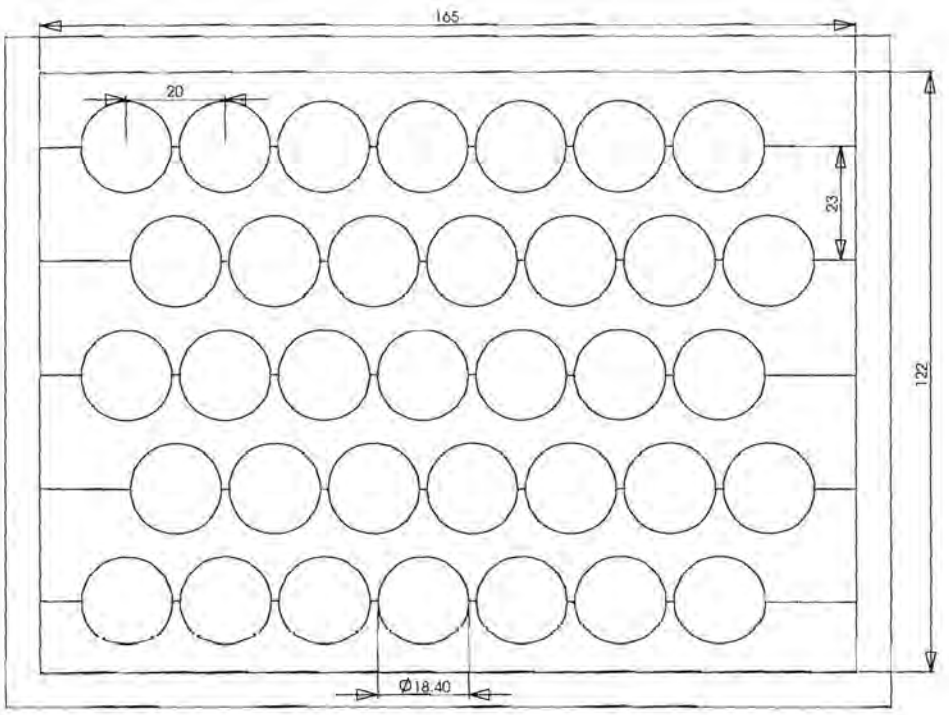

Fig.5.3 b Top view of a manifold with some relevant dimensions in mm.

The heat transfer unit comprises 70 tubes of 18.4mm diameter and 2m long. This corresponds to a surface area of $8m^2$. At the top, the heat transfer unit is fixed on a plate separating the 2 vacuum compartments through two vapour manifolds. At the bottom, each "air mattress" is connected through a small tube to a main plastic tube – the liquid collecting manifold – that is used to collect the distillate before it is pumped from the vacuum vessel.

5.3 Vacuum Vessel

The vacuum vessel was manufactured by an engineering company specializing in borehole casings, from 3mm thick mild steel reinforced with 20mm thick external circumferential ribs at 660mm intervals. Top and bottom plates are also of 20mm steel. It has an inside diameter of 400mm and a total height of 2310 mm, and is shown in figure 5.4. It has a main compartment (everything up to the flange about 290mm from the top), and an upper one which houses the vapour compressor.

Fig 5.4 The uninsulated 2.35m tall vacuum vessel showing 200mm windows, stand and scaffolding. The pulley block is used to raise and lower the small top compartment (housing the turbo centrifugal compressor, and at a pressure $p + \Delta p$ above that of the main compartment).

The upper compartment is at the increased pressure $p + \Delta p$ of the compressor outlet. Between the main and the top compartments is a removable separator plate of 15mm polypropylene, which has at its centre a suction port leading to the centrifugal compressor inlet.

The main compartment has five windows, and a removable bottom lid, and is held by the stand and scaffolding. The windows - three of 200 mm and two of 160 mm diameter – are

to enable one to check on the wetting of the polymer heat transfer elements. They also facilitate access to the inside. In operation the windows have 6 mm thick heat toughened glass disks - 165 mm diameter for the small and 204 mm for the big windows. The bottom small window is now sealed with a stainless steel disk with a vacuum hose connector – to couple the vessel to the vacuum pump.

The separator plate separates two regions of different pressures: p in the main compartment, where evaporation takes place *outside* the film tubes, and $p + \Delta p$ in the upper compartment, which contains manifolds leading to the *inside* of the film tubes. Figure 5.5 shows a bottom view of the configuration adopted. Below the separator plate, a plastic tube extending from outside the vessel, is used as inlet for saline water. The tube is connected through a T-junction to a series of multiply drilled small tubes (liquid distributors) placed between adjacent air mattresses-like HTE's, with enough holes to wet each film tube on each side of each small tube with an even film of saline water. Thus each small tube acts as a saline water distributing manifold, which is further equipped as detailed in Chapter 6.

To prevent corrosion of the vessel, two coats of a phenolic epoxy tar coating (TCN300) were applied directly to the cleaned, sandblasted carbon steel. The coating took weeks to harden – into an uneven surface resembling a tarred road.

Vacuum seal. The flange sealing surfaces and O-ring grooves were distorted by the welding process, and needed re-surfacing – on a huge lathe bigger than that of the manufacturer. These surfaces were then painted with a marine epoxy (Copon) which hardened within an hour or so into a smooth hard surface more suitable for vacuum sealing. But even now (at least one of) the many seals (5 windows, 415mm diameter bottom seal, 2 seals of 415mm diameter at the separator plate, plus many smaller diameter seals)are far from satisfactory. It would have been much better to require from the manufacturer a pre-test and guarantee of the seal - even if this had more than doubled the cost of the vessel. Perhaps at least the *sealing surfaces* should also have been of 304 or 316 *stainless* steel.

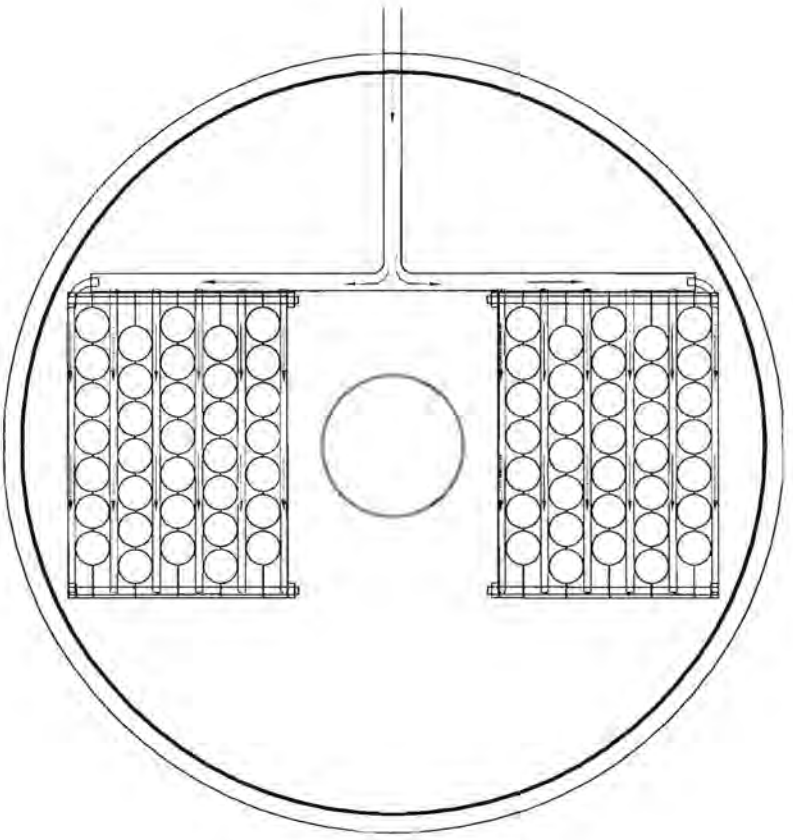

Fig. 5.5 Schematic bottom view of the separator plate with the water inlet and the liquid distributors tubes. Two manifolds used to join the air mattresses (five each) are presented. The evaporating vapour reaches the compressor through the orifice (circle) at the centre of the plate.

5.4 System Auxiliaries

The auxiliary components connected to the vacuum vessel include a vacuum pump, water pumps, a turbo centrifugal vapour compressor, a specially made water cooled high speed rotary vacuum seal, specially made (in Germany) high speed bearings (with ceramic balls), a small plate heat exchanger, feedwater heater, and measuring instruments.

5.4.1 Vacuum Pump

Two types of vacuum pump were tested. The first pump was a small plastic ejector type water jet pump. Due to the low pressure of the water supply it evacuates the vessel too slowly – even when connected to two water taps in parallel. It can of course not achieve

the desired absolute pressure of 1 mbar under dry conditions that we deem necessary as indicator of an adequate vacuum seal (zero infiltration of unwanted non-condensible gases).

The other pump is an oil-type vacuum pump (LH – Leybold – Heraeus, Trivac, D16A). This evacuates the vessel faster, and to absolute pressures of about 1 mbar when dry.

5.4.2 Water Pumps

In the system three water pumps are employed. One is used to maintain continuous circulation of ice water through the small **plate heat exchanger** used as a **condenser** to trap the water vapour evacuated from the vacuum vessel – preventing it from reaching the vacuum pump. For removing the distillate and the concentrate brine from the vacuum vessel, and re-circulating part of the brine, two air-operated double-diaphragm pumps (Wilden P.025) were employed – with all wetted solid parts of polypropylene [1].

Unfortunately the diaphragm pumps – located on the floor below the desalinator – are unable to retrieve the distillate and the brine from the vacuum system when the absolute pressure in the latter is below 10 kPa. This is despite the claim [1] that it is "capable of pulling a high vacuum". Thus we built an apparatus based on a barometric principle to extract these by gravity. Unfortunately this is somewhat inconvenient, as the distillate is now collected 4 stories (12 m) below the apparatus. And the barometric pump needs careful priming and (like everything else) air-tight seals. And staff at widely different levels.

5.4.3 Centrifugal Vapour Compressor

The specially designed and built centrifugal turbo compressor is mounted inside the small upper compartment. It is driven by a shaft passing through a rotary vacuum seal cooled and sealed with a trickle of water. As the seal is just a millimetre below a specially made imported bearing, it must be carefully wetted – and the surplus water continuously removed by suction – to keep the expensive bearing dry. A special grooved high speed drive belt passes over a 210 mm pulley mounted on the shaft of a 3 kW, 2 900 r p m electric motor, and drives a 30 mm pulley on the impeller shaft at about 20 000 r p m.

Fig 5.6 Upper part of the vacuum vessel with the motor for the compressor. The inverted orientation of the motor is to get the correct sense of rotation of the impeller.

See figure 5.6. [Initially we had bought a 2.2 kW industrial router – with 12.7 collet chuck and the valuable feature of a *speed controllable from 9 000 to 27 00 r p m.* Unfortunately all routers rotate in the same sense (direction) – the opposite of that of all readily available impellers for turbo machinery. And the bearing of the router appeared incapable of safely supporting even the dynamically balanced 127 mm diameter impeller at speeds much above 12 000 r p m. Fortunately, we were able to return the router for a full refund a few days after buying it. But the change caused a huge delay, as the compressor needed modification. In all, it took more than 2 years to get the compressor operational, as the manufacturer had another project (a gyrocopter) of higher priority to it.]

The compressor was designed for a low compression ratio (1.02 - 1.04) to give a small temperature difference (below 2°C) in the evaporator/condenser.

5.4.4 Measuring Devices

The pressure in the main compartment is measured with a simple Bourdon type gauge giving the pressure relative to atmospheric on a scale 0 to -100 kPa. When testing the vacuum sealing, a gauge giving the *absolute* pressure on a scale 0 - 25 mbar (0 - 2.5 kPa) is used.

When the compressor is running, the pressure difference between the compartments is measured by a (coloured) **water manometer.** We found, to our surprise, that the initial manometer gave a non-zero reading when both sides were at equal pressure – even when both were open at atmospheric pressure! The cause was capillary effects and different surface tension of the glass on the 2 sides – induced during the heated bending of the tube. No amount of ultrasonic detergent cleaning would remove this – the only solution was to have a U bent out of much larger diameter glass tubing.

The feed water flow rate is measured with a calibrated 1/4 inch Fisher and Porter rotameter. This was calibrated using a stopwatch and large measuring cylinder. The feed water is supplied from a big tub. A glass thermometer indicates the temperature of water from the **specially built flow-through feed water heater**. Flow into the desalinator is regulated by a valve, and the heating power by a variable transformer. For a *laboratory* MVCD heat recovery flat plate heat exchangers to recover heat from the brine and distillate streams (to pre-heat the feed) was not deemed necessary or cost-effective.

Our experience suggests that a *heating element* in the brine at the bottom of the desalinator would be useful – to speed the warm-up of the apparatus from a cold start. It could be switched on even before the vacuum pump (which needs circulating ice water to protect it) – to warm the apparatus by condensation of water vapour from the warmed water.

5.5 Experimental Procedure

The schematic setup of the vertical vapour compression desalinator designed to operate between 50 and 65°C is shown in figure 5.7. In this temperature range the scaling potential is very low for seawater and for most industrial effluents. Although scale does not adhere to untreated non-polar polyolefin surfaces, it is expected to adhere to some

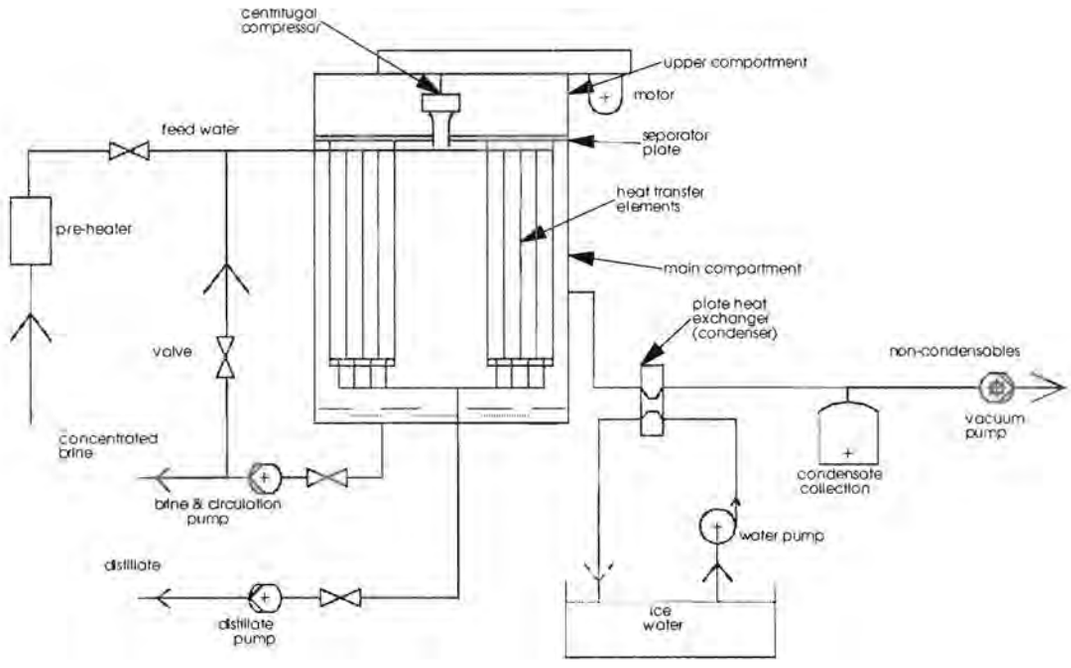

Fig. 5.7 Schematic diagram of the desalinator with auxiliares.

extent to surfaces treated for wettability – see chapter 6. This treatment is needed in order to utilize film-wise evaporation. The evaporator-condenser has vertical air mattress-shaped HTE's joined together as described in section 5.2. Until now, the testing of the desalinator has started with the evacuation of the vessel under *dry* conditions. This was to test the overall tightness of the various vacuum seals, which needed to be covered with silicone sealer to make them effective. At an initial absolute pressure of about 1 kPa pre-heated feed water is drawn into the vessel. Inside, the feed water is dispersed over the outer surface of the plastic film tubes through the saline water distributors. A small part of the water moving downwards evaporates. For efficient evaporation – due to transfer of latent heat of condensing vapour inside the HTE's – it *should flow down as a film* to the bottom of the vessel from where it is pumped out of the evacuated apparatus. Part is discharged, and part recirculated with the pre-heated feed.

The vapour from the evaporated liquid is drawn into the compressor. By increasing the

pressure the compressor raises the saturation temperature (at which the vapour condenses). Compressed vapour flows via the manifolds into the film tubes. There it condenses releasing latent heat which is transferred through the tube walls to evaporate feed water flowing on the outside surface of the plastic films. Thus, additional vapour is produced and the process repeats itself again and again. However, the saline water *did not actually flow down the HTE's as a film.* In the time it took for the silicone sealer to dry (several days inside the "crevices" between mating surfaces), the film elements dried out, and their wettability was irreversibly reduced – see chapter 6. The result was that – as far as could be judged by looking through the windows – **only about 5 - 10% of the film heat transfer surface was wetted.** Water was seen to be dripping and running in narrow streamlets – instead of flowing filmwise. Thus it is no surprise that the performance of the apparatus (as judged by the amount of distillate formed inside the HTE's) was disappointing.

5.6 Recommendations

An alternative procedure would be to put several centimetres of water in the bottom of the apparatus once the bottom plate is in position with its bolts tightened. The pump for re-circulating this water to the top of the HTE's is then "switched" on (by opening a valve for compressed air) in order to (try to) keep the HTE's wet. One proceeds to tighten all other apertures and connections, and carefully applies silicone sealant to all of these. After about 24 hours the heating element inside is switched on to speed up the curing of the sealant. The interior is kept at about 60°C for the following 24 hours to complete the curing process. With the apparatus already warmed up, it could be evacuated and started up fairly quickly.

However, there is some doubt as to how successful this would be. Even the day or so of dryness needed to assemble new HTE's into the apparatus with also the distillate collecting manifolding in some difficult-to-reach positions (and tightening all the seals) can affect their wettability. Pumping water onto the already dry HTE's will not wet more than about 30% of their surface. Merely bolting on the bottom might be insufficient, as its 415mm diameter seal might leak. And the procedure does not allow one to test the

tightness of the vacuum seals, which requires dry conditions.

What is really needed is a laboratory apparatus:–

(a) that permits *inspection during operation* of the *full* heat transfer surface of *at least* one HTE to check the wetting. This is essential before any measurements or optimization of the key parameter U can be made – or even seriously contemplated. Optimizing the heat transfer coefficient U is a key to any serious design of a new type of desalinator [4]. This feature is also needed for studying how scale is formed from highly concentrated industrial wastes, and what surface treatments will lead to good wetting, but avoid or minimize scale adhesion.

(b) that can be made vacuum tight in minutes – not days;

(c) where the HTE's can be easily flooded over their entire external surface *after closing the apparatus;* or

(d) where they can be assembled (and the apparatus closed) *before drying out.*

In a production apparatus, requirement (c) (if needed together with (d):– keeping the HTE's wet before & during installation) will be a key to success. This is impossible to attain in a vertical setup, but rather easy in a **horizontal tube configuration**. Furthermore, recent work has shown that a horizontal system – which is outside the scope of this thesis – also leads to simpler, less expensive HTE's, to much improved wetting, and to far simpler (spray type) saline water distribution.

Indeed it will have about a *thousand times fewer water distributors* (now of the full bore type, rather than the more easily clogging capillary type used for the vertical configuration). These are of critical importance [5] as they

(A) can clog;

(B) need to be monitored; and

(C) when blocked, must be promptly and quickly replaced without cooling down the

apparatus.

If requirements (B) and (C) are not met, irreversible damage will result to the HTE's, which will dry out in parts, and may lose their wettability or scale up.

5.7 Summary

The assembly of the air mattress-like heat transfer elements (HTE's) using the adopted manifold pieces to build a single heat transfer unit was successfully accomplished. Also specifying, obtaining, installing (and where needed, designing and constructing) the various auxiliaries.

Although this would have at least doubled the cost of the vacuum vessel, it would have been much better to have required the contractor who built it to have pre-tested it against leaks, and to give a guarantee on this. Perhaps also the sealing surfaces should have been of stainless steel. The use of silicone to improve the sealing of vacuum vessel - to prevent leakages - was labourious.

A laboratory polymer film apparatus should satisfy the requirements (a) - (c) – or (a), (b) & (d) – of the previous section. A production desalinator should at least satisfy the key requirement (c) – as well as requirements (B) and (C). These requirements can only be met (at affordable cost) in a *horizontal* (film) tube desalinator.

5.8 References

1. *"Engineering Operation and Maintenance"*, Wilden technical manual, EOM-P.025P 8/00.

2. J. Bijkersma, *Pressure losses at the tubular inlet section of a low temperature differential heat exchanger*, M Eng thesis, RAU, 2003.

3. J. Bijkersma and L. Pretorius, *Design parameters to minimize pressure loss for an axisymmetric inlet section evaluated*, 3rd International Conference on Heat Transfer, Fluid Mechanics, and Thermodynamics , Cape Town, South Africa, 2004.

   Also (same title) J. Bijkersma, L. Pretorius and J. P. Meyer, SACAM Conference,

Johannesburg, South Africa, 21-23 January, 2004.

4. E. Ghiazza and P. Peluffo, *A new design approach to reduce water cost in MSF Evaporators*, Proceedings of IDA conference, Paradise Island, Bahamas, 2003.

5. V. Baujat and T. Bukato, *Research and development towards the increase of MED units capacity,* Proceedings of IDA conference, Paradise Island, Bahamas, 2003.

6 Wettability and Wetting

6.1 Introduction

6.1.1 Efficient Evaporation

Pool boiling (used in older, pre-1950 multi-effect stills) is inefficient at low ΔT_e, as both the static pressure head and the considerable pressure effects of surface tension on the formation of tiny steam bubbles must be overcome. *Falling film evaporation* is used in all modern multi-effect (ME) and vapour compression (VC) desalinators.

The *falling film* refers to a thin film of saline *water* trickling ("falling") down a heat transfer surface - whether this be a metal tube or a polymer film heat transfer element. A falling film evaporator presents a large surface area for evaporation, and a heat transfer coefficient h_e for evaporation that (in the Nusselt theory) *increases* as ΔT_e decreases. It is thus particularly suitable for high efficiency stills, which require small ΔT_o and hence even smaller ΔT_e.

Efficient, i.e. falling film evaporation requires that the evaporation surface of the polymer heat transfer element be thoroughly *wettable - hydrophilic*. A thin, preferably uniform and continuous water film should flow downwards on the heat transfer surface.

The most efficient condensation, by contrast, is dropwise condensation, [1,2,3] which needs a *hydrophobic* - water repellent - surface. Therefore the ideal is a surface that is strongly hydrophilic (water attracting, and therefore wettable) on the evaporating side, but strongly hydrophobic on the condensing side.

6.1.2 Surface Modification

It is well known that the polar liquid water does not wet polyolefins, which are non-polar and mildly hydrophobic. This is due to the low surface tension of polyolefins (~ 30 mN/m) compared to water (~ 70mN/m). The surface tension and wettability of a polyolefin surface can be increased by subjecting it to a suitable surface treatment. Possible chemical surface treatments include exposure to corona discharge, to gaseous ozone (O_3), to gaseous SO_3, to oleum, to chromic acid, to sulfamic acid, and

oxyfluorination. During oxyfluorination the polyolefin surface is exposed to a fluorine - oxygen - nitrogen gas mixture. This results in functionalization of the surface: charged, dipolar and/or polarizable sites are created. All of these tend to increase the affinity for water, which comprises dipolar molecules.

Wettabililty is a material property while wetting depends on the wettability and on the recent - *temporary* - history of the hysteresis of the material.

6.1.3 Unwanted Capillary Action

Once the evaporating outer surface has been made wettable, an unwanted capillary action arises in the space between adjacent film tubes: Saline water flowing down the outside of the set of tubes tends to move to the region where the weld line separates adjacent tubes (see figure 6.1). This depletes and/or removes the water film from the rest of the surface. Thus it can happen that most or all of the water eventually flows along the weld lines - where little heat exchange can take place between condensation inside and evaporation outside - leaving the regions where evaporation *should* take place dry. Such large dry areas are unacceptable [10]: in the process of drying out they can form *scale,* and, once dry, they do not contribute to the evaporation.

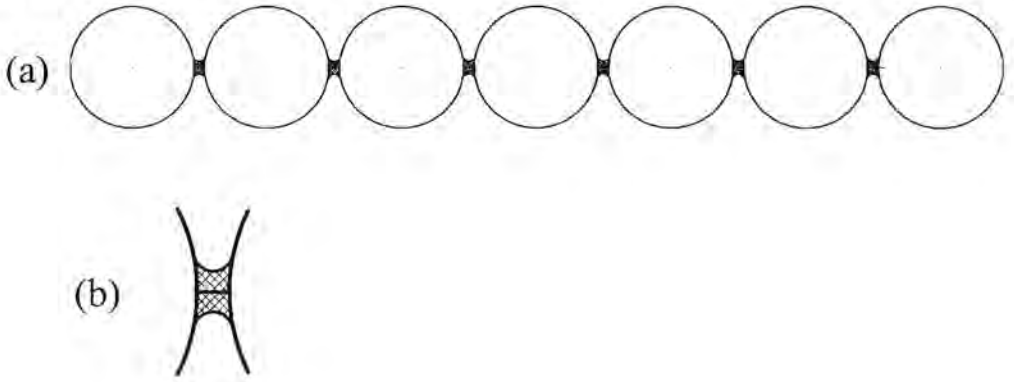

Fig.6.1 (a) Capillary action between adjacent film tubes, in the region of the weld lines, between adjacent film tubes (b) a close-up view of the capillary zone. In our test setup, each "air mattress" has seven film tubes. Water is drawn into the region between adjacent tubes - that is, into the film region nearest to the weld lines.

As side-wise conduction will be minimal in a thin (~30μ) polymer film (with low conductivity $k \approx 0.2$ to 0.4 W/mK), the condensation directly opposite to the dry areas will also cease, so that the total area for heat transmission between condensation and evaporation will be essentially the total area wetted by saline water. It was originally

thought that if the areas of the weld lines, and adjacent to them were masked (with masking or PVC tape) during the wettability treatment the natural hydrophobic character of the polymer film might be sufficient to prevent this unwanted capillary action. Unfortunately, this did not happen - most water still flowed down the vertical "furrows" between adjacent tubes. This may be for either (or a combination) of the following reasons:

(a) The untreated polymer is perhaps not sufficiently hydrophobic.

(b) Traces of the tape adhesive remain in the weld area after the masking/PVC tape is removed. These traces make the film somewhat hydrophilic in the very region where they are supposed to *prevent* the wettability treatment.

(c) The masking is not sufficient to prevent some of the highly reactive chemicals to reach the region.

Another solution tried for this problem was to use spacers (see figure 6.2) that would keep the "air mattress" tubes in a constant staggered spacing relative to the tubes of the next "air mattress". They were also designed to collect the water flowing down the "furrows" next to the weld lines, and to re-direct this water to positions halfway between "furrows".

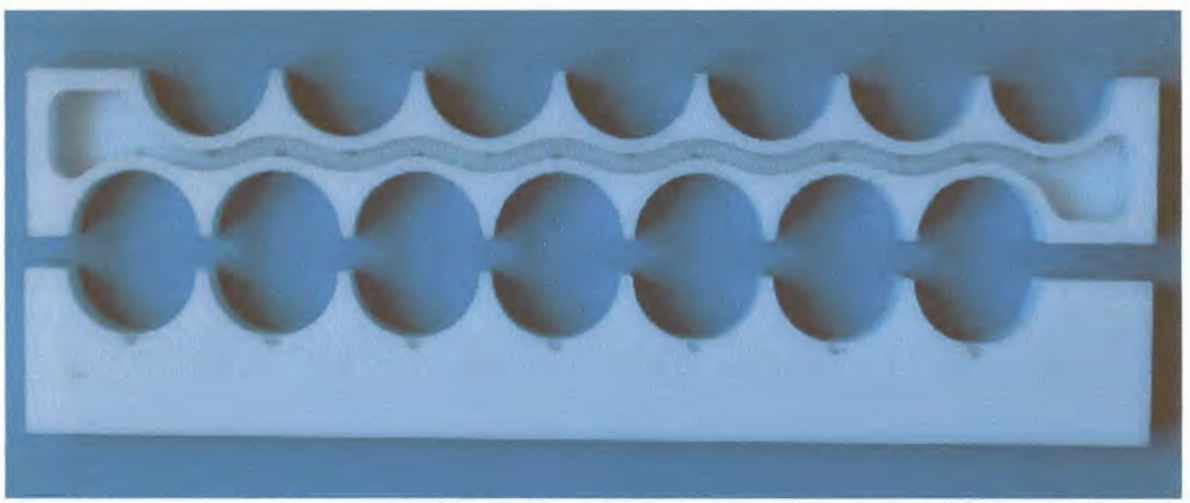

Fig.6.2 Spacers used to keep the "air mattress" tubes in a constant staggered spacing relative to the tubes of the next "air mattress". The lower spacer is upside down.

This, too was not as successful as we had hoped. The reason appears to be that on inflating the "air mattresses", the polymer film stretches by an amount that is difficult to

predict - as it will depend on both the pressure of inflating, and on the temperature (which strongly influences the elastic modulus of the polymer film). The "air mattresses" then no longer accurately match the dimensions of the specially made spacers. Therefore they do not effectively collect the water from the "furrows".

By far the best solution appears to be a modification of the original - to apply a thin layer of silicone (a *strongly hydrophobic* material) to strips over and surrounding the weld lines *after* the wettability treatment (which also increases the adherability). This at present still somewhat labourious solution has proved 100% effective against the undesired capillary action. A flexible tape, adhesive on one side but strongly hydrophobic on the other, would also be effective. So far, we have not been able to find such a tape, and it is not clear whether such tape exists, or can be easily manufactured. PTFE impregnated fibre-glass cloth is available in a form that *is* adherable on one side and strongly hydrophobic on the other, but is not nearly flexible enough.

We now discuss the testing of the wettability of plastic films - to see which will be suitable for use in the still.

6.2 Wettability Test

An experimental setup used to perform the wettability tests of the oxyfluorinated "air mattress" plastic films is shown in figure 6.3. It comprises two basins, one at the bottom to collect the water and the other at a variable height and used as the water source. A flexible tube with a tap connects the top basin to two small distributor tubes (5mm ID) through a T-junction. Each distributor tube has seven holes - one at the centre of each film tube, halfway between the weld lines - to spread water evenly on the plastic films to be tested. In one distributor tube the diameter of the holes was 1.0 mm; in the other it was 1.4 mm.

Closely fitting white plastic tubes were inserted carefully (so as not to tear the thin film) inside the welded plastic film in order to attain the desired round shape for the test. The assembly of the plastic films with inserted tubes was held at the top and at the bottom.

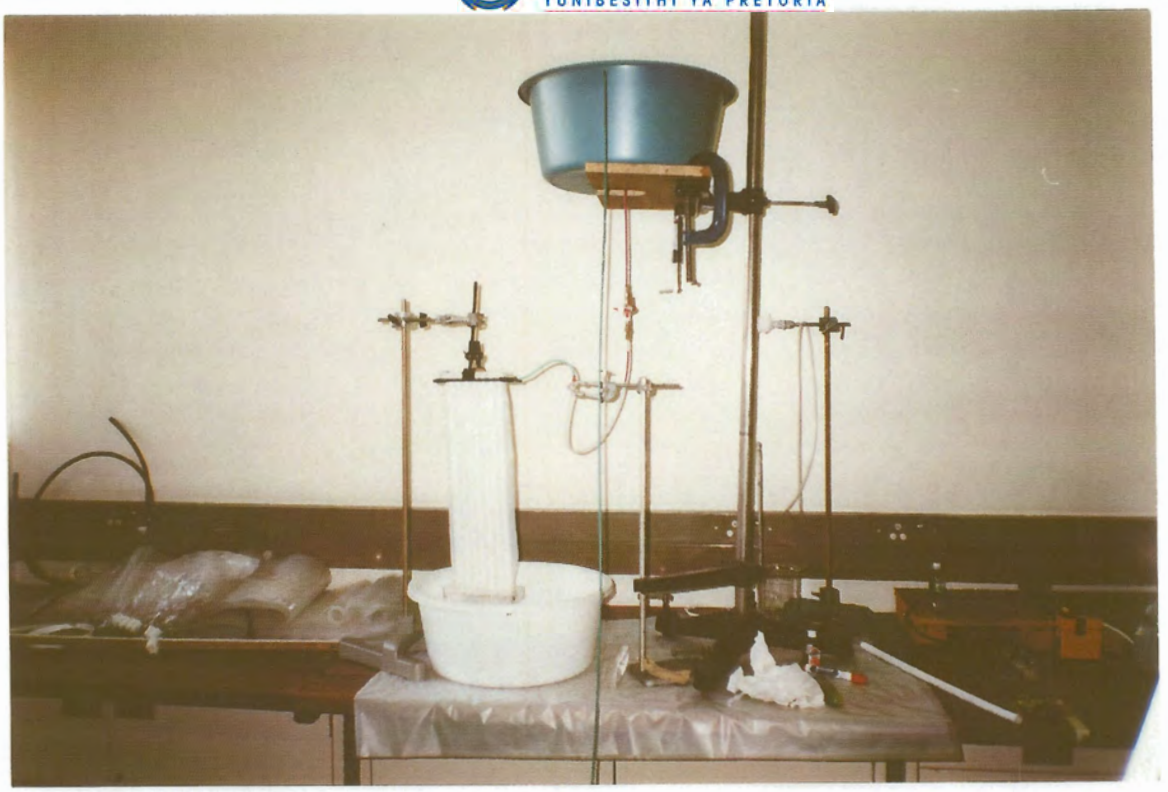

Fig.6.3 Experimental setup for wettability test.

The figure 6.4 allows a close-up visualization of the amount of water streaming in each weld line by looking at the water level in each glass tube.

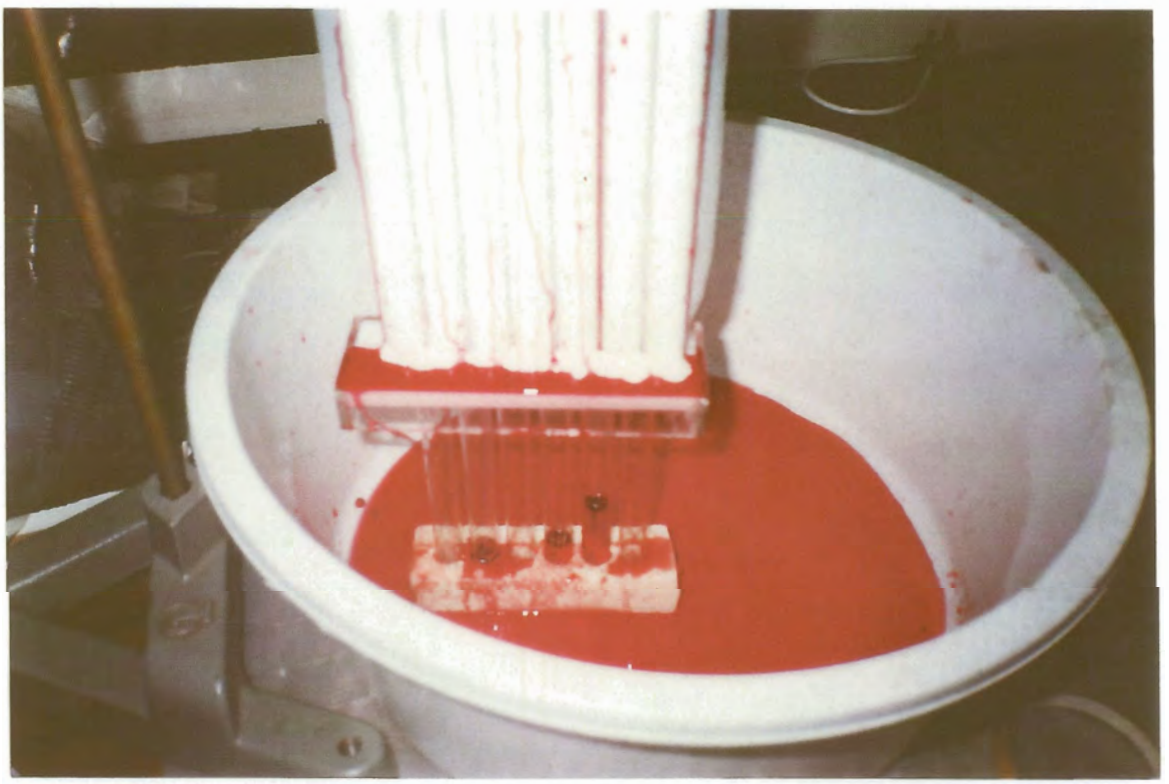

Fig. 6.4 Close-up view of the setup for separation of the fluid streams.

Figure 6.5 is a drawing of the used separation unit. The dashed lines represent the (chemical) test tubes. White silicone putty P sloping towards the apertures A was used (see figure 6.5b) to guide the flow streaming along the weld lines towards the apertures A. Each of the 6 apertures (one for each weld line *between* tubes) on one side of the air mattress had below it a test tube to collect the water streaming through that aperture. Water flowing on the air mattress surface, but not near the weld lines, would flow to be collected in the basin (outside the test tubes).

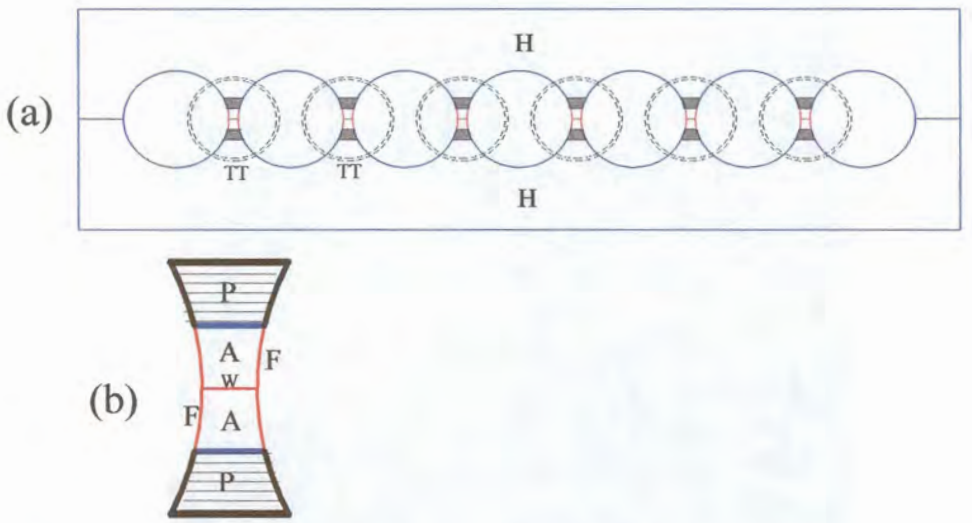

Fig.6.5 (a) Drawing of the separation unit with the white holders H and test tubes TT (dashed lines), (b) close-up view of the separation region (A= aperture, W= weld line, F= plastic film, and P= Putty).

Water from the top basin was used to wet the plastic film by letting it flow downwards at different flow rates determined by changing the height of the top basin. The water was coloured with red food colouring liquid to facilitate its visualization on the white back-ground represented by the plastic film. A camera was used to record the images of the water flowing downwards on the welded plastic film, at different flow rates, and for different surface treatments.

The insertion of closely fitting white tubes in the "air mattress" tubes to attain the required round shape was not a suitable method for tests involving "air mattresses" of two metres long as needed for the desalinator. This procedure was abandoned in favour of one more resembling the real situation of the system in operation. Compressed air inflated the "air

mattresses". The use of 2m long oxyfluorinated air mattresses in the wettability tests required some alterations of the experimental setup. In figure 6.6 the new setup is depicted. In this setup the top basin was removed. A small fountain pump (EDEN 130G)

Fig.6.6 Improved experimental setup for wettability test.

was employed to circulate the water from the bottom basin to the liquid distributor.

6.3 Test Results

In the first tests plain coloured water was used to wet the films, which were of bi-axially stretched polypropylene (PP). The wettability was poor. In the following tests, coloured water was mixed with a *surfactant* to reduce its surface tension. This improved the wettability. With the new setup, no surfactant was used, as in a production desalinator it might cause environmental problems (for the brine disposal), and would also involve the cost of the surfactant. Instead every effort was made to improve the wettablity of the plastic films by optimising the surface treatment process.

The test results are presented in the following sections.

6.3.1 Test without Surfactant

From the figure 6.7, it can be seen that (red coloured) water wets the tested oxyfluorinated plastic film, but not very well.

Droplets can be observed in the picture. On each film tube a flow stream starts at the hole in the liquid distributor: half-way between the weld lines on the plastic film surface. It spreads somewhat and also meanders. Where water enters the region of the weld lines, it tends to stay there, moving vertically, and finally enters a glass tube. As seen in figure 6.4, different tubes collect different amounts of water - showing that the water flow on the plastic film is not homogeneous.

This could be because the used plastic film was not adequately oxyfluorinated (too low a treatment time, temperature or concentration). Thermodynamics suggest that it is also possible that long exposure of the treated surface (which has increased the surface tension and energy) to dry conditions *after* treatment could have caused components of the high energy surface to migrate inwards thus decreasing the charged/polar/polarizable nature of the surface, and its wettability. The exposure of a treated film to dry air for long can also cause [4,6] the lowering of the surface tension due to, for instance, absorption by the surface of low energy contaminants from the atmosphere.

6.3.2 Test with Surfactants

The results obtained in the previous experiments were not satisfactory. In the following tests, coloured water was mixed, separately, with two different surfactants (NP9 and AL2575 from Uniquema) in different concentrations to lower the surface tension of the solution. This improved the wettability of the plastic by lowering the surface energy of the water. For these tests the first setup and testing procedure was used. Five litres of coloured water were mixed with each surfactant at 10^{-5} dilution by volume. The solution was spread on the same plastic film previously used in the tests without surfactant.

The result of the first attempt was poor. Consequently the surfactant's concentration was doubled, tripled and finally kept at ten times the initial concentration. However, no satisfactory results were obtained at any of the used concentrations of either surfactant.

The use of the *same* plastic film employed in the first experiment (without surfactant) could be the reason for the poor results obtained also this time.

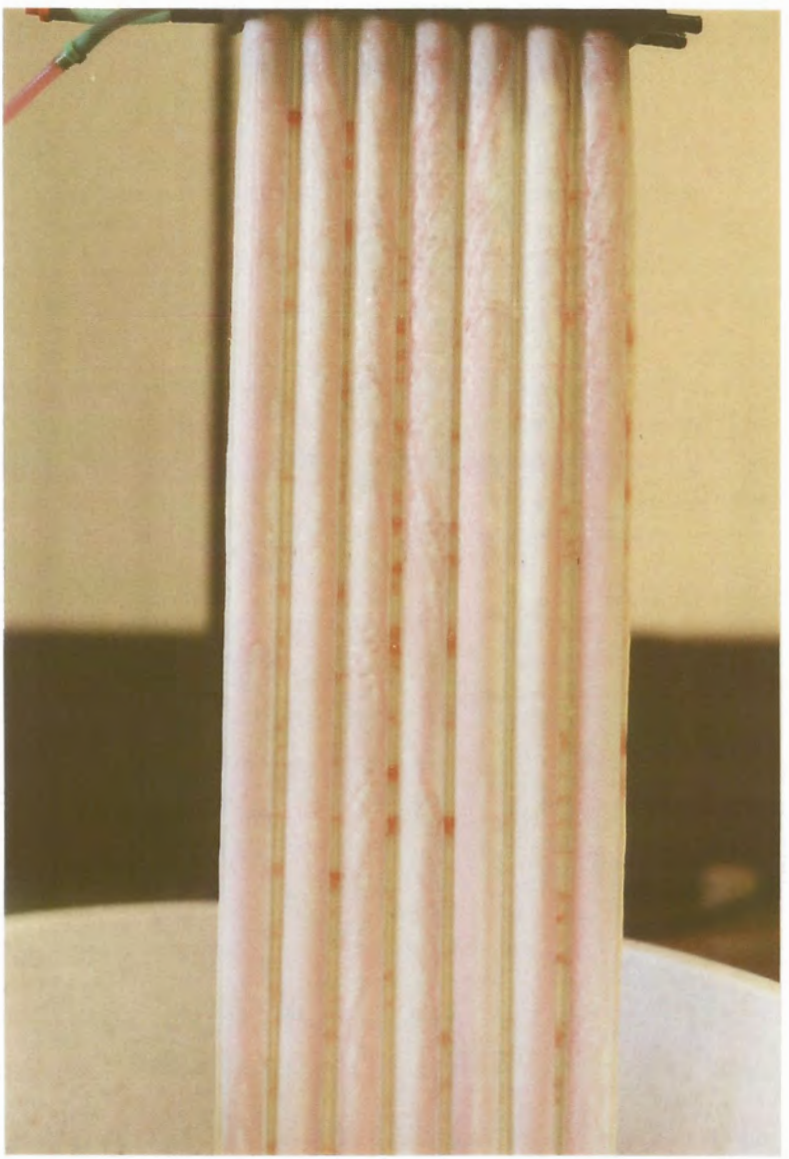

Fig.6.7 Visualization of the streams flowing downwards.

Before the tests with surfactant the plastic film was exposed for many days to dry air instead of being kept in a wet environment. This could have had a negative effect on the treated surface.

We had some indications that additives used in the polypropylene film itself was creating problems with the wettability. Anti-block, slip and other additives often contain waxy low molecular mass oligomers which readily migrate to the surface. Two situations can now arise:

(a) If such migration occurs *before* oxyfluorination (or other surface treatment), then these *mobile* additives (instead of the film itself) are made wettable. As they subsequently move, the surface is no longer wettable.

(b) If a clean surface is oxyfluorinated (or else teated for wettability), then subsequent migration of mobile oligomers (which have low surface energy) to cover the surface will swamp the wettable surface with non-wettable material.

We therefore had film made in a specially formulated grade of high density polyethylene (HDPE) material, containing an absolute minimum of such mobile components/additives. Only the second batch of such film was satisfactory - from the second film blowing company.

Experiments followed with these HDPE films. Before oxyfluorination, some were masked around the weld lines to prevent oxyfluorination in these regions - most with masking tape, others with PVC insulation tape. These films were subjected to three different treatment times - 10, 100 and 1000 seconds. The wettability of the films was tested. In these tests the surfactants were used at a dilution of 10^{-4}. The plastic films were kept always wet in a device built for this purpose. Surprisingly the non-masked films - one shown in figure 6.8 - show better wettability than the masked ones. (Perhaps out-gasses from the tape reacted with the reactive fluorine or oxygen). However, the amount of water flowing down the "furrows", is (as expected) less in the masked films - but only *slightly* less.

In the non-masked category, the film oxyfluorinated for 1000 seconds shows better wettability than the one treated for 100 seconds. Confirming this trend, the film treated for 10 seconds had the poorest wettability in that category.

In the category of the masked films, the "100 sec" oxyfluorinated film was - suprisingly - better than the one treated for "1000 sec". This result is not understood. We suspect a labelling error.

In general, the use of surfactants to complement the oxyfluorination process have

enhanced significantly the wettability of water on the plastic films. However, results dependent on surfactants do not seem acceptable for a practical desalinator.

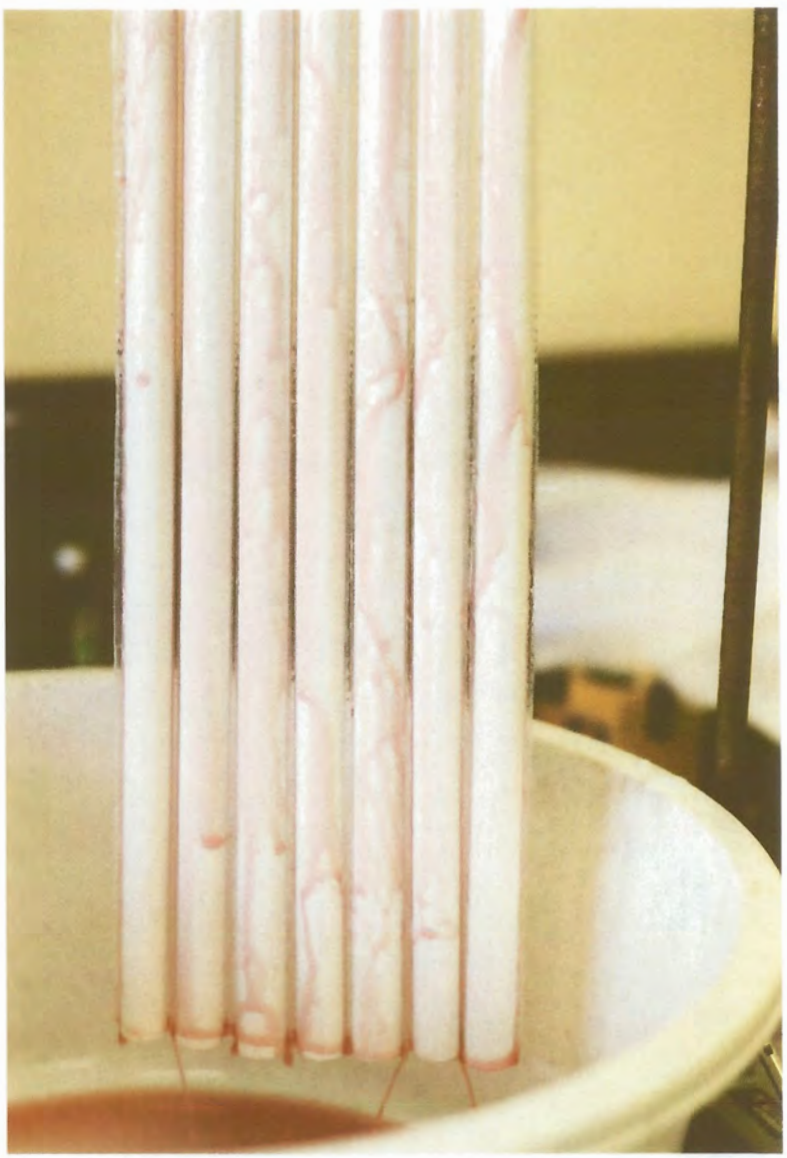

Fig.6.8 View of the flow on a non-masked oxyfluorinated plastic film.

Thus, adjustments of the oxyfluorination conditions were undertaken: - Sets of one and two metre long welded plastic films were sent for oxyfluorination under enhanced treatment conditions (time & concentration of the gas mixture). For the oxyfluorination of plastic films of 2m long, a device was specially built to hold these films equally spaced in spiral layout inside the cylindrical reactor. The testing of the wettability of these oxyfluorinated films was done using the improved setup. There is a limit to what is possible with oxyfluorination, as too high a concentration of these reactive gases causes

melting, carbonisation, or even ignition, of the film. The best obtained results with enhanced conditions were better than before, but still not satisfactory.

It was accidentally found that by slowly "*wiping*" the inflated tubes with rubber gloves *while water was flowing over the surface,* the wetting of the plastic films improved dramatically. Thus, tests were done to compare the efficiency of about 40 wiping tools of different shapes and materials. The tests indicate that tools with a smooth round contact surface were the most efficient. Whether the wiper material was hydrophilic or hydrophobic made little difference. But *slow* wiping was markedly more efficient than fast.

It appears that the surface treatment - with a very reactive fluorine-oxygen mixture - causes a roughening of the surface. (In a future project atomic force microscope experiments will be done to investigate this hypothesis) It is known [6] that *rough surfaces* show some *hysteresis* effects - *advancing and receding contact angles* for a liquid such as water differ for such surfaces. What happens with *slow* wiping of the air mattresses *with water flowing* against a treated surface, is that *water is dammed* by the smooth wiper against the "air mattress" film. Once wet, as long as water is (even slowly) flowing, the surface remains wetted rather uniformly - in a near ideal manner.

From a practical point of view, the wiping (say once per hour, or per day) may also - like the sponge ball method used in MSF systems - help to remove scale *as it is being formed* (when it is still soft, due to an incomplete crystallization process) [11]. Inside the system, the wipers may also serve as *spacers* between the "air mattresses". But having a mechanically moving system to wipe each of the thousands (or millions) of tubes inside the vacuum system of a large desalinator, with hot saline water all around, may pose serious problems with the reliability and availability of the system.

With the use of wipers, the problem of the flow along the "furrows" centred on the weld lines still remained a problem, as can be seen in figure 6.9. As mentioned before, different approaches were tried to address that problem. The use of a layer of strongly hydrophobic silicone on the weld lines seems to be the best options so far. The combined action of

wiping the films and using thin layers of silicone on the weld lines improves the wettability significantly. The achievement of complete wettability via oxyfluorination has

Fig. 6.9 Flow dripping through the weld lines of an oxyfluorinated film.

proved unsuccessful after several years' work. Thus, another surface treatment - sulfonation of the specially formulated HDPE film - is in the early stages of being tested. This process uses gaseous sulfur trioxide (SO_3). Figures 6.10 and 6.11 show the first sulfonated films in our wettability test. The brown colour of the films is due to the sulfonation process. At this early stage the first sulfonated films appear to be more wettable than the best oxyfluorinated ones.

6.4 Surface Tension Measurements

Knowledge of the surface tension of a solid is vital for the assessment of its wetting capability by a given liquid. The wetting behaviour of a liquid on a solid surface can be evaluated by measuring the contact angle between the liquid and the solid. Theoretically, a surface is wetted by a liquid if the contact angle between both is less than 90° [6,12].

Complete wettability is achieved if the contact angle is zero degree. It occurs when the surface tension of the solid exceeds that of the liquid.

Fig. 6.10 Sulfonated film with water flowing on its surface.

Fig. 6.11 Another sulfonated film.

When free of oily contamination, all metal heat transfer surfaces used in thin film evaporation (cupro-nickel, titanium, aluminium brass, other aluminium alloys and various grades of stainless steel) are *completely wettable* by water. Clearly, complete wettability plays an important role in achieving a *total wetting* of the evaporating surface - which is essential for efficient and reliable operation of a multi-effect (ME) or vapour compression (VC) desalinator [10]. We consider it also essential for desalinators with polymer heat transfer surfaces. Clearly, an evaporation surface contaminated with oil - or feedwater so contaminated - will not be acceptable for efficient and reliable operation of an ME or VC desalinator.

Table 6.1 lists - for comparison - the surface tension of water and of some polymers.

There are different methods for the determination of the contact angle of a liquid on a given solid surface. The most commonly used methods are sessile drop, captive bubble and the Wilhelmy plate technique. With some methods one can measure only one contact angle (static). This contact angle does not characterise the interaction solid-liquid since solid surfaces are often rough, uneven, and inhomogeneous.

Temperature(°C)	Material	Surface tension (dynes/cm)
25	Water	72
	Sea water	73
25	Polypropylene	30.1
25	Polyethylene	35.7
	Silicones	20 - 26
	Polyamide	46
	PTFE	18

Table 6.1 The surface tension values of some polymeric materials for comparison with that of water.

The Wilhelmy plate method [15] is the technique used in this work. It was chosen because it provides more information about the solid-liquid interaction. Thus, a *contact angle hysteresis* is obtained - the difference between the advancing and the receding

contact angles.

The advancing (maximum) and receding (minimum) angles are automatically calculated by the computer from the force exerted as the sample is dipped into the liquid or withdrawn from it. The equation used by the computer to calculate the dynamic contact angles is:

$$\cos\theta = \frac{F}{\sigma p} \tag{6.1}$$

where F is the insertion/withdrawal force measured by the balance, p the perimeter of the sample in contact with the liquid, σ the surface tension of the liquid probe; and θ the angle formed by the tangent to the point of contact at the solid-liquid-vapour boundaries.

6.4.1 Experimental Setup

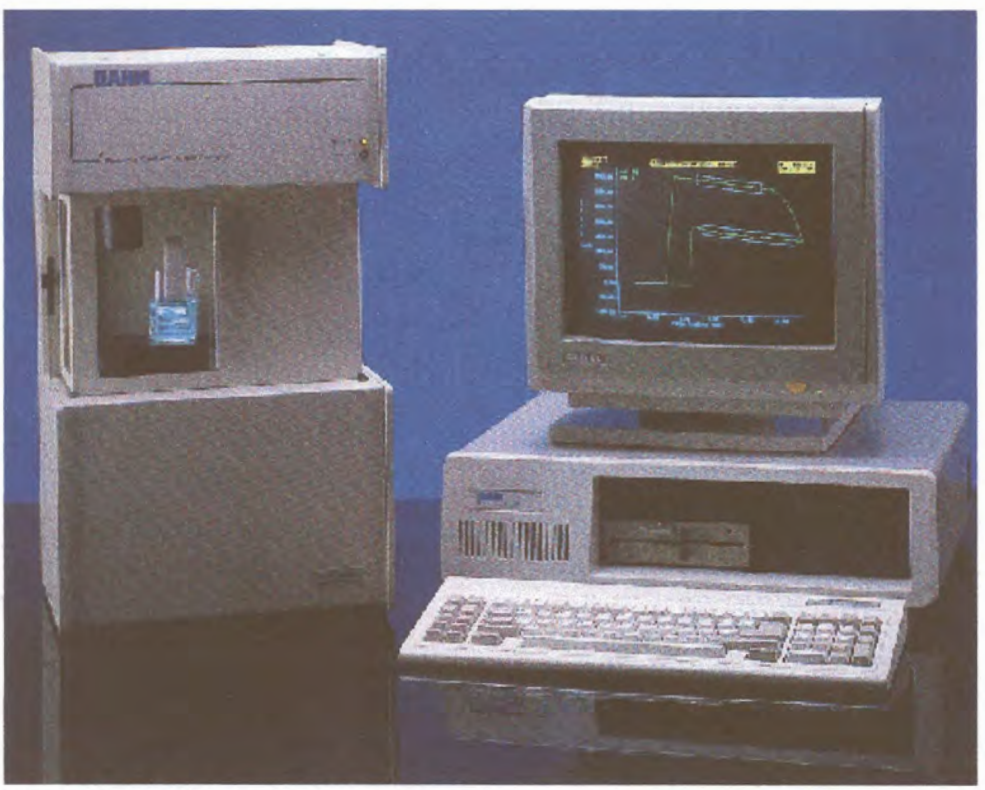

Fig.6.12 A DCA series 322 Analyzer.

The instrumentation used for the dynamic contact angle is shown in figure 6.12. It comprises a DCA series 322 Analyzer (from CAHN), a computer, and a printer. The DCA Analyzer includes a microbalance and a movable stage, on which the container with the wetting liquid is placed.

The computer controls the DCA through special software that calculates automatically the contact angles (advancing and receding) and the surface tension.

The samples for the dynamic contact angle measurements, comprising small pieces (30mm x 12.5mm x 39μ) of plastic film, were thoroughly cleaned. For this, they were introduced into a small container filled with tap water mixed with a commercial surfactant and immersed in an ultrasonic bath for 15min. Thereafter, they were thoroughly rinsed with distilled water and dried. The samples were then introduced into the reactor for oxyfluorination in two sets of five each using oxyfluorination times of 400 and 800s.

The testing of each *sample* started with the measurement of its to be wetted perimeter with a digital vernier caliper. Then it is held vertically suspended by an electro-balance in a fixed position. A container with the probe liquid of known surface tension (e.g. water) is placed on the movable stage. In operation the stage moves up and down at a constant velocity of 40μm/s. The sample is immersed into and withdrawn from the liquid. The wetting force on the sample is continuously measured as function of the immersion depth. A printer attached to the apparatus plots the obtained force *versus* depth of immersion, and calculates the advancing and receding contact angles.

The dynamic contact angle hysteresis curve for the samples, subjected to different conditions, is presented in figures 6.13, 6.14 and 6.15. The sample of figure 6.13 had not been surface treated. The results are summarised in table 6.2.

	Dynamic contact angle (degrees)		
Oxyfluorination time	advancing	receding	hysteresis
untreated	84.5	69.9	14.6
400 s	69.2	54.4	14.8
800s	51.8	35.4	16.4

Table 6.2 Dynamic contact angles for PP sample.

As expected in all samples, the advancing contact angles are higher than the receding ones. The contact angle hysteresis increases with the oxyfluorination time. This is under-

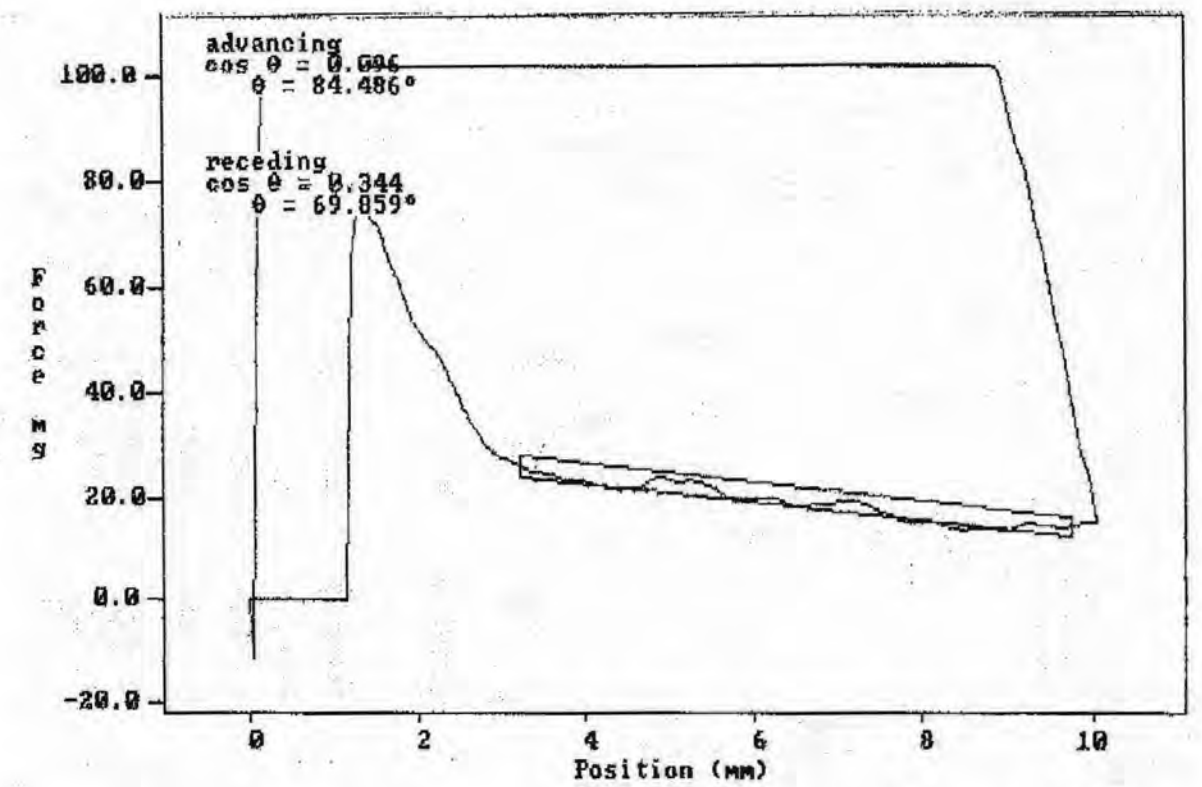

Fig.6.13 Dynamic contact angle hysteresis curve for untreated uniaxially stretched PP film.

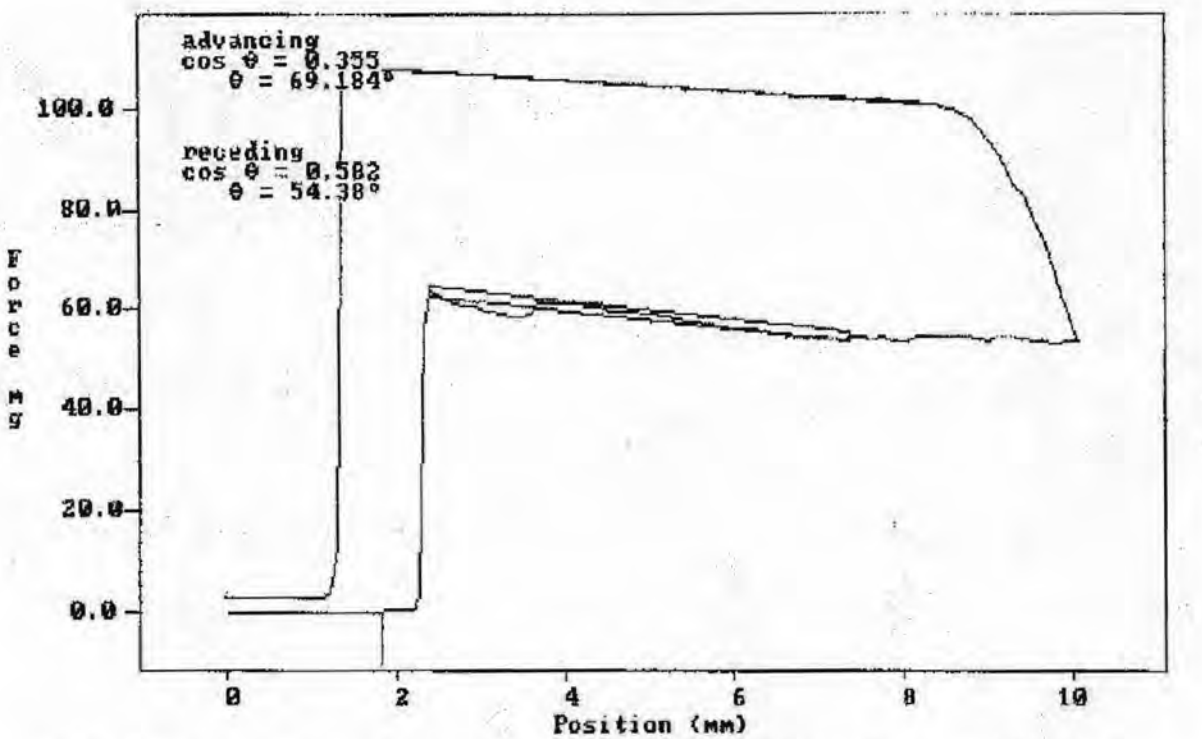

Fig. 6.14 Dynamic contact angle hysteresis curve for a 400s oxyfluorinated PP film.

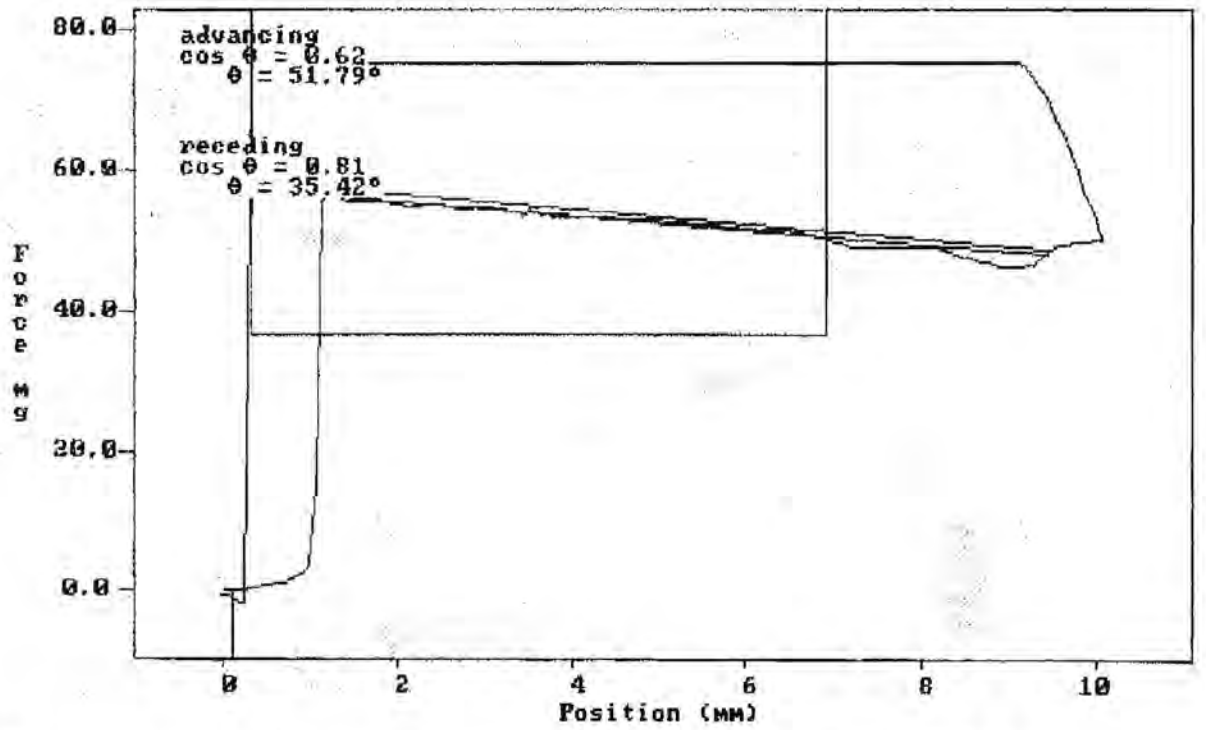

Fig. 6.15 Dynamic contact angle hysteresis curve for a 800s oxyfluorinated PP film.

standable, for the treatment process changes the surface morphology.

The contact angles decreases with the treatment time. With this trend in mind the surface treatment time were increased. However, complete wettability (zero contact angle θ) could not be achieved by oxyfluorination.

6.5 Liquid Distributor

For good heat transfer, an adequate distribution of water (flow mode) onto the outer (evaporation) surface of the thin film "air mattress" heat exchanger element is needed to keep the entire outer surface (except the areas near the weld lines) wet. The distribution of the fluid onto the surface should be even, uniform and at a sufficiently low rate to have film-wise evaporation. The design, construction and materials of the liquid distributor must be such as to avoid or at least minimize the occurrences of blockages.

The following configurations of the liquid distributor were tested:

A) A high density polyethylene (HDPE) distributor tube (5mm ID), with seven holes of one millimetre diameter each, spaced axially 20mm apart. Due to the known ease of

blockage of such small holes, versions with micro-tubes instead of simple hole were tested.

B) A similar HDPE distributor tube with inserted polypropylene (PP) micro-tubes of 1.1 mm inside diameter and 5 mm long: - 7 holes to each side at an angle of 45° from the vertical - to wet "air mattress" elements placed on both sides of the distributor. The tubes facing left are staggered with respect to the ones facing to the right, as the "air mattress" tubes are likewise staggered (see figure 6.16).

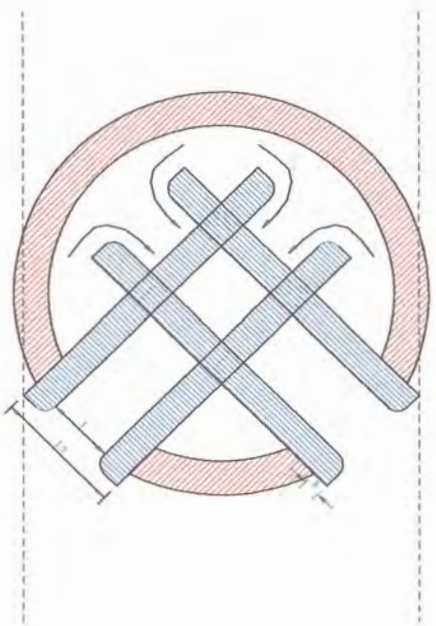

Fig. 6.16 Cross sectional view of the liquid distributor with the inserted micro-tubes.

C) In another setup stainless steel micro-tubes (0.8 mm ID) replaced the PP ones.

For the tests the liquid distributor comprised only one set of micro-tubes all located on the same side of the HDPE plastic tube.

Tests were performed to determine the water head h at which the flow pattern coming from the liquid distributor varies from droplet to jet mode were conducted using the test facility shown in figure 6.17. The setup comprised two basins. The one, usually kept at

fixed height, was used as water source. The other, at the bottom, was used to collect the water discharged from the first basin.

Fig. 6.17 Setup for liquid distributor testing.

The liquid distributor was connected to the top basin through a flexible tube with a tap to interrupt the flow when necessary. The liquid distributor was set at 40 mm below the bottom of the top basin.

A small fountain pump (EDEN 130G) was used to fill the top basin with water to a level sufficient to effect jet mode. With the pump off and the tap open, water from the top basin was released through the liquid distributor into the bottom basin. As the liquid level dropped, the flow pattern varied from jet mode (at the beginning) to jet-droplet mode and

finally to droplet mode. For comparison, with the liquid distributor exhibiting droplet mode the pump was switched on again to refill the top basin and the inverse transitions were observed.

The water levels inside the basin where the changing of flow mode occurs were measured with an ordinary ruler. The corresponding water head h - at the flow distributor - for the three configurations is shown in table 6.3. The values for both directions differ slightly in all configurations, specially in the transition from mixed to droplet mode and vice versa.

Configuration	h (mm) jet <–>jet-droplet	h (mm) jet-droplet <–>droplet	Observation
A	124	91	downwards
	126	95	upwards
B	146	63	downwards
	150	70	upwards
C	131	64	downwards
	130	67	upwards

Table 6.3 Water head h for the configurations A, B, and C in the transitions jet - mixed, mixed - droplet, and vice versa.

The determination of the h values for the transition from mixed to droplet mode and vice versa was difficult due to the frequent blockages experienced in the liquid distributors, specially in configuration A.

The holes and the inserted micro-tubes had to be constantly cleaned during the tests. This could have affected the measurements.

As expected the water head h in all configurations reduces from jet via mixed to droplet mode. The factor of reduction is almost equal in configurations B and C. The frequent blockages experienced in configuration A have affected the results in the transition from mixture to droplet mode thus making the reduction factor of A less than that of B and C. Comparatively, configuration A looks more attractive given the low h values in the

transition jet to mixture mode. However, the uncertainty of the reliability of the h values in the other transition makes configuration C a better option.

To establish the nature (laminar, transitional or turbulent) of the flow inside of the distributor the Reynolds number was determined for the three configurations. Transitional flow tends to be unstable - therefore to be avoided. The Reynolds number is given by

$$R_e = \frac{\mathrm{v} d_h}{v} \tag{6.2}$$

where v is the fluid velocity, v the kinematic viscosity, and d_h the hydraulic diameter.

The hydraulic diameter - determined for a tube with one inserted micro-tube (see figure 6.16) is given by

$$d_h = \frac{4A_c}{P} \tag{6.3}$$

where A_c is the cross-sectional area for flow and P the wetted perimeter.

The fluid velocity is given by

$$\mathrm{v} = \frac{\dot{m}}{\rho A_c} = \frac{\dot{V}}{A_c} \tag{6.4}$$

where $\dot{m}$ is the fluid mass flow rate, ρ the fluid density, and $\dot{V}$ the fluid volume rate.

The average fluid volume rate was obtained by measuring the volume of the fluid collected during 30 seconds in a set of three measurements for each configuration. This was done at the water head where the flow was about to change from jet to mixed mode.

Using the equations (6.2), (6.3) and (6.4) the Reynolds number was calculated by

$$R_e = \frac{\dot{V} d_h}{v A_c} \tag{6.5}$$

In the calculation of R_e for configuration A (tube without obstruction), d_h was replaced by the inside tube diameter. The fluid kinematic viscosity v was evaluated at the temperature of 295K [7].

The obtained values of the Reynolds numbers are shown in table 6.4. The results are far less than the critical value of 2300, where the transition from laminar to turbulent flow inside a round tube normally starts. However, given the existence of obstruction due to the inserted micro-tubes in the configurations B and C, the theoretical critical Reynolds number for similar case is expected to be lower than 2300, since obstruction promotes turbulence.

Configuration	R_e
A	840
B	852
C	440

Table 6.4 Calculated Reynolds numbers for the three configurations with the flow in jet mode.

The calculated Reynolds numbers are nevertheless still far from 2300. Therefore the flow inside the tube in all configurations can be considered as laminar. This is good for the required uniform spreading of the fluid on the plastic film surface.

6.6 Summary

The wettability of the plastic films is essential for the falling film evaporation used in all modern multi-effect and vapour compression desalinators. The surface treatments (oxyfluorination and sulfonation) on the used polymer films did improve their wettability to water. The use of surfactants to complement the surface treatment has enhanced

significantly the wetting of the films. However the results obtained so far are still not satisfactory.

The wiping of the surface of the oxyfluorinated films was another alternative to further improve the wetting of the plastic films. However it appeared to be a complex options to implement in the prototype desalinator, despite the advantages for its use for removing scale and acting as spacers between the "air mattresses".

To avoid the unwanted capillary action in the space between adjacent film tubes the use of hydrophobic silicone was by far the best solution.

The wettability of the plastic films was quantitatively estimated by determining the contact angles between the liquid (water) and the sample (treated and untreated plastic films) using the Wilhelmy plate technique. The obtained results show a relationship between the oxyfluorination time and the contact angles.

The configurations of the liquid distributor is vital for the desired even, continuous, and uniform spreading of the water on the heat transfer surface to promote falling film evaporation. The use of HDPE plastic tube with inserted metallic micro-tubes appears to be the best solution to avoid undesirable blockages in the liquid distributor.

The flow in all tested liquid distributors' configurations lies inside the laminar region.

6.7 References

1. A. F. Mills, *Heat and Mass Transfer*, Chicago, Irwin 1995.

2. F. P. Incropera and D. P. DeWitt, *Introduction to heat transfer*, New York, Wiley, 1990.

3. A. Bejan , *Heat transfer*, New York, Wiley, 1993.

4. M. Anand, R.E. Cohen, and R.F. Baddour *Surface modification of low density polyethylene in a fluorine gas plasma*, Polymer, 1981 vol. 22.

5. F. J. du Toit and R.D. Sanderson, *Surface fluorination of polypropylene, 1.*

Characterization of surface properties, Journal of Fluorine Chemistry 98 (1999) 107 - 114.

6. F. Garbassi, M. Morra, and E. Occiello, *Polymer Surfaces: from Physics to Technology*, Chichester, Wiley, 1996.

7. Y-H Wei and A.M. Jacobi, *Vapor -shear, geometric, and bundle-depth effects on the intertube falling-film modes*, paper presented at 1st International Conference on the heat Transfer, fluid mechanics, and thermodynamics, Kruger National Park, South Africa, 2002.

8. J. A. Fox, *An introduction to engineering fluid mechanics*, London, Macmillan,1974

9. D. M. Brewis and I. Mathieson, *Adhesion and bonding to polyolefins*, Shawbary, Rapra Technology Ltd, 2002.

10. V. Baujat and T. Bukato, *Research and development towards the increase of MED units capacity*, proceedings of IDA conference, Paradise Island, Bahamas, 2003.

11. E. Ghiazza and A.M. Ferro, *The scaling of tubes in MSF Evaporators: A critical review across 20 years of operational experience*, proceedings of IDA conference, Manama, Bahrain, 2002.

12. Lin Tu, *Development of surface fluorinated polypropylene fibres for use in concrete*, PhD-thesis, Rand Afrikaans University, Johannesburg, 1998.

13. L. Ramm-Schmidt, H. Eriksson, P. Koistinen, and V. Tiainen, *Liquid distributor for an evaporator*, USA patent 5904807, 1999.

14. R. Defay and I. Prigogine, *Surface tension and absorption*, London, Longman, 1996.

15. K. T. Hodgson and J. C. Berg, *Dynamic Wettability Properties od Single Wood Pulp Fibers and their Relationship to Absorbency*, Wood and Fiber Science 20(1) 1988 3 -17

List of Symbols

A_c : cross-sectional area for flow (m^2)

d_h : hydraulic diameter (m)

F : insertion/withdrawal force measured by the balance (N)

h_e : heat transfer coefficient for evaporation (W/m^2K)

k : conductivity of polymer film heat transfer material (W/mK)

$\dot{m}$: fluid mass flow rate (kg/s)

p : perimeter of the sample in contact with the liquid (mm)

P : wetted perimeter (m)

R_e : Reynolds number

v : fluid velocity (m/s)

$\dot{V}$: fluid volume rate (m^3/s)

ΔT_o : temperature difference per effect (K or C)

ΔT_l : temperature difference for heat transfer between condensing vapour and evaporating saline water In- and outside film tubes (K or C)

ΔT_e : temperature difference between a heated polymer film surface next to evaporating saline water, and its vapour.

θ : angle formed by the tangent to the point of contact at the solid-liquid-vapour (degrees)

ν : kinematic viscosity (m^2/s)

ρ : fluid density (kg/m^3)

σ : surface tension of the liquid probe (dynes/cm)

Anex

List of companies

Companies	Activity
CSIR-Rapid prototyping	manufacturing of the first version of manifolds
Tee Kee Engineering, Pretoria	building of the vacuum vessel
Gordon Bennet (Pty) Ltd	painting of the vacuum vessel with a special phenolic epoxy - two coats of TCN 300
Master Machining cc	building of the compressor
Prestec	N. C. machining of manifold pieces